A PROTOCOL FOR SAMPLING ECOHYDROLOGICAL TRAITS IN NEPAL'S TERAI ARC LANDSCAPE
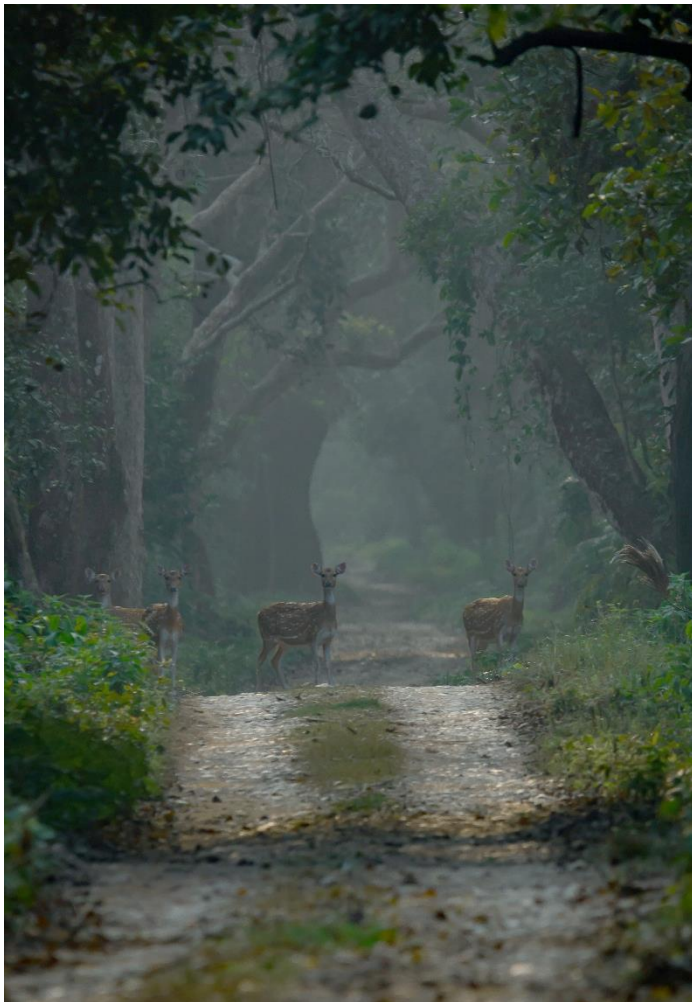
Author: Stephen Maycock

MSc Thesis – Water Science and Management

Student No.: 7299540

Supervisor: Dr. Hugo. J. de Boer

Date: 03 July 2023

Contact:

stephenmmaycock@gmail.com
s.m.cromaycock@students.uu.nl

Photo taken by Stephen Maycock (2023)

Acknowledgements

Abstract

The Terai Arc Landscape (TAL) of Nepal is a global priority conservation area for the Bengal Tiger (*Panthera tigris tigris*). The Bengal Tiger faces numerous threats to its survival, including a decrease in prey availability as a result of the degradation and loss of critical habitats such as grasslands and wetlands. Fluctuating groundwater tables can potentially contribute to the loss of these habitats as grasslands thrive with shallower groundwater levels. The potential impacts of human development and climate change on groundwater in the region necessitates the investigation on the dynamic relationship between hydrologic and vegetation processes. This Master's thesis forms a part of the "Save the Tiger! Save the Grasslands! Save the Water!" (Tiger) project that aims to contribute to the conservation efforts of tiger habitats in the TAL through recognizing the significance of ecohydrology and its impact on these crucial tiger habitats.

The primary objective of this research is to develop a protocol to facilitate the systematic collection of consistent and reliable data on Leaf Area Index (LAI), Fractional Vegetation Cover (FVC), and Surface Soil Moisture (SSM) - key parameters that describe ecohydrological relationships. Moreover, a secondary objective is investigated, utilizing the data acquired through implementation of the developed protocol to validate satellite products to explore the potential of upscaling in-situ data.

The protocol demonstrated its ability to capture consistent and reliable data for LAI and FVC across various vegetation types, showing potential for application across different regions in the TAL. Additionally, the study explored the viability of a smartphone-based LAI method, the PocketLAI, which proved to be a feasible alternative to the more established and high-cost AccuPAR-LP80, albeit requiring further investigation on the effect of specific smartphone models and LAI retrieval. While the protocol captured consistent SSM data, improvements are necessary to enhance the reliability of these measurements. The validation of satellite products revealed significant relationships with in-situ LAI and FVC. Despite largely underestimating LAI and FVC values, the results have important implications for monitoring patterns of these parameters across the TAL.

Further iterations of the protocol, implemented across different fieldwork campaigns within The Tiger Project, are crucial for establishing a robust protocol. Such a comprehensive protocol will have invaluable implications for conservation efforts towards tiger habitats and form a fundamental platform for future research and analysis in the TAL.

Table of Contents

1. Introduction

An unprecedented loss of biodiversity is being experienced on a global scale, with evidence suggesting that current extinction rates are vastly higher than estimated background extinction rates (Bellard et al., 2022). There is general agreement that there are five major drivers for this loss: habitat destruction, over-exploitation of natural resources, biological invasions, climate change, and pollution, although many other local perturbations and stressors are also important (Brook et al., 2008). Almost one-quarter of the 5692 species of mammals are threatened with extinction, with further increases in human pressures exacerbating this crisis (Di Marco et al., 2018). One such species particularly threatened by these pressures is the Bengal Tiger *(Panthera tigris tigris),* classified as 'Endangered' in the IUCN red list.

The conservation of tigers has garnered much attention in recent years due in part to its charisma and popularity, but also its impacts on biodiversity and ecosystem functioning, as it is the apex predator in its occurring habitats (Nittu et al., 2022). Tiger habitats provide numerous environmental and socio-economic benefits ranging from water provision for local and downstream communities, increased natural hazard resilience, mitigation of climate change effects through carbon sequestration as well as a variety of medicinal benefits (WWF, 2022). This led to the formation of the Global Tiger Initiative, an alliance of 13 tiger range countries with the overarching aim to double the population of wild tigers in 2022 as compared to that of 2010 (WWF, 2022). Furthermore, this recognition of the benefits of conserving tiger habitats for both biodiversity and socio-economic development led to the creation of the Dutch-Nepali project "Save the tiger! Save the Grasslands! Save the Water!" (hereafter, 'The Tiger Project'). The Tiger Project aims to understand both the ecological and hydrological dynamics of tiger habitats for the sustainable conservation of these important ecosystems in the context of the Terai Arc Landscape in Nepal (UU, 2022). This thesis aims to contribute to the Tiger Project through exploratory research into the development of a sampling protocol to aid in the monitoring of ecological and hydrological dynamics to better inform conservation management for the sustainable preservation of tiger habitats.

1.1 Background

Nepal was the first country in the Global Tiger Initiative to succeed in doubling its tiger population (DNPWC and DFSC, 2022). The Terai Arc Landscape (TAL) is a global priority transboundary conservation landscape for tigers and is home to several other threatened endemic species such as the greater one-horned rhinoceros, Asian elephant, and swamp deer (DNPWC & DFSC, 2022). In addition to being a biodiversity hotspot, it is also the most densely populated region of Nepal supporting the agriculture and livelihoods for more than half of the population (CBS, 2014). The balance between human development and ecological conservation is therefore criticial and has been under pressure in the past century. Ever increasing anthropogenic development within the TAL, notably before the formation of the national parks, led to the region suffering from extensive poaching, human expansion, and deforestation, much like other natural areas in Asia (Kral et al., 2017). These drivers, particularly poaching, were the main causes of the tiger population decline in the 20th century.

As a result of this, tiger conservation efforts have historically been dominated through actions and measures that mitigate tiger poaching (Panthi et al., 2019). These actions have evidently been successful, and poaching is no longer the dominant threat to future tiger populations in Nepal. The major challenges currently are the continued threat of tiger habitat loss and degradation as well as a loss in prey-base due to the degradation specifically of wetlands and grasslands (Dhakal & Baral, 2015). This results in an additional conservation issue as old and weak tigers are forced out of diminishing natural habitats by more dominant tigers, increasing human-tiger conflicts as their search of food leads to livestock and humans (Dhungana et al., 2016). Thus, special attention to the conservation of tiger habitats including these vital prey ecosystems, is crucial for the continued success of tiger conservation and biodiversity conservation in the TAL whilst minimising wildlife conflicts and maintaining socio-economic growth in the region.

Tigers are an umbrella species and are dependent on their prey base, largely herbivores, that in turn are dependent on grasslands for their required nutrients and food diets (Dhakal & Baral, 2015). Carter et al. (2013) also found that tigers preferred areas with more grasslands and dense understory vegetation growth due in part to the abundance of prey, but also increased cover for hunting activities. The abundance of these grasslands is primarily associated with disturbances that prohibit the natural successional growth of this vegetation to later successional stages, forests. (Bijlmakers, 2020). In the TAL, these disturbances were attributed predominantly to

anthropogenic activities that included burnings, harvesting of grass, and livestock grazing that all acted in combination with natural disturbances such as fire, wildlife grazing, and fluvial processes (Thapa et al., 2021; Bijlmakers, 2020).
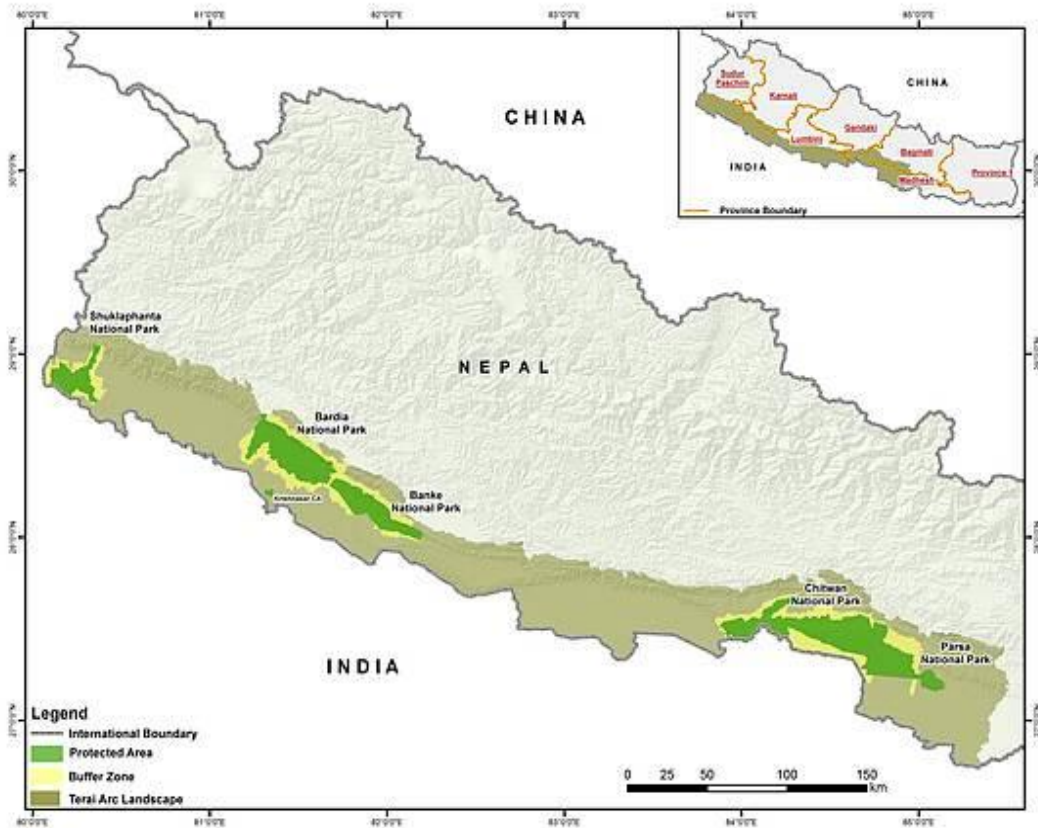
Figure 1. The Terai Arc Landscape (TAL) (brown shading) depicting the six major protected areas (green shading) and buffer zones that enable increased landscape connectivity (WWF, 2021; Dhakal & Baral, 2015).

Anthropogenic disturbances came to a somewhat sudden halt since the formation of protected areas (green areas in figure 1) within the TAL beginning in 1970. With no harvesting and cutting of grass, no livestock grazing, and reduced fires, tall grasslands proliferated in place of short grasslands (grazing lawns) and were therefore allowed to follow their natural succession to shrubs and forests (Lehmkuhl, 1994). This has resulted in the decline of grazing lawns over the years, posing a threat to the endangered faunal communities that are dependent on these early successional habitats (Kral et al., 2017). To prevent further encroachment from woody species and the proliferation of tall grasslands at the expense of grazing lawns, local communities are permitted to harvest grass to be used as building material and additional cutting and burning of grasslands is carried out as a part of park management strategies each year during the dry season (Brown, 1997). Whilst these management strategies have been successful in retarding successional change towards forests (Lehmkuhl, 1994), the number of people entering the park for these controlled instances of harvesting has drastically decreased

in comparison to previous decades, possibly due to a shift in construction materials needed for housing (thatch to sheet roofs), which has allowed once more for the establishment of tall grasses at the expense of grazing lawns (Thapa et al., 2021).

Fluvial processes can also potentially contribute to the favouring of late-stage successional vegetation (forests) as a result of falling groundwater tables. Figure 2 depicts the interaction between fluvial processes and successional stages of vegetation, notably that lower groundwater tables (for example, as a result of decreasing streamflows) favour trees with deep roots whilst grasses flourish with frequent inundation and shallow groundwater tables (Merritt & Cooper, 2000; Hai-liang et al., 2007). The TAL is currently predicted to experience changes in fluvial processes that will result in reduced groundwater availability, thus endangering the grasslands further. The two major contributors to these changes being: climate change where it is foreseen that the hydrology of the Himalaya will be impacted resulting in lower baseflows in the rivers that feed into the TAL, as well as economic development with current and planned large-scale irrigation and potential hydropower projects that will remove water from the rivers in the TAL (Wester et al., 2019).
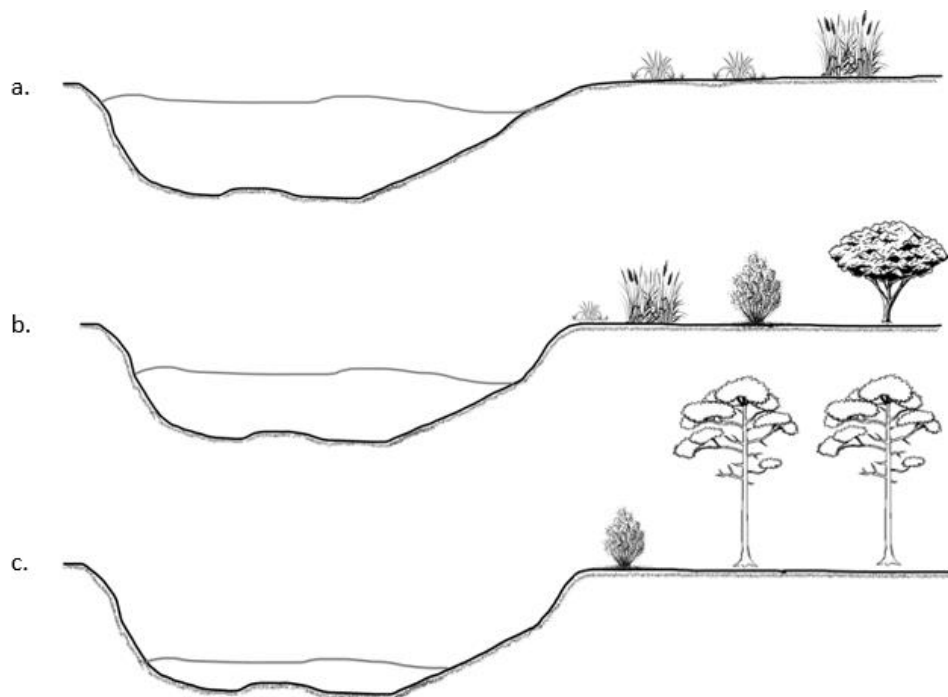
Figure 2. Simplified depiction of successional vegetation changes as a response to water level. a) High river water level (shallow groundwater table) promotes early successional vegetation - grazing lawns and short grasslands; b) Medium water levels decrease abundance of grazing lawns, favouring tall grasslands and shrub growth; c) Low water level (deep groundwater table) promotes late-stage successional vegetation - tree and forest growth with deep-rooted vegetation.

1.2 Ecohydrology

Ecohydrology is at the core of these relationships between fluvial processes and grassland and vegetation dynamics. The Tiger Project argues that extensive knowledge on the ecohydrology of the TAL is therefore necessary for the continued and sustainable conservation of tigers and dependent biodiversity whilst still ensuring concurrent sustainable development. Two widely used parameters for the study of vegetation processes in relation to terrestrial water cycles are Leaf Area Index (LAI) and fractional vegetation cover (FVC) (Li et al., 2022).

LAI is defined as the one-sided leaf area per unit ground area and has been related to net radiation, net primary production of a canopy, as well as influencing the partitioning of rainfall between evaporation, throughfall, and runoff (Kala et al., 2014). Given its interactions with radiation, the water and carbon balances, LAI has long been considered a key component of ecological modelling and more recently ecohydrological modelling (Parton et al., 1996; Ma et al., 2019). FVC is defined as the fraction of surface, or vertical projection area, covered by vegetation and is closely related to LAI in its applications, also showing strong correlations to LAI on a variety of spatial scales (Li et al., 2022).

Soil moisture is another parameter that is widely used for the study of vegetation and water processes as it plays a significant role in regulating runoff, vegetation production, and evapotranspiration (Adab et al., 2020). Surface soil moisture (SSM) in particular refers to the water content of the top ~15cm of the soil layer and is an important parameter in describing fundamental water and energy fluxes at the land surface/atmosphere interface (Wang & Qu, 2009).

LAI, FVC, and SSM, form the focus of this thesis as they, simplistically, can be used to describe and quantify the complex ecohydrological interrelationships as shown in Figure 3. These relationships are key in understanding the dynamics between vegetation and groundwater hydrology and therefore the successional vegetation change as a result of fluvial and climate processes.
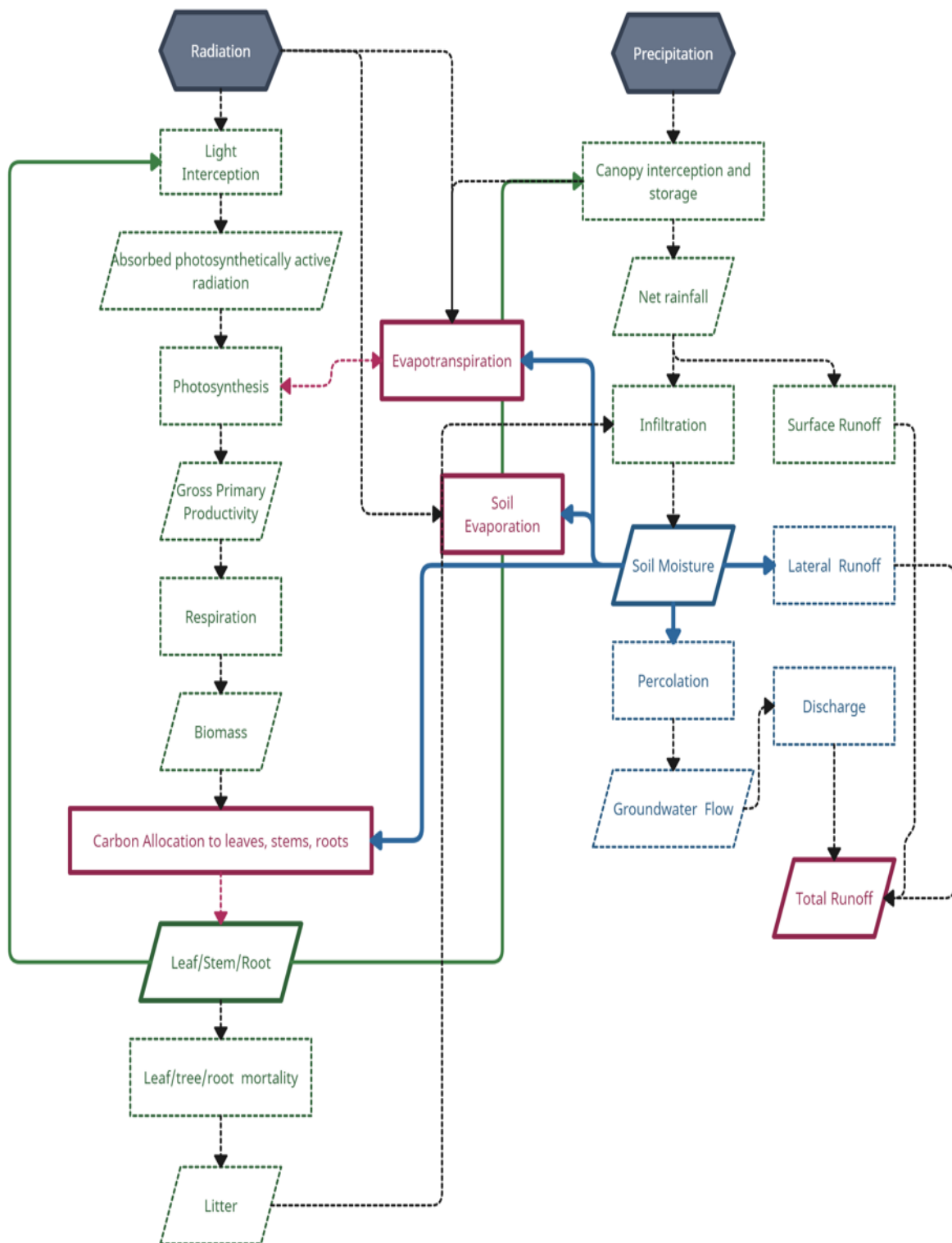
Figure 3. The basis of ecohydrological interactions between hydrology and vegetation processes, split by precipitation and radiation processes, adapted from Chen et al. (2015). Green boxes indicate influence from LAI/FVC, blue boxes influence from SSM and red boxes indicating direct influence from both LAI/FVC and SSM. LAI/FVC is a direct measurement of Leaf/Stem/Root (solid green box). SSM a direct measurement of soil moisture (solid blue box). This thesis argues that an intimate knowledge of these relationships will directly connect with an increased understanding of successional vegetation changes as a result of fluvial and climate processes.

Methods of data collection for LAI, FVC, and SSM field measurements have been extensively researched and tested over the past decades, particularly in an agricultural context (Weiss et al., 2004; Stafford, 1988). In-situ LAI measurements can be categorised as direct (destructive) or indirect (non-destructive). Direct methods are used as the reference LAI in validation studies as they are the most accurate when calculating LAI as a result of directly harvesting the leaves, a time-consuming process that is also often destructive to its environment (Bréda, 2003). Indirect methods rely on the transmission of light and radiation through the canopy and are generally preferred despite their lower accuracy, due to their non-destructive means. However, the instruments can prove costly, and the LAI estimates can be heavily dependent sky conditions as well as canopy structure (Bréda, 2003).

In-situ FVC measurements are predominantly visually estimated using grid-based or point-intercept methods (Smith et al., 1990). This carries large risks of researcher bias and therefore FVC is more generally derived from established remote-sensed vegetation indices such as the normalised difference (NDVI), soil-adjusted (SAVI), atmospherically resistant (ARVI) and other vegetation indices (Jiapaer et al., 2011; Younes et al., 2019). In-situ SSM measurements generally exploit the electrical properties of the soil (impedance, capacitance, dielectric constant, and soil resistivity), and are therefore often probe-based point measurements, although other modern methods – infrared rays, neutron scattering, gamma attenuation – are increasingly used and detailed in Lekshmi et al. (2014).

There is a distinct gap in the study of hydrology and its relationship on vegetation dynamics in the TAL. This gap becomes more apparent with the consistent collection of ecohydrological data, specifically LAI, FVC, and SSM in the region. For the Tiger Project to succeed in describing the long-term dynamics between grasslands and hydrology, there exists the need for consistent data collection of these parameters, encompassing multiple seasons. This entails the large-scale collection of in-situ data in a uniform and comparable manner across the TAL, thus requiring the use of a standard protocol that describes the sampling techniques of LAI, FVC, and SSM in the context of the TAL. To be successful in gathering the vast amount of data needed to describe long-term dynamics, the protocol will need to be used by researchers and locals with a variety of backgrounds that are in the field, and will therefore focus on accessibility, ensuring minimal cost, time, and technical requirements.

Whilst being invaluable for accuracy and validation, in-situ measurements pose the inherent problem of being spatially discontinuous and are therefore difficult to operationalize on a landscape scale (Dube et al., 2019), a critical aspect in achieving the goals of the Tiger Project. This and the fact that most of the tiger habitats in the TAL are situated within wildlife inhabited protected areas, necessitates the eventual upscaling of in-situ data to satellite sensing. Satellite sensing would overcome the inherent safety and logistical challenges of these environments, minimizing damage to important ecological systems, all while providing data at a landscape scale over large temporal scales. For satellite sensing to be reliable, extensive validation between in-situ and satellite data needs to be conducted in the geographical context of the TAL. Reliable satellite sensing will prove paramount to the success of the Tiger Project, contributing to the sustainable conservation of tiger habitats and respective ecosystems in the TAL that are so important for biodiversity and human livelihoods.

2. Objectives and Research Questions

The overarching goal of this thesis is to contribute to the "Save the tiger! Save the Grasslands! Save the Water!" project for the conservation of tiger habitats within the Terai Arc Landscape. A protocol for the collection of LAI, FVC, and SSM in this specific environmental context will be developed and forms the primary objective of this thesis. This protocol will need to be implementable and easy-to-use by members of the Tiger Project in order to provide consistent results over multiple field visits.

The secondary objective of this thesis is to provide a so-called ground truthing for established satellite-derived methods to quantify LAI, SSM, and FVC in the Terai Arc Landscape. Satellite-derived data will therefore be compared with observations from the field collected during this study. To realise these two objectives, the thesis will be guided by the following aims and research questions.

Aim 1: To develop and test a protocol for the sampling of leaf area index, fractional cover, and surface soil moisture to quantify ecohydrological properties of natural heterogenous plots in the Terai Arc Landscape.

An additional aspect of developing the protocol will be to detail the most cost- and time-efficient LAI measuring techniques with regards to two indirect (non-destructive) methods. Therefore, it will also investigate the following research question:

Research Question 1: To what extent can an affordable smartphone-based indirect LAI method be considered a viable alternative to a more established, technical and higher-cost indirect LAI method in heterogenous vegetation in the Terai Arc Landscape?

The protocol will then be tested, and the data used to attain the ground-truth measurements required for the following aim:

Aim 2: To investigate the potential of satellite products in determining leaf area index, fractional cover, and surface soil moisture in the Terai Arc Landscape.

This aim deals with the upscaling of in-situ measurements obtained, thus simultaneously investigating the effectiveness of the methods outlined in the protocol as well as the potential of satellite products in quantifying the LAI, FVC, and SSM of the TAL. The SeNtinel Application Platform (SNAP) biophysical processor as described in Weiss and Baret (2016) is

used for the retrieval of LAI and FVC, and the Optical TRApezoid Model (OPTRAM) as developed by Sadeghi et al. (2017) for the retrieval of high resolution SSM. The following research questions are used to guide this aim:

Research Question 2: To what extent can the SNAP biophysical processor be used to accurately retrieve LAI and FVC in the Terai Arc Landscape?

Research Question 3: To what extent can the OPTRAM method be used to accurately retrieve SSM in the Terai Arc Landscape?

The consistency and reliability of the data collected using the protocol was tested by additional independent researchers from HAS University of Applied Sciences (HAS) in the field, and these results are shown and analysed in the context of the above aims and research questions.

3. Materials and Methods

The following section introduces the study site of the research and details the methodologies used to achieve the two objectives of this thesis, as visualized in figure 4.
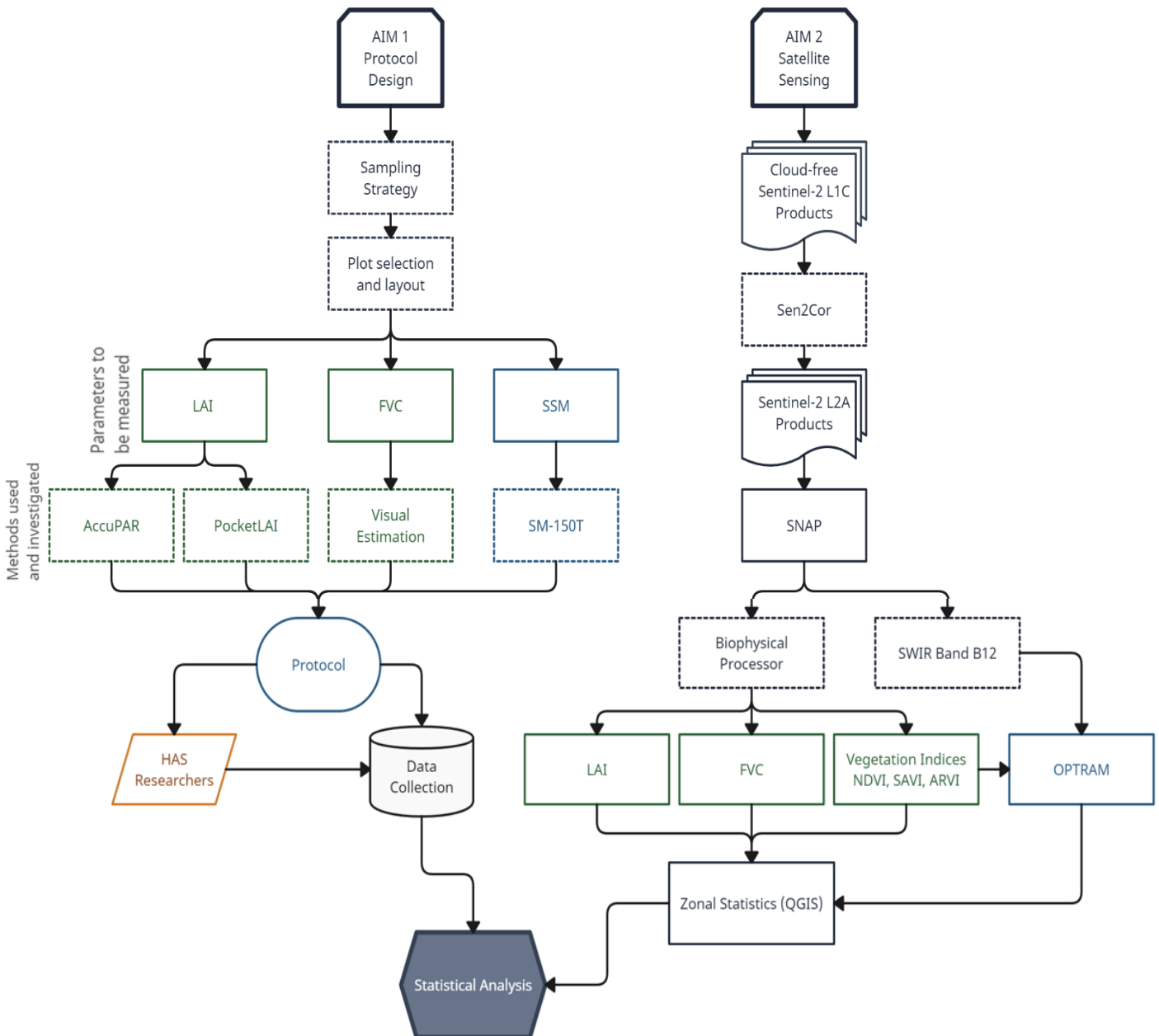
Figure 4. Step-by-step flowchart for the methodologies employed in this research. The left branch detailing the process in developing the protocol, ending with the protocol being used to collect data in this thesis as well as by researchers from HAS. The right branch depicting the process used to quantify satellite-derived LAI, FVC, SSM, and the vegetation indices. The outcomes of both branches are then compared by means of statistical analysis.

3.1 Study Site

The study area of this thesis is the Karnali floodplain and its surroundings on the western portion of Bardiya National Park (BNP; figure 5), an important protected area designated under IUCN category II, and one of the largest national parks within the TAL in Nepal. BNP was first established in 1976 and currently has a core zone area of 986km^2 that is surrounded by a buffer zone of 507km^2. BNP was chosen as the case study for this thesis as it has been documented to have undergone the disturbances affecting grasslands detailed in the introduction and forms a vital 'living lab' in the context of the Tiger Project. Fluvial disturbances are of particular importance in BNP as a result of the changes experienced by the Karnali River, the most notable being the shift in its dominant discharge channel from the BNP-bordering Geruwa branch to the western Kauriala branch after the monsoon season of 2009 (Sinclair et al., 2017; see figure 5 for context). This combined with gravel mining and the irrigation schemes being proposed in the Karnali, upstream from Bardiya, will result in further reduced discharges along the western boundary of the park (Geruwa) and therefore potentially reduce groundwater heads near the Karnali floodplain (Berghuis, 2019; Bijlmakers 2020). Furthermore, the Karnali river is the only snow-fed river in BNP and climate impacts on the Himalaya may exacerbate these decreases in discharge and groundwater levels (Shrestha et al., 2018).

The climate of BNP follows a monsoonal pattern with three distinct seasons (Upadhyaya et al., 2018). The monsoon season occurs through June to September. Groundwater is recharged, intermittent and ephemeral streams are activated, and 90% of the Karnali river's discharge is provided as a result of the 1000-1500mm of average rainfall during this season, approximately 80% of the total annual precipitation (DHM, 2017). Winter, or post-monsoon (September-February), is extremely dry with little to no precipitation and is followed by summer, or pre-monsoon (February-July) where temperatures can reach 45°C (Bijlmakers, 2020; Upadhyaya et al., 2018).

The vegetation of the park is dominated by three main habitats: tallgrass floodplain, riverine forests, and Sal forests, which alone accounts for about 70% of the vegetation cover in the park (Wegge & Storaas, 2009; Upadhyaya et al., 2018). The eastern section of the Karnali floodplain, the central region of interest in this thesis (red delineated area in figure 5), can be broadly classed into eight vegetation types as found in Dinerstein (1979a) and in Bijlmakers (2020) (presented later in figure 7).
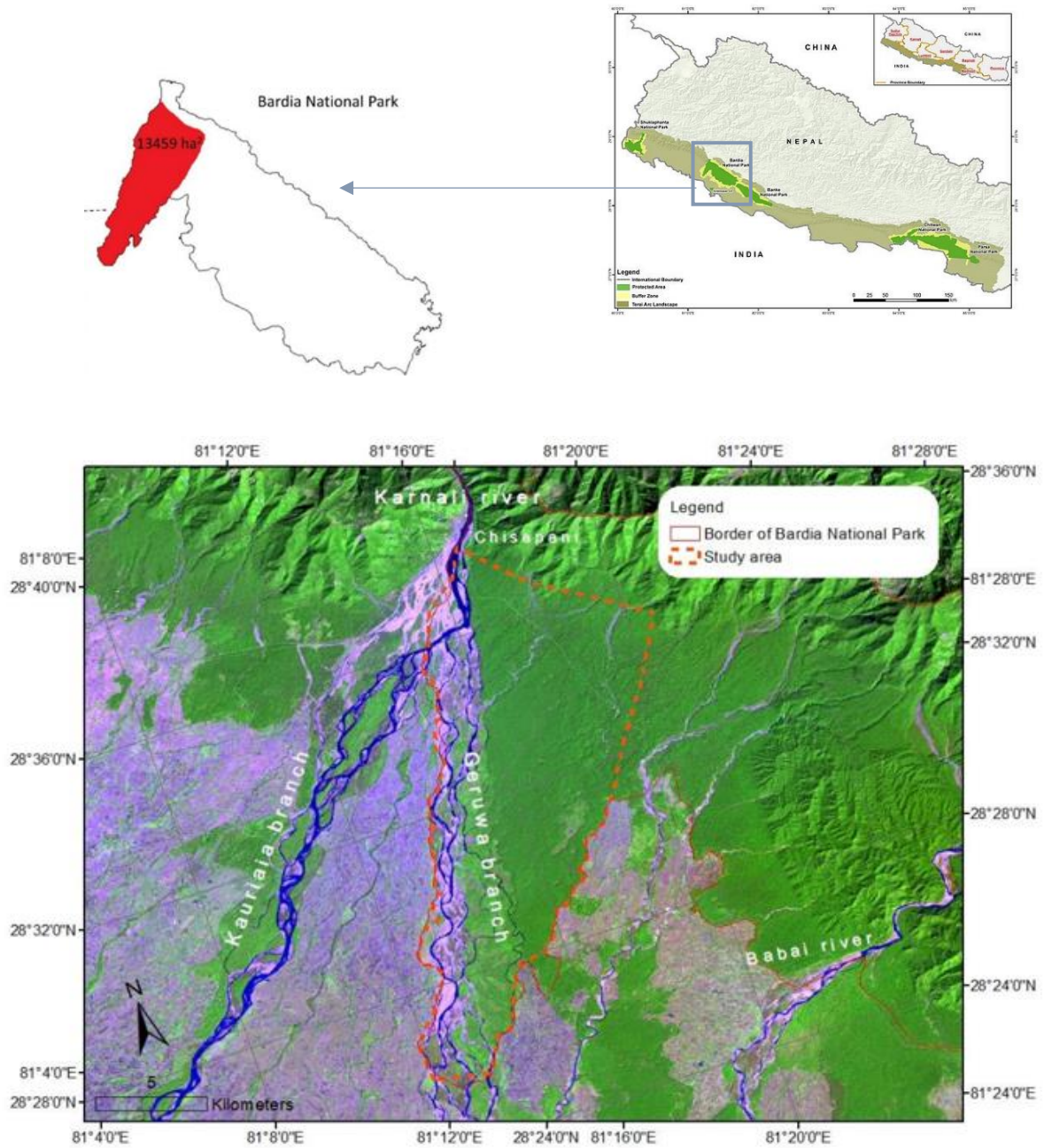
Figure 5. Top: Location of Bardiya within the Terai Arc Landscape (WWF, 2021). Highlighted in red is the Karnali floodplain, the study area for the fieldwork conducted. Bottom: The mega fan of the Karnali river that is located at the western border of BNP (Bijlmakers, 2020). Note western branch of Karnali (Kauriala) and eastern branch that borders BNP (Geruwa).

3.2 Protocol Design

The approach taken for designing the protocol is based upon literature, notably in the medical field, as this is the most documented and rigorous regarding the creation of research protocols. This literature was used as a guide to determine the general design and structure of a protocol and what is considered to be 'good practice' in the developing of a protocol. The primary goal of this protocol is that it is accessible and time efficient. This will ensure that future data collection can be carried out by all people connected with the Tiger Project, with varying backgrounds and skill levels, in a bid to ensure that ground-truth data can be consistently collected over time without the need for extensive training or expensive equipment.

Furthermore, given the nature of the environment, an emphasis was placed on spending as short amount of time as possible at each plot for safety reasons and to have as little impact on the ecosystems as possible. Collecting measurements within a short time with minimal changing conditions will also be beneficial given the sensitivity to light conditions experienced by indirect LAI measurement methods. Figure 6 shows the aspects that guided the structure of the protocol developed in this research, as adapted from Rout and Aldous (2016) and a protocol checklist from Washington University (DEH, 2001).
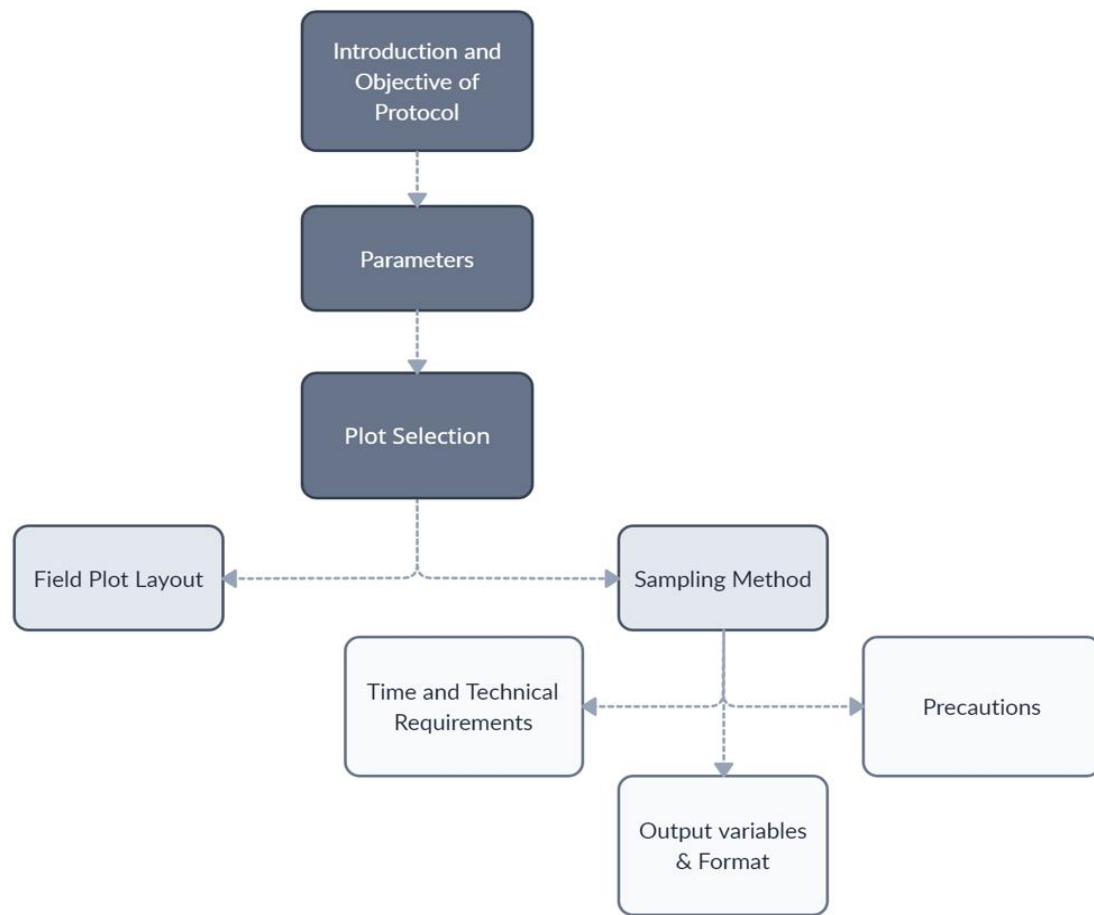
Figure 6. Structure of protocol to be developed. The objective and implications of the protocol are presented before introducing the parameters that will be sampled. In this thesis, these parameters are LAI, FVC, and SSM. A general field plot layout is then presented after a description on the selection of plots. This is all followed by detailed sampling methods for each parameter.

The introductory section of the protocol will follow the design of a vegetation sampling protocol as proposed by Andrade et al. (2019). A brief overall objective of the sampling and consequent implications will be given, including an acknowledgement of the spatio-temporal impacts that guide the study approach for such a sampling objective. Any other aspects that pertain to the sampling of all parameters will also be discussed before moving forward to each parameter. The introduction will then be followed by a section that introduces and defines the parameters to be discussed in the protocol.

In the context of this thesis, these parameters will be LAI, FVC, and SSM. Each parameter will then be described in detail regarding their respective sampling methods as shown in figure 6. The protocol presented in the results section and Appendix A was developed based on the results and experiences of the initial field data collection process.

3.3 Field data collection

This section details the methodologies behind the field observations collected during this research that were used to develop and subsequently implement the sampling protocol.

Sampling Strategy

The fieldwork was undertaken in the post-monsoon season during the months of January and February 2023. The fieldwork was separated into two parts, reflecting the objectives of this thesis. Initial data collection for the development of the protocol was carried out and followed by further data collection using the newly developed protocol to investigate the secondary objective. In total, 30 plots were non-randomly selected to be representative of the three major vegetation classes, Sal forest, riverine forest, and grasslands (short and tall). The locations of the plots were selected based on the vegetation class results of Bijlmakers (2020; figure 7) as well as local knowledge of the different vegetation types.

Each plot size was 30m x 30m, corresponding to the plot size in Bijlmakers (2020). The specific plot locations were heavily determined by safety constraints regarding wildlife, meaning sparser understory for increased visibility. Furthermore, accessibility by vehicle and foot, whilst still ensuring the plots cover a variety of vegetation classes was a driving factor in the location of the plots. 10 of the 30 plots (protocol plots) were selected for the primary objective of developing the protocol. These plots were sampled in two time slots, 10:00-12:15 and 12:15-14:30 (hereafter morning, and afternoon respectively) to determine any potential effect of time. This was to agree with recommendations regarding the use of one of the indirect LAI instruments (AccuPAR LP-80) that measurements should be done within approximately 2 hours of solar noon (Pokovai & Fodor, 2019), roughly 12:15 for the month of field data collection (GeoTimeDate, 2023).

The locations of protocol plots were selected to ensure multiple visits to the same plots could be done with relative ease whilst maximizing the number of plots sampled in a day and were therefore chosen to be in close proximity to the main National Trust for Nature Conservation (NTNC) camp. NTNC is the primary local organisation in collaboration with The Tiger Project aiding in the facilitation of fieldwork in the national parks within the TALA list of the plots including the date and time of sampling and vegetation classification can be found in Appendix B.
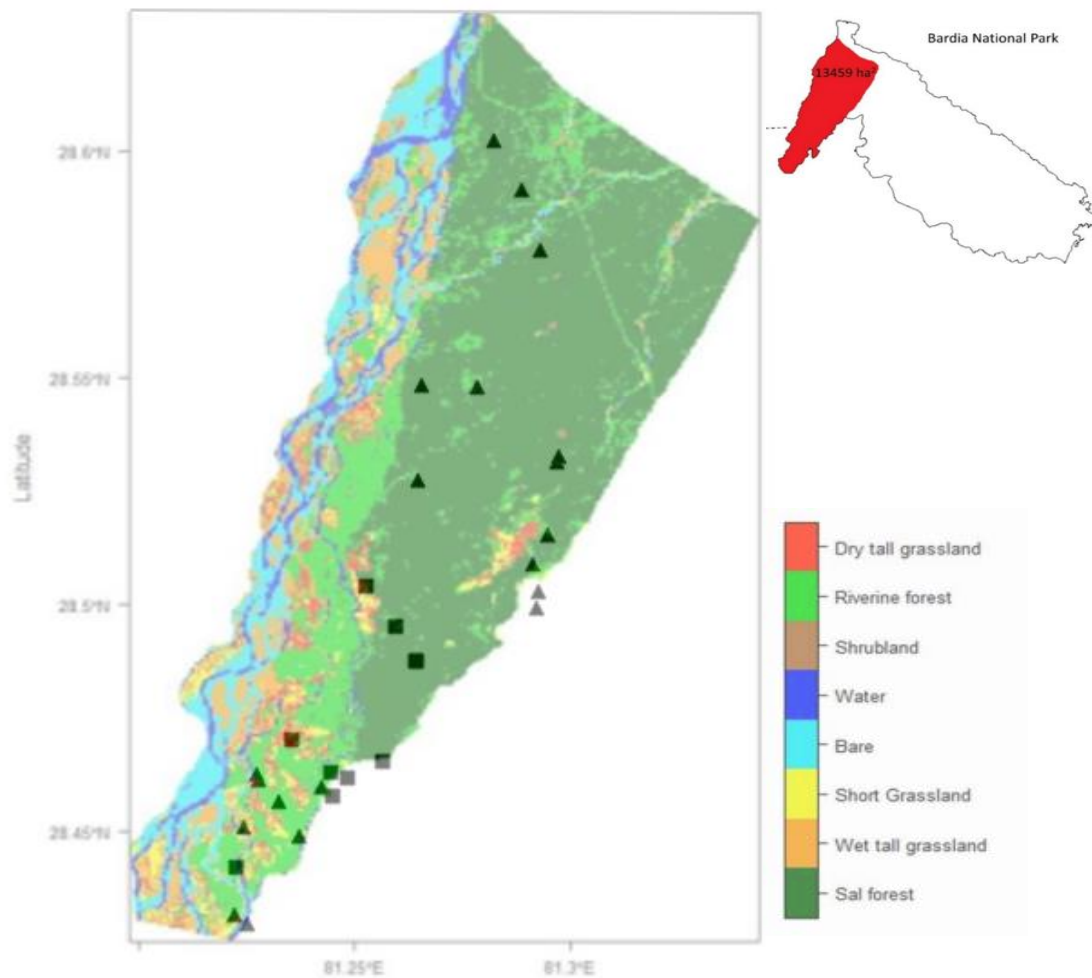
Figure 7. Karnali floodplain field plots analysed in this study. Squares indicate the 10 protocol plots used in the development of the protocol. Triangles indicate the 20 other plots that tested the protocol and were used in combination with the 10 protocol plots for the satellite analysis. Plots overlaid on vegetation class map from Bijlmakers (2020).

The smallest grid spacing selected for plots was 5m, resulting in the plot layout shown in figure 8 for the field data collection for the development of the protocol. All LAI and FVC measurements were separated into canopy and understory measurements to facilitate the distinguishing of potential canopy and understory influences on satellite products.
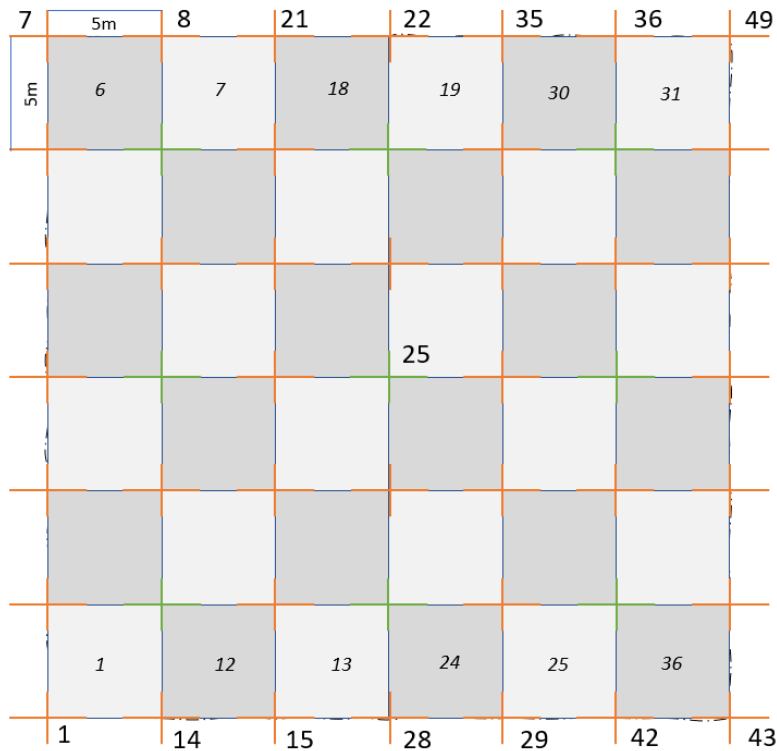
Figure 8. General plot layout for protocol plots. AccuPAR and SSM measurements were taken every 5m (crosses). Gridded squares represent canopy cover for 5m x 5m estimations.

AccuPAR LP-80

The AccuPAR LP-80 ceptometer is a well-established instrument to obtain indirect LAI estimates, designed for use primarily in crop monitoring (Finzel et al., 2012; Decagon, 2016). The AccuPAR uses gap-fraction analysis to provide LAI estimates, a method of measuring LAI that uses light to determine the fraction of unvegetated background from a viewpoint above or below the vegetation being sampled (Bréda, 2003; Finzel et al., 2012). The AccuPAR does this by measuring photosynthetically active radiation (PAR) above and below the canopy of vegetation being sampled (Decagon, 2016). PAR is measured by the 80 linear sensors on its 80cm rod. The AccuPAR's integrated processor then calculates the LAI using a simplified version of the Norman-Jarvis radiation transmission and scattering model (Decagon, 2016):

$$LAI = \frac{\left[\left(1 - \frac{0.5}{\sqrt{x^2 + tan\theta^2}}\right)f_b - 1\right] \times ln\frac{PAR_b}{PAR_a}}{0.9(1 - 0.47f_b)} \qquad (1)$$

Where x is the leaf distribution parameter (the default value of 1 was used as recommended by the manual when no knowledge of the specific leaf angles are known); f_b is the fraction of beam radiation (the ratio of direct beam radiation from the sun to radiation from other ambient sources); PAR_a and PAR_b the above- and below-canopy PAR measurements respectively; θ is

the zenith angle of the sun. The general location (Kathmandu for this study) is input into the AccuPAR which enables the zenith angle to be calculated automatically within the device. The AccuPAR also uses the location provided to determine potential PAR (PAR outside the atmosphere), as well as the PAR measured and outputs f_b values automatically during measurements. The sensors were calibrated each day of sampling according to the manual. Incident f_b, θ, and all PAR values were noted during sampling to manually calculate the LAI to obtain variations within the protocol plots, as the AccuPAR automatically calculates an average LAI and does not display LAI at each point.

Several studies have noted the accuracy of the AccuPAR and other ceptometers to be highly dependent on the sky conditions (Pokovai & Fodor, 2019; Pask & Pietragalla, 2012) and therefore suggest the use of the AccuPAR in forest plots to be accompanied by an external sensor that is placed in an open stand nearby and logs above-canopy PAR every few minutes. An external sensor was not available for this research and therefore, incident above-canopy PAR readings were taken for each plot. Care was taken to ensure these incident readings were taken no further than a 5-minute walk away from the plot to avoid drastic changes in sky conditions between incident reading and plot measurements. Furthermore, if a change in sky condition (such as a cloud passing over) was observed during plot measurements, the incident reading and subsequently, the plot measurements were retaken.

A distinction between canopy and understory LAI was made, where understory LAI includes understory vegetation in addition to canopy influences above the understory vegetation being measured, and canopy LAI is an estimate of only the canopy LAI. Canopy measurements were taken holding the device level at 1.5m ensuring that there was no influence of understory vegetation on the light sensors. Isolated instances where below-canopy PAR readings exceeded above-canopy PAR, resulting in a negative LAI estimate, were excluded from analyses.

The grid spacing shown in figure 8 was used for the canopy LAI AccuPAR measurements with each cross representing a point of measurement resulting in 49 data points at each plot. These readings are expected to vary spatially and therefore, the maximum number of sampling points for the selected grid size (5m) was chosen as the starting point to account for spatial heterogeneity within the plots (Hyer & Goetz, 2004). Furthermore, given the sensitivity to light penetration and canopy structure, two perpendicular readings at each point (98 total readings), in the same directional layout as shown by the crosses in figure 8, were also taken

for further investigation. Plot canopy LAI estimates were then obtained by averaging the point measurements.

A 10m x 10m grid (16 points, figure 9) was investigated to determine whether less points at each plot, taking less time, will provide similar canopy LAI estimations to the 49 points. This was done for the measurements taken at the protocol plots.
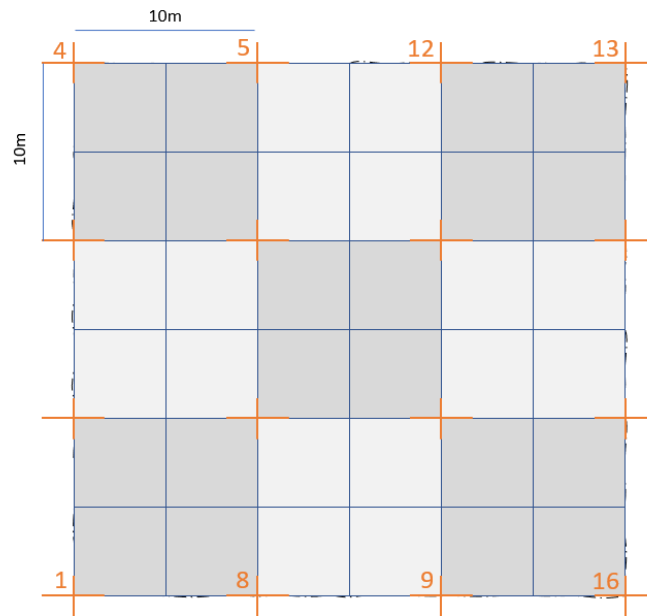
Figure 9. 10m x 10m grid for reduced number of AccuPAR sampling points.

Understory LAI measurements were done on a subjective analysis of the understory present. This was as a result of many plots having sparsely distributed understory vegetation that were often not captured in 5m grids in the same manner as the canopy. This was observed during the protocol development phase with most understory LAI measurements in a grid manner primarily capturing only the canopy, excluding important clumps of understory vegetation. Therefore, a subjective sampling scheme consisting of 16 points was investigated. The AccuPAR was held 0-20cm above the ground with the vegetation of interest covering the entirety of the light bar. For smaller vegetation where 80cm was too long, sensors were deactivated on the AccuPAR, thus reducing the effective length of the light bar to a suitable length for the vegetation. Care was taken to ensure representative sampling of understory vegetation types was sampled (when present) as well as for light conditions (sun rays penetrating through the canopy). The averaged understory LAI (which inherently includes the canopy above the point measurement) was then used in combination with the understory vegetation cover estimates (described shortly), as well as the averaged canopy LAI to provide a total plot LAI estimate using the proposed equation:

$$Plot\ LAI = LAIu * UC + (1 - UC) * LAIc \tag{2}$$

Where LAI_u and LAI_c are the averaged LAI measurements for the understory and canopy respectively and UC is the percentage of ground cover by understory vegetation.

PocketLAI

The PocketLAI is a smartphone-based application for indirect LAI estimates developed by Confalonieri et al. (2013) as an alternative to higher cost indirect instruments such as the AccuPAR. The PocketLAI uses the smartphone's accelerometer and camera to automatically take images from below the canopy at a view-angle of 57.5° as the user rotates the smartphone along its main axis (figure 10). This angle is used as it allows the light transmission model employed by the application to be independent of leaf angle distribution (Warren-Wilson, 1963; Orlando et al., 2015). Images are then processed with an automatic segmentation algorithm to derive the gap fraction and subsequently the LAI (Orlando et al., 2015).

The sampling scheme for the PocketLAI was based on the sampling scheme proposed in Orlando et al. (2015) for a continuous canopy. However, this methodology did not include distances between trees or plot size, and therefore three methods are developed and investigated in this thesis for heterogenous canopies. Upon visual inspection, it was found that for canopy measurements (plant height>1.5m), the PocketLAI had a frontward horizontal distance field-of-view of approximately 30m (the plot size), and sideward horizontal distance of approximately 15m when held at ~1.8m. Therefore, plot center measurements were taken as according to Orlando et al. (2015), plot border measurements were taken at spacings of 15m along the border of the plot, and an average of these two methods was also calculated. These will be referred to the 'center', 'border', and 'average' methods respectively. As recommended by Confalonieri et al. (2013), a minimum of four photos were taken at every measurement, with their averages being calculated within the application to provide the point measurements at each point. These were later averaged to provide plot canopy LAI for each method. The proposed scheme can be found in figure 10.
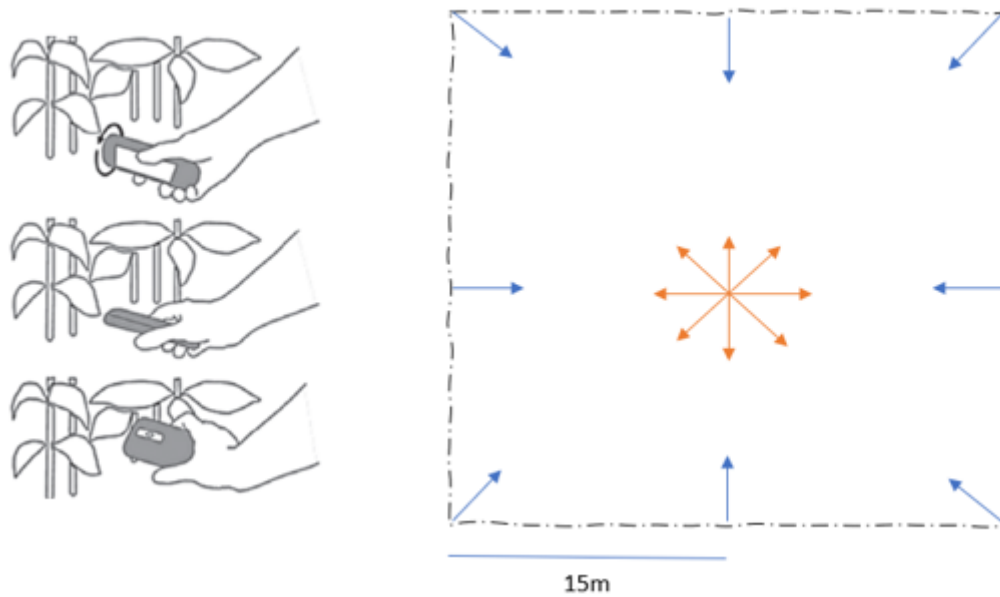
Figure 10. Left: The manner in which to rotate the device starting from its longitudinal axis and rotating slowly upwards (Orlando et al., 2015). Right: PocketLAI sampling scheme. The border measurements are represented by the blue arrows, and the centre measurements by the orange arrows.

The different methods (border, centre, and the average between the two) were investigated further with the data from all the plots during the testing of the protocol, in addition to being analysed for the 10 protocol plots, to gain a more detailed understanding using more data points to determine which method is more reliable in comparison to the AccuPAR LAI results. The same process as for the AccuPAR was used for understory measurements and subsequently total plot LAI estimates. For these understory measurements, the device was held no closer than 20cm to the stem of the vegetation and ~10cm from the ground.

Fractional Cover

Fractional cover was visually estimated within the plots using 5m x 5m grids (Smith et al., 1990). 10m x 10m grids were also investigated to determine whether 9 estimations would be able to describe the plot with similar results to 36 estimations and thus, once more shortening the time needed at each plot. This was carried out independently by two researchers and later compared to avoid bias. Intervals of 5% were used to estimate the fraction of vegetation that essentially obstructed the sky (canopy estimation) or ground (understory). All points were averaged to obtain canopy and understory vegetation cover for each plot.

SM150T

SM150T uses the principle of capacitance on an operating frequency of 100MHz to calculate the soil water content with a measurement error of 3% ($\pm 0.03 m^3 m^{-3}$) (Delta-T Devices, 2016). To obtain surface soil moisture data, the sensor, consisting of two metal rods with a length of 5.1cm, separated by 2.2cm, was gently inserted into the ground at the same 49 locations as the AccuPAR measurements (crosses shown in figure 8). The points of measurements were cleared of any vegetation to ensure the probe was fully inserted to maximise the rods' depth into the soil, taking care not to compact or disturb the topsoil where possible. Further care was taken to avoid rocks or impenetrable ground to prevent damage to the probe.

Additionally, a 9-point grid (figure 11) was investigated to determine whether less points would provide similar plot SSM estimates as the full 49-point grid. This grid was chosen with the idea that each point would provide SSM estimates on a 10m x 10m grid basis and averaged for a plot estimate. Additionally, the location of these point measurements would be different to that of the reduced AccuPAR grid (figure 9) and thus minimise soil disturbance from researchers recording AccuPAR data.
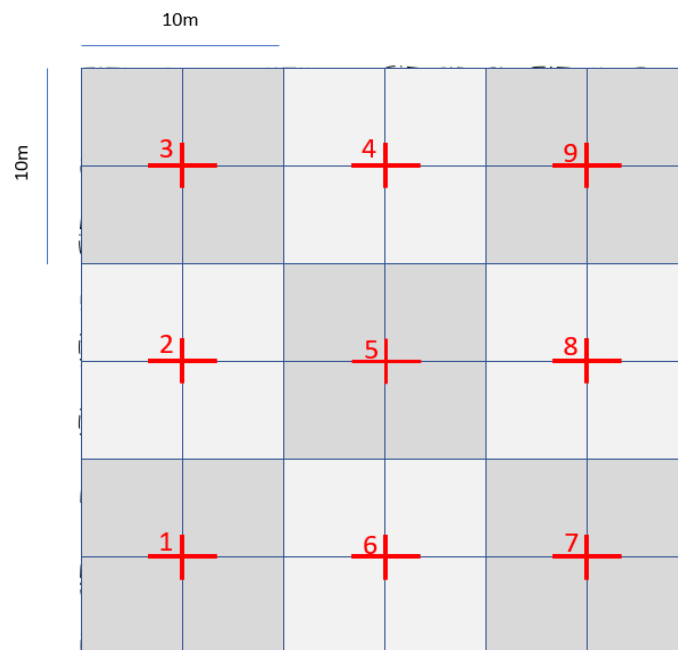
Figure 11. 9-point grid proposed for reduced number of surface soil measurements.

Vegetation Classification

Vegetation classification was carried out for plot descriptions in an attempt to implement the protocol across a range of vegetation types. Whilst not being a specific goal or aim of this thesis, describing vegetation types may be beneficial for future research investigating vegetation changes as well as for additional research within The Tiger Project. This study described vegetation classes based on the classes presented in Bijlmakers (2020; figure 7) with the help of local experts.

3.3.1 HAS Field Data

The protocol developed upon analysing the initial 10 protocol plots, as presented in the results section, was handed over to three researchers from HAS Applied Sciences University. Canopy LAI data using the AccuPAR and PocketLAI, as well as SSM data was obtained using this protocol in the same study area (Karnali floodplain) as well as another area within BNP, the Babai Valley to the east of the study area. The canopy LAI data was also obtained for two other major protected areas within the TAL, Chitwan National Park (CNP) and Shuklaphanta National Park (SNP) to the east and west of BNP respectively (refer to figure 1 for context).

Only the data that was comparable to methods used in this thesis was included in analysis. Therefore, only plot sizes of 30m x 30m that were sampled within two hours of solar noon were selected. Furthermore, only plots that had available corresponding cloud-free satellite images were used. This fieldwork was conducted during the months of March and April 2023 and the location, date and time of sampling, and vegetation classification of these plots can be found in Appendix B.

3.4 Satellite Data

SNAP-Derived Products

Sentinel-2 MultiSpectral Imager images consisting of 13 bands (table 1) were downloaded from the ESA Copernicus Open Access Hub (https://scihub.copernicus.eu/dhus).

Table 1. Spectral and spatial resolution of the Sentinel-2 MSI bands (Somvanshi & Kumari, 2020).

Sentinel-2 MSI Bands	Spatial Resolution (m)	Central Wavelength (nm)
Band 1: Coastal Aerosol	60	443
Band 2: Blue	10	490
Band 3: Green	10	560
Band 4: Red	10	665
Band 5: Red-edge 1	20	705
Band 6: Red-edge 2	20	740
Band 7: Red-edge 3	20	783
Band 8: NIR	10	842
Band 8a: NIR narrow	20	865
Band 9: Water vapour	60	945
Band 10: SWIR Cirrus	60	1375
Band 11: SWIR	20	1610
Band 12: SWIR	20	2190

Sentinel-2A or B level-1C products that were sensed within at least five days of the ground measurements were downloaded for the tile T44RNS. The products used for each plot can be found in Appendix B. To attain level-2A products, the Sen2Cor application (v2.11.0) (https://step.esa.int/main/snap-supported-plugins/sen2cor/) was used on each product to atmospherically correct the top-of-atmosphere (TOA) reflectance, providing bottom-of-atmosphere (BOA) products from the original Level-1C products. This was done by running the L2A_Process.bat file on each of the products.

The Level-2A products were then loaded in the SeNtinel Applications Platform (SNAP) by opening the respective MTD_MSIL2A.xml files. Subsets of the original tile (N: 28.66 W: 81.21 S: 28.43 E: 81.33) were created to focus only on the study area itself. In order to run the Biophysical Processor within SNAP that outputs LAI, FVC, and the Vegetation Radiometric Indices (NDVI, SAVI, and ARVI), all bands need to be at equal resolutions. Using the raster

tool, the products were resampled to 20m using the band B5 as a reference, and the nearest neighbour method and mean method for upsampling and downsampling respectively.

The S2 Biophysical Processor, that employs radiative transfer models (RTMs) for its calculations, was then run to output LAI and FVC. The following bands are used by the Biophysical Processor, B3, B4, B5, B6, B7, B8A, B11, B12, as well as the viewing zenith, solar zenith, and relative azimuth angles (Kganyago et al., 2020; Weiss & Baret, 2016). Equations 3-5 are used within SNAP to output the vegetation indices.

$$NDVI = \frac{NIR-Red}{NIR+Red} \qquad \text{(Tucker, 1979)} \qquad (3)$$

$$SAVI = \frac{NIR-Red}{NIR+Red+0.5} \times (1.5) \qquad \text{(Huete, 1988)} \qquad (4)$$

$$ARVI = \frac{NIR-(Red-(Blue-Red))}{NIR+(Red-(Blue-Red))} \qquad \text{(Tanre \& Kaufman, 1992)} \qquad (5)$$

Where NIR is band 8, Red is band 4, and Blue is Band 2.

The final processed products were then outputted as GeoTIFF images for easier processing in QGIS. The same methods as detailed above were carried out to obtain the satellite products for the HAS data. Tiles T44RMT and T45RTL were downloaded for SNP and CNP respectively and the products used for this analysis can be found in Appendix B.

Optical Trapezoid Model (OPTRAM)

The OPTRAM method was proposed by Sadeghi et al. (2017) based on the linear physical relationship between soil moisture and shortwave infrared transformed reflectance (SWIR) and therefore the assumption that STR (the SWIR transformed reflectance using equation 6) forms a trapezoidal shape when used against NDVI or other similarly derived vegetation indices, as shown in figure 12 (Sadeghi et al., 2017). These relationships result in the development of equation 7 to predict the soil moisture for each pixel in a satellite scene.

$$STR = \frac{(1-SWIR)^2}{2 \times SWIR} ; \quad 0<SWIR<1 \qquad (6)$$

$$SMC = \frac{i_d+s_dNDVI-STR}{i_d-i_w+(s_d-s_w)NDVI} \qquad (7)$$

Where i_d and i_w are the intercepts of the dry and wet edge respectively, and s_d and s_w the slopes of these lines (figure 12). NDVI is used in addition to SAVI and ARVI for this study to determine which vegetation index performs better in the TAL. Band 12 was used for SWIR values. Sadeghi et al. (2017) also notes that the linear relationship from which the model is

developed is only valid for saturated soils and not oversaturated soils (standing surface water) as STR will increase with increased water however, the actual soil moisture cannot increase past its threshold of being fully saturated. Hence, the wet edge will fall below the top line in these instances (figure 12). Therefore, in an attempt to avoid this, surface water pixels were masked in SNAP using the mask 'scl_vegetation' before extracting Band 12. Furthermore, plots with SSM values >1 obtained after application of OPTRAM were excluded. The vegetation indices were plotted against the STR values for the entire respective subset scenes created during the SNAP process as described previously. This was done using the *rasterio* extension in python. The straight lines representing the wet and dry edge were then visually plotted to surround the majority of pixels and the corresponding intercepts and slopes determined.
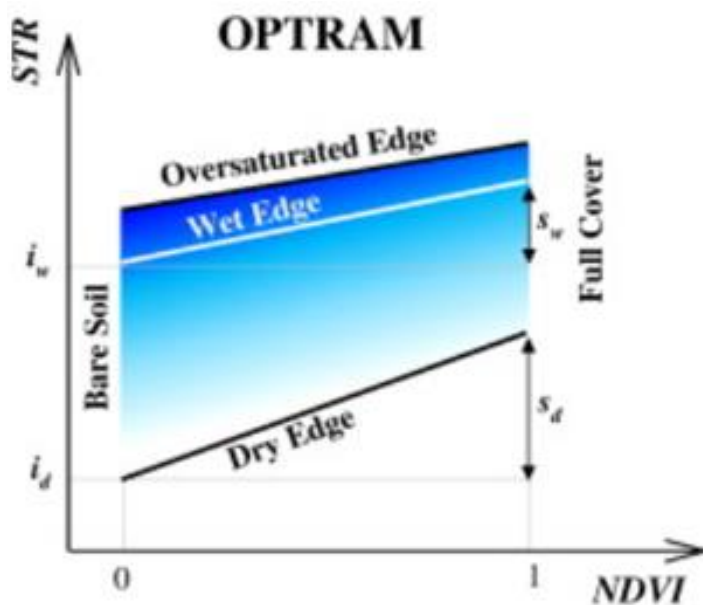
Figure 12. Sketch illustrating the STR-NDVI space and parameters (Sadeghi et al., 2017)

QGIS

The GeoTIFF files exported from SNAP containing the biophysical and vegetation indices data and the B12 bands for each product were imported into QGIS v3.16.14. A layer for the plots was created using the coordinates collected as centre points for squares with a resolution of 30m. The data for each of the extracted bands that fell within the plots was then calculated using the zonal statistics tool, giving the final SNAP-derived LAI, FCover, NDVI, ARVI, and SAVI values. The STR products created during the implementation of OPTRAM were output as GeoTIFFs for the respective scenes, and also imported into QGIS to obtain pixel specific STR values for the plots (using zonal statistics).

3.5 Statistics

Protocol Development

The data was first analysed regarding any potential differences between sampling in the morning (10:00-12:15) and afternoon (12:15-14:30). This was done using a paired t-test and creating boxplots for all comparisons (SSM, AccuPAR LAI, and PocketLAI).

The SSM and AccuPAR LAI data of 49 points at every plot was then compared to the reduced number of points (9 points for SSM and 16 for the AccuPAR). Given that the 9 points and 16 points were taken from the original 49-point sample, a one-sample t-test is used to determine whether the smaller sample sizes differ significantly from the known original sample. Once more, boxplots accompanied these tests for visual comparisons.

Protocol Testing

Descriptive statistics (mean, median, standard deviation) were calculated and presented for the 30 plots of this thesis as well as for the plots sampled by HAS to provide an overview of the data collected by the protocol. These were organized according to vegetation class. Correlation analyses were performed on the different PocketLAI methods and the AccuPAR results to determine the suitable PocketLAI method to be used in further analyses, as well as on the total plot estimates using the understory LAI measurements obtained by the AccuPAR and PocketLAI to determine the PocketLAI's viability as an alternative. Field data was organised with respect to its corresponding satellite products and correlation analyses were performed between the in-situ data and the satellite-derived data.

All correlations were done using a reduced major axis (RMA) regression analysis to account for uncertainties in both axes' measurements. This was done using the pylr2 package in python which outputs the slope and intercept as well as the correlation coefficient r.

Furthermore, R^2 values, root mean squared error (RMSE; 0 to $+\infty$, optimum 0), mean absolute error (MAE; 0 to $+\infty$, optimum 0) (Chai & Draxler, 2014), model efficiency (EF; $-\infty$ to $+1$, optimum $+1$) (Nash & Sutcliffe, 1970), and coefficient of residual mass (CRM; from $-\infty$ to $+\infty$, optimum 0; positive values indicate underestimation and vice versa) (Loague & Green, 1991) were computed for each data comparisons to quantify each relationship investigated. R^2 values were calculated by squaring the r result obtained through the RMA regression.

The following equations were used:

$$MAE = \frac{1}{n}\sum_{i=1}^{n}|P_i - O_i|$$ (9)

$$RMSE = \sqrt{\frac{1}{n}\sum_{i=1}^{n}(P_i - O_i)^2}$$ (10)

$$EF = 1 - \frac{\sum_{i=1}^{n}(O_i - P_i)^2}{\sum_{i=1}^{n}(O_i - \bar{O}_i)^2}$$ (11)

$$CRM = \frac{\sum_{i=1}^{n}(O_i - P_i)}{\sum_{i=1}^{n}O_i}$$ (12)

All analyses were initially performed on the data obtained from the fieldwork conducted for this study before including the additional data from HAS. A further distinction between the data from the Karnali floodplain and the other areas in the TAL (collected by HAS) was made to determine whether the protocol as developed within the Karnali in BNP, is applicable in other regions of the TAL.

4. Results

The following section presents a shortened version of the final protocol, followed by an overview of the data and values collected at each of the plots using the protocol. The secondary objective is then explored consisting of the validation of satellite-derived data using the ground-truth data obtained by using the protocol.

4.1 Protocol

The final protocol was a result of the findings and analysis of the protocol development phase that are presented in Appendix C, as well as experience gained whilst taking measurements at the protocol plots. Only the field plot layout and general sampling strategy is presented from the final protocol in this section to avoid repetition with the details for each sampling method as already described in the *Materials and Methods* section. This shortened protocol, including the relevant information as described in *Materials and Methods* with a brief in-person demonstration of the sampling methods, was given to the HAS researchers to be able to implement the protocol for their data collection. The full protocol including all elements mentioned in *Material and Methods* (introduction, implications, sampling objectives, parameter definitions, and the step-by-step guide for sampling methods; figure 6) can be found in Appendix A.

The field plot shown in figure 13 is suggested for the sampling of LAI using the AccuPAR-LP80 and PocketLAI, FVC for understory and canopy through visual estimation, and SSM using the SM-150T. Point measurements should be numbered in a snake pattern (as indicated) starting in a south-north direction as this will help comparability between potential repeat samplings.

The plot borders and, if possible, 5m transects, should be marked using a rope or similar whilst sampling to ensure point measurements are consistent in their locations. This will also considerably speed up the sampling process. The coordinates of the centre point and the four corners of the plot should be taken.

Field Plot Layout
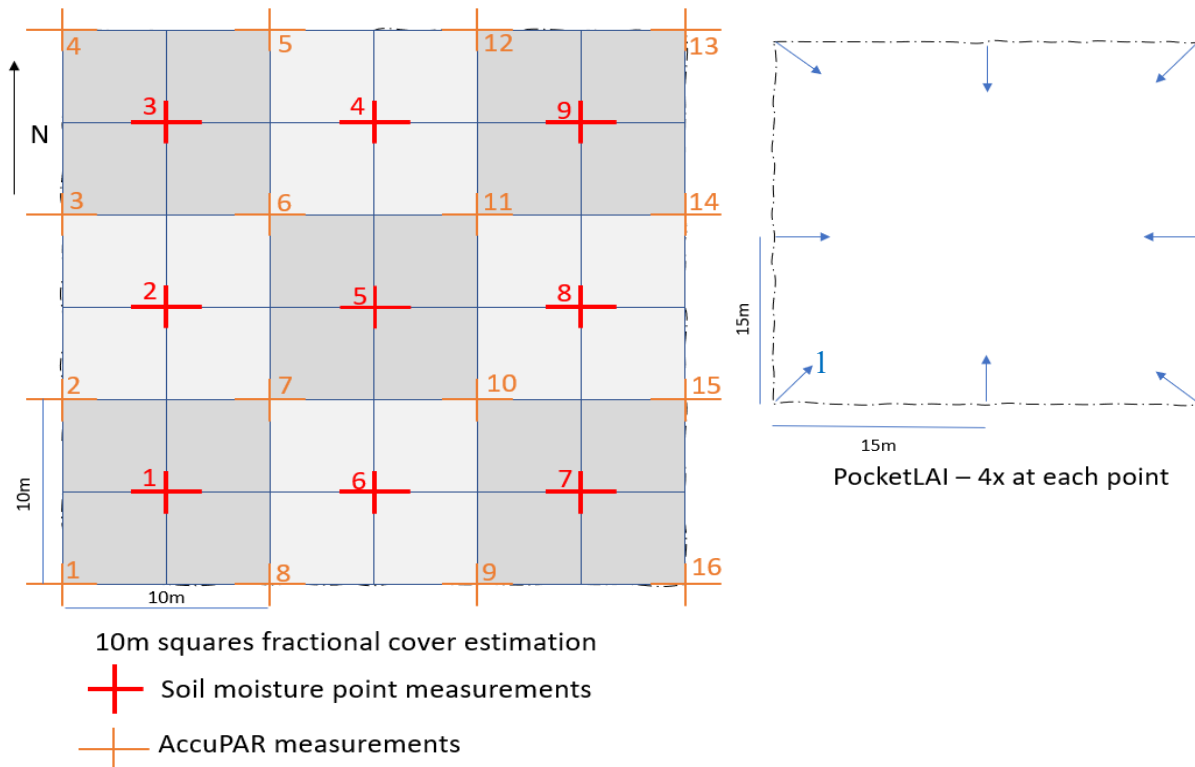
Figure 13. Field plot layout for the sampling of LAI, FVC, and SSM.

Sampling Strategy

Plots must be sampled within 2 hours of solar noon ideally sampling as close to solar noon as possible, particularly in winter when beam radiation is generally lower than in summer. Sampling should take place in clear sky conditions, especially when using the AccuPAR, however if this is not possible the sky conditions should be observed and described, and f_b and PAR readings should be noted. The dominant vegetation class (forest, grassland) of the plot should be observed and if possible, further classification (Sal forest, riverine forest, short grasslands, tall grasslands) as well as dominant vegetation species can be noted as this will enable further detailed analysis if desired and can potentially contribute to other investigations within the Tiger Project. Canopy vegetation is regarded as vegetation with a height >1.5m. For all LAI measurements using both the AccuPAR and PocketLAI, try to avoid woody elements that may obstruct the camera (PocketLAI) or incoming light and sunrays (AccuPAR).

Other general remarks regarding observations of any other details regarding external (e.g., wind, weather) or plot-specific aspects (e.g., burnt or cut vegetation) are recommended. All data should be stored electronically and uploaded or sent to the relevant database or researchers responsible for data treatment.

Sampling Methods

All general sampling methods are as described in the *Materials and Methods* section of this thesis. For a full step-by-step guide, see the final protocol in Appendix A.

4.1.1 Data Collected

Data from the fieldwork conducted for this thesis in the Karnali was obtained from a total of 30 plots consisting of 10 grassland plots, 10 Sal forest plots, 8 riverine forest plots, and 2 'mixed' forest plots. The mixed forest plots were plots that were situated where the change of two major vegetation classes occurred, resulting in species from both classes being present. Canopy LAI was taken in all forest plots and 3 of the grassland plots, understory LAI was taken in all plots apart from 2 Sal forest plots as no understory was present. Both understory and canopy vegetation cover, as well as SSM was obtained for all plots.

HAS obtained data for 34 additional forest plots consisting of 17 Sal forest plots, 10 riverine, 2 mixed, and 5 general forest plots, where the sub-class was not defined. 6 plots were located in the Karnali – the study area of this thesis, 7 plots were located in another region of BNP, the Babai Valley, 13 in SNP, and the remaining 8 in CNP. Canopy LAI data was obtained for all plots with SSM data obtained only for 12 of the plots in BNP. No FVC or understory LAI was obtained using the protocol. Figure 14 visualizes the types of vegetation classes sampled across the fieldwork of this thesis and HAS.
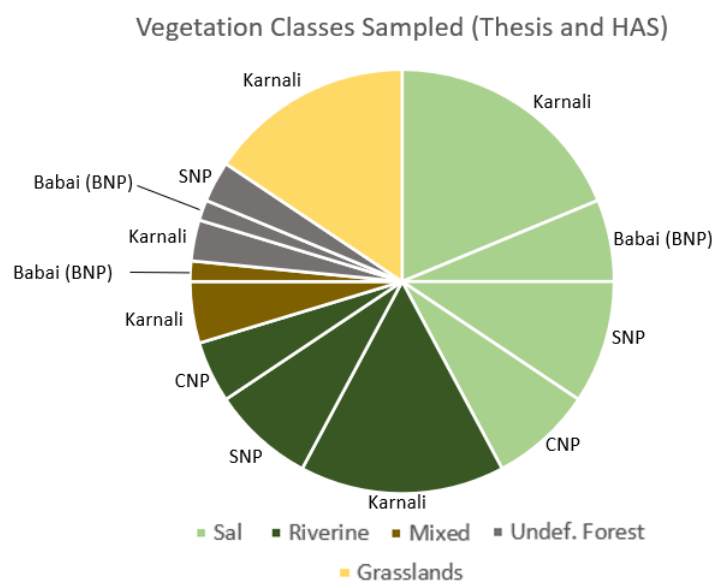
Figure 14. Types of vegetation classes, including the region, on which the protocol was used.

The following boxplots present the range of values obtained at each plot for canopy LAI, FVC, and SSM, separated by forests and grasslands (figures 15-17) and then further into specifically Sal forests and riverine forests (figures 18-20). Data obtained at the plots of this thesis and that obtained by HAS is also distinguished. Additional results presenting canopy LAI obtained by the PocketLAI and total plot LAI can be found in Appendix C.
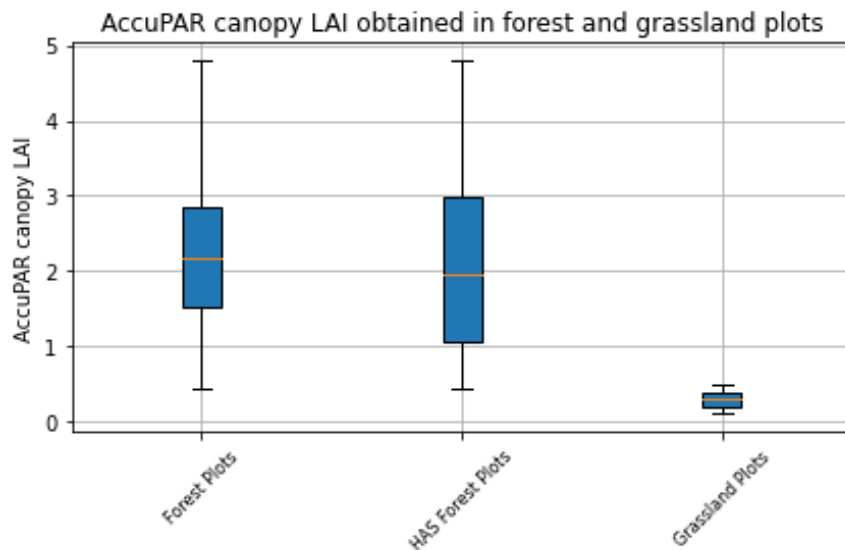
Figure 15. Canopy LAI values recorded with the AccuPAR at forest and grassland plots.

Forest canopy LAI data is comparable between the results of this thesis and that obtained by HAS with the ranges of the LAI obtained overlapping greatly as is seen in figure 15. There is a distinct difference as expected, between grassland plots and forest plots.
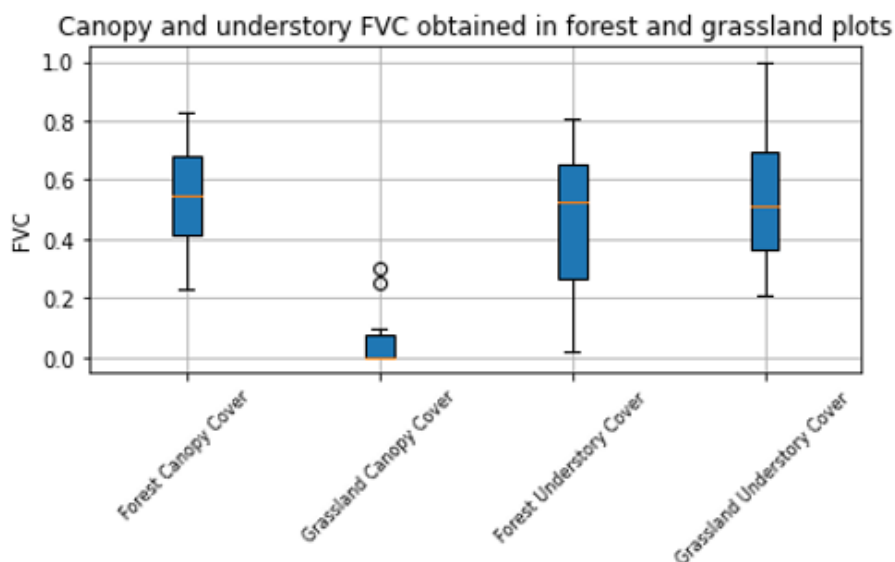
Figure 16. Canopy and understory FVC at forest and grassland thesis plots.

Figure 16 depicts a distinct difference between forest and grassland canopy values. There is overlap in the range for understory vegetation cover between grasslands and forests, with forest plots generally having less understory vegetation cover.
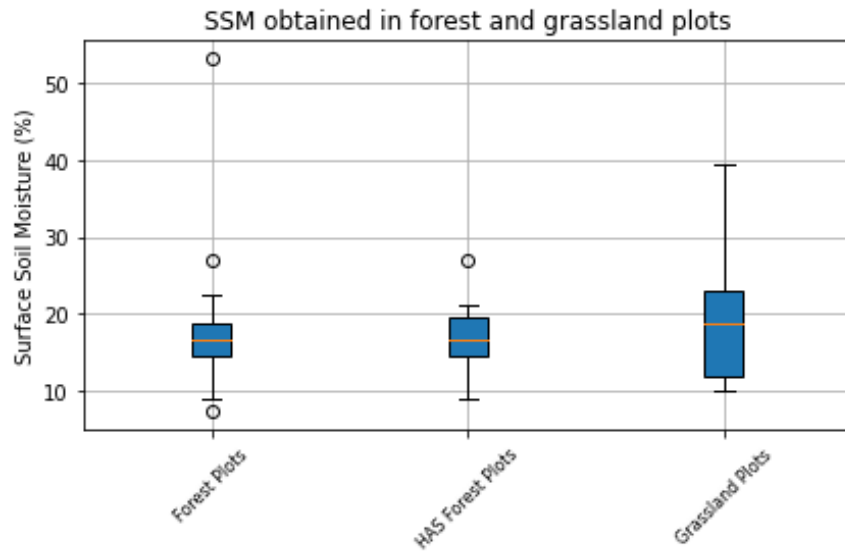
Figure 17. SSM obtained at forest and grassland plots.

The SSM values obtained in this thesis are comparable with those obtained by HAS for forest plots as shown in figure 17. SSM values obtained in grassland plots show a larger range that appears to be marginally higher than the range of SSM values for forest plots.
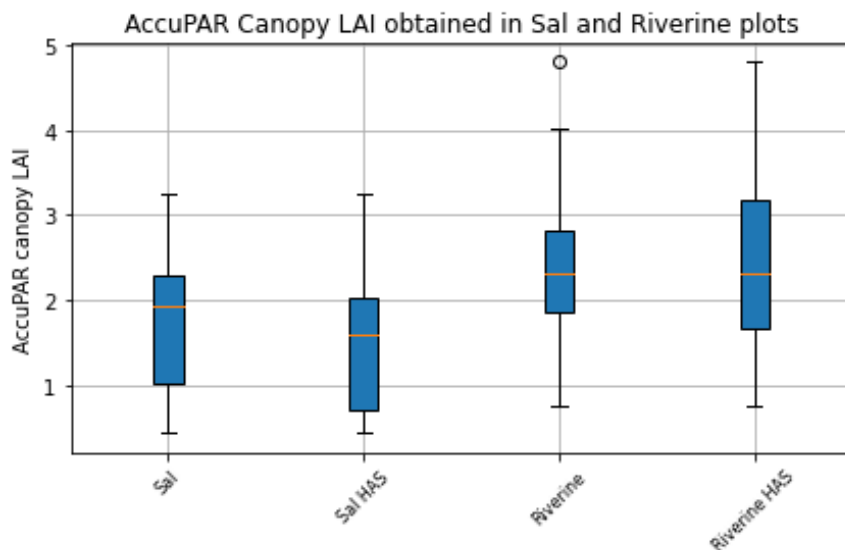
Figure 18. Canopy LAI values recorded with the AccuPAR at Sal forest and riverine forest plots.

When distinguishing forest plots further by Sal forests and riverine forests, it is evident that riverine plots on average show higher LAI values than Sal plots as seen in figure 18. Once

more, data obtained by HAS show similar ranges for both forest types to the data obtained in this thesis.
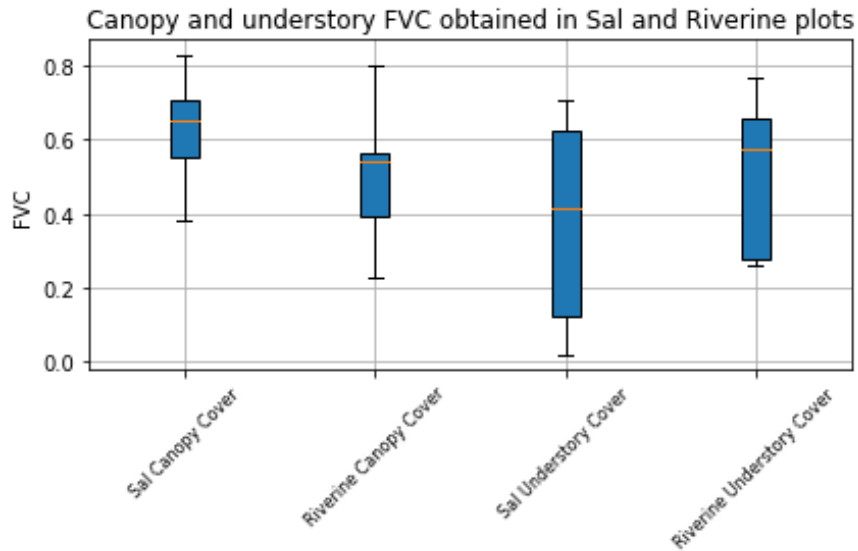
Figure 19. Canopy and understory FVC at Sal forest and riverine forests plots

Figure 19 shows a general pattern where larger canopy cover tends to result in lower understory cover, and vice versa. Differences in the ranges of FVC between Sal forests and riverine forests are evident for both canopy and understory cover.
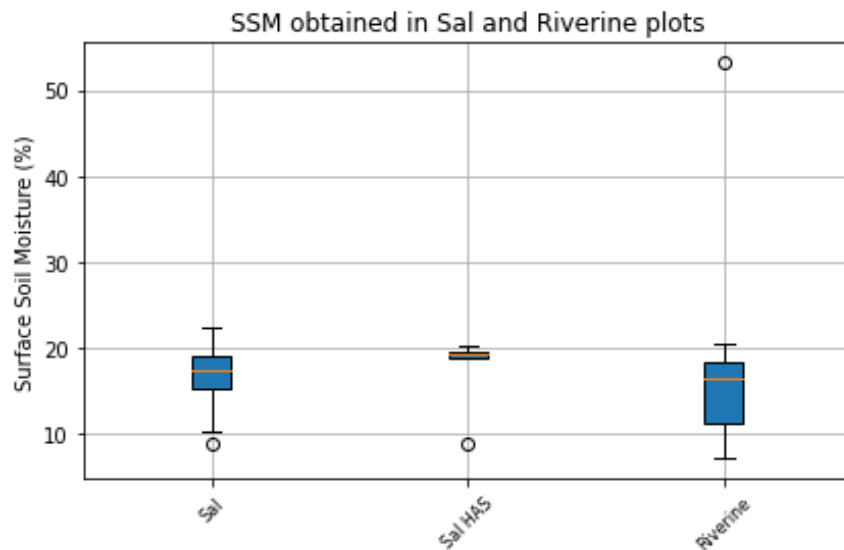
Figure 20. SSM obtained at forest and grassland plots.

The range of SSM in Sal forest plots is considerably smaller for the values obtained by HAS as can be seen in figure 20. The values are, however, still comparable in magnitude with those obtained at the thesis plots. Riverine plots tended to have marginally lower SSM than Sal forest plots, with the exception of an outlier above 50%.

4.2 Protocol Testing

This section, primarily addressing objective 2 regarding satellite-sensing potential, will be organized according to the parameters investigated. All values used in the analyses including the satellite-derived values can be found in Appendix B.

4.2.1 Leaf Area Index

The relationship between the PocketLAI and AccuPAR is first presented in figure 21 with a comparison between total plot LAI estimates for the plots studied in this thesis (using equation 2). This is followed by a comparison between the canopy LAI estimates obtained by the PocketLAI and AccuPAR, including the results from HAS, before the results obtained from these devices are related to the satellite products.
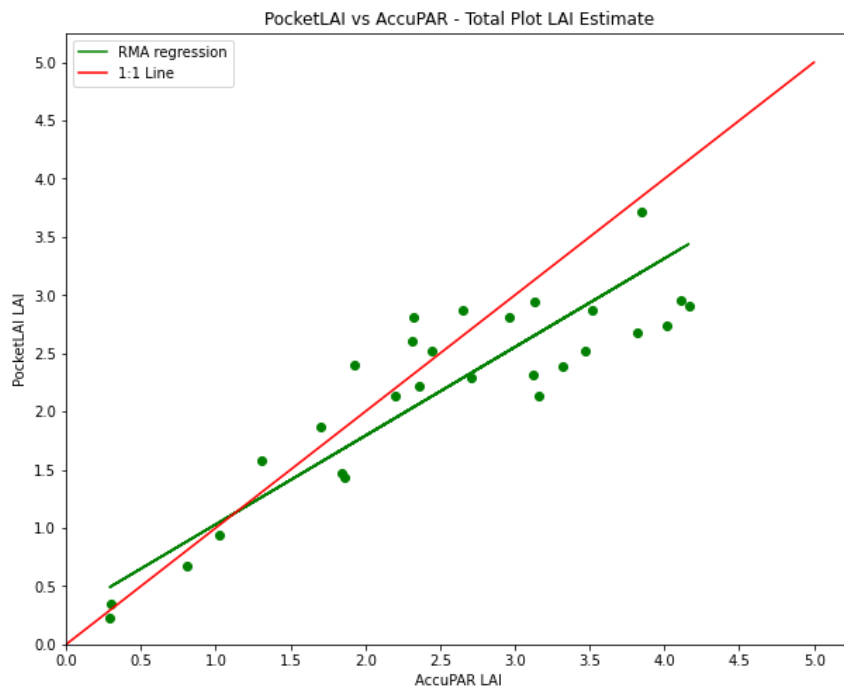
Figure 21. Relationship between PocketLAI and AccuPAR for total plot LAI estimates using equation 2.

Table 2. Statistical results from analysis comparing PocketLAI and AccuPAR for total plot estimates.

	n	MAE	RMSE	CRM	EF	R2	p-value
Karnali floodplain (thesis plots)	28	0.48	0.63	2.64	0.67	0.78	0.00

There is a good agreement between PocketLAI and AccuPAR total plot LAI estimates as shown with a high R^2 value of 0.78 and EF value of 0.67 (table 2). Upon inspecting figure 21, a slight saturation is apparent for AccuPAR LAI >2.5, however the RMA regression still shows

closeness to the ideal 1:1 relationship. As a result of this saturation, the PocketLAI tends to underestimate the LAI (CRM > 0).
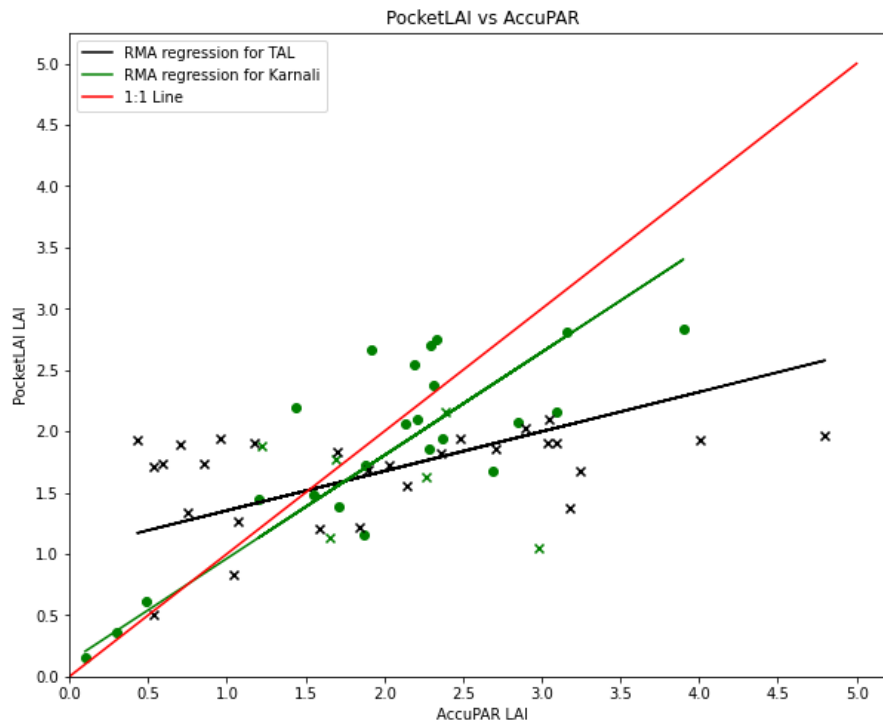
Figure 22. Relationship between PocketLAI and AccuPAR. Crosses represent values obtained by HAS researchers, with dots representing the values obtained in the fieldwork of this thesis.

Table 3. Statistical results from analysis comparing PocketLAI and AccuPAR canopy LAI.

	n	MAE	RMSE	CRM	EF	R2	p-value
Karnali floodplain (thesis plots)	23	0.42	0.53	−0.24	0.64	0.67	0.00
Karnali floodplain (thesis + HAS)	29	0.47	0.63	0.51	0.43	0.51	0.00
TAL (Babai, SNP, CNP; HAS)	28	0.90	1.10	−7.44	0.10	0.15	0.04
Combined	57	0.68	0.89	−6.93	0.21	0.27	0.00

The difference between the two RMA regressions (Karnali and TAL) and the ideal 1:1 relationship is immediately evident upon inspection of figure 22, with data obtained in the Karnali performing better. The RMA regression for the TAL data is further shown to not be a good description of the data with a low R^2 value of 0.15 (table 3; p-value = 0.04). The EF value for the thesis data (0.64) indicates that the PocketLAI sufficiently captures canopy LAI when compared to the AccuPAR, however for the rest of the data this value falls below 0.5 (0.21 for all the plots combined) indicating that the PocketLAI does not tend to capture comparable LAI values to the AccuPAR throughout the TAL. Overall, the PocketLAI tends to overestimate LAI (CRM = -6.93), particularly in the lower LAI ranges of the AccuPAR. Once more, there appears

to be a slight saturation of PocketLAI values for AccuPAR LAI > 2. Furthermore, LAI obtained with the PocketLAI by HAS (crosses in figure 22) is generally saturated between 1.5 and 2.0 regardless of the ranges shown in the AccuPAR, impacting the statistical results.
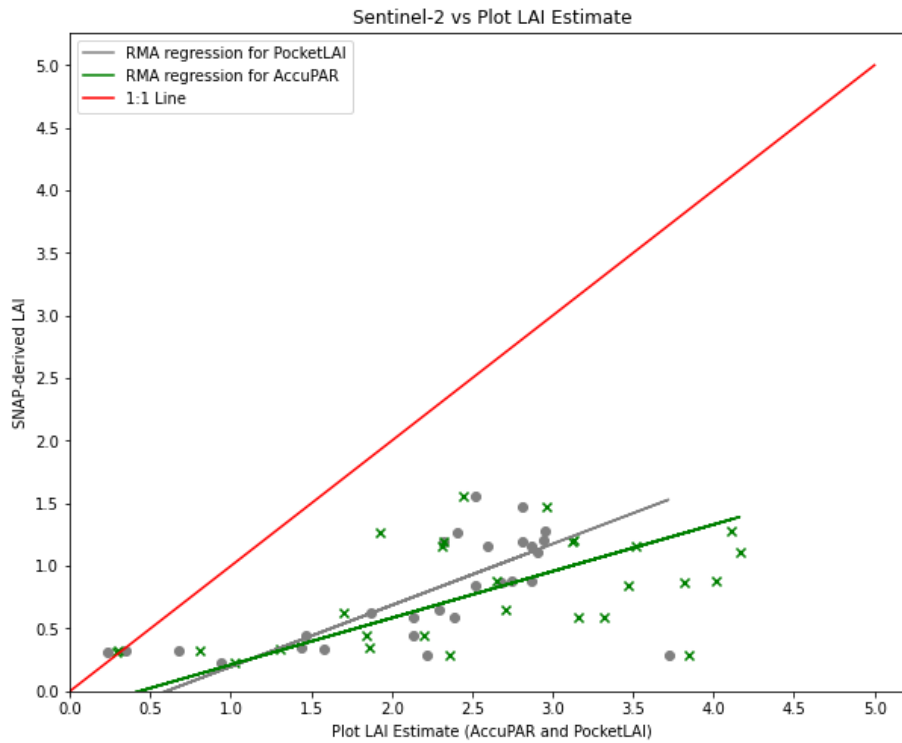
Figure 23. Relationship between SNAP-derived LAI and plot LAI estimates using equation 2.

Table 4. Statistical results from analysis comparing SNAP-derived LAI with plot LAI estimates using equation 2.

		n	MAE	RMSE	CRM	EF	R2	p-value
Karnali floodplain	AccuPAR	28	1.75	1.99	17.68	-2.3	0.27	0.01
(thesis plots)	PocketLAI	28	1.42	1.56	16.72	-2.51	0.38	0.00

Figure 23 shows the relationship between SNAP-derived LAI and the total plot LAI estimates, obtained using equation 2. Overall, SNAP-derived LAI performed with poor accuracy against the total plot LAI estimates from both the AccuPAR and PocketLAI. This is shown with high MAE and RMSE values as well as negative EF values (table 4). Whilst the RMA regression shown in figure 23 indicates a discernible pattern despite a large underestimation (CRM > 16), low R^2 values (<0.4) signify that the correlations and patterns between SNAP-derived LAI and plot LAI should be taken with some caution.
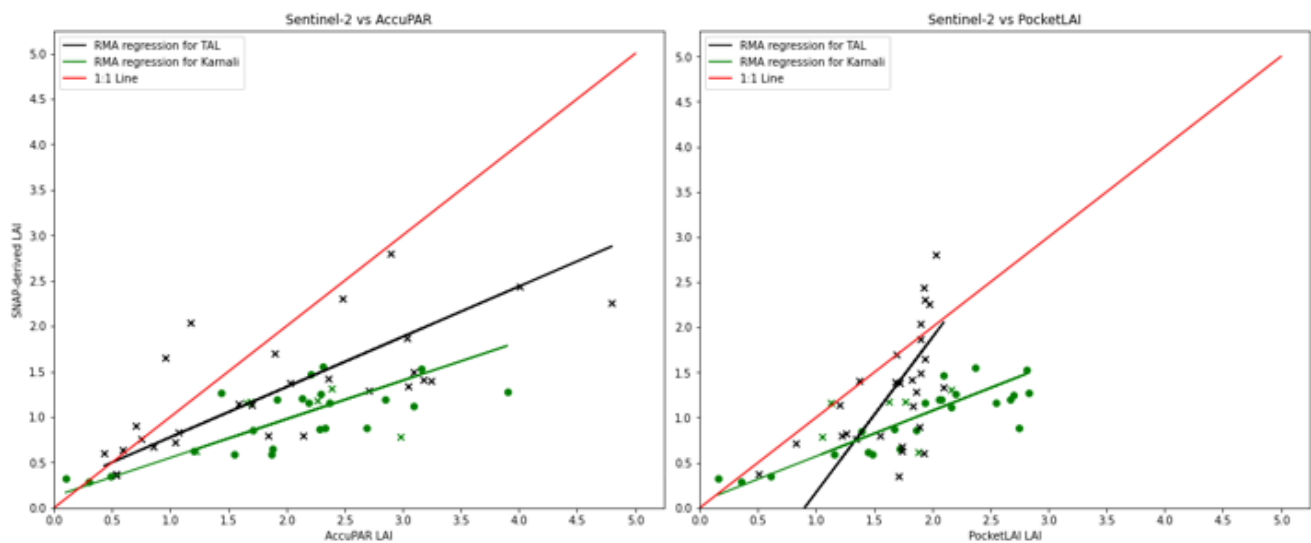
Figure 24. Relationship between SNAP-derived LAI and canopy LAI obtained with the AccuPAR (left) and PocketLAI (right).
Crosses represent values obtained by HAS researchers, with dots representing the values obtained in the fieldwork of this
thesis. Green points are LAI values in the Karnali and black points in the TAL.

Table 5. Statistical results from analysis comparing SNAP-derived LAI with AccuPAR and PocketLAI canopy LAI.

		n	MAE	RMSE	CRM	EF	R2	p-value
Karnali floodplain	AccuPAR	23	1.06	1.23	8.36	-0.94	0.55	0.00
(thesis plots)	PocketLAI		0.92	1.02	9.38	-0.85	0.74	0.00
Karnali floodplain	AccuPAR	29	1.05	1.22	11.12	-1.15	0.47	0.00
(thesis + HAS)	PocketLAI		0.85	0.96	11.28	-0.89	0.61	0.00
TAL (Babai, SNP, CNP;	AccuPAR	28	0.79	1.05	5.88	0.17	0.51	0.00
HAS)	PocketLAI		0.51	0.64	6.23	-1.94	0.32	0.00
Combined	AccuPAR	57	0.92	1.14	16.99	-0.29	0.44	0.00
	PocketLAI		0.68	0.82	17.51	-1.08	0.25	0.00

The SNAP-derived data performs better when compared to just the canopy LAI than the plot LAI, with all MAE and RMSE values being lower than 1.25, most of which <1.0 as seen in table 5. The RMA regressions in figure 24 indicate that the AccuPAR data obtained by HAS in the TAL lies closer to the ideal 1:1 line than those taken in the Karnali in BNP. This is supported by the EF value of 0.17 for the canopy LAI, which despite being low, is the only positive EF value implying that SNAP-derived data is most accurate compared to the in-situ canopy LAI in this instance. On the other hand, there is a more significant correlation for both PocketLAI and AccuPAR data obtained at the plots investigated in this thesis, with higher R^2 values demonstrating a stronger ability for the SNAP-derived data to capture general patterns as observed by the in-situ data. Similar to what was observed with the plot LAI estimates, SNAP-derived data tends to systemically underestimate LAI when compared to canopy LAI having positive CRM values, although less so than with the total plot estimates.

4.2.2 Fractional Vegetation Cover
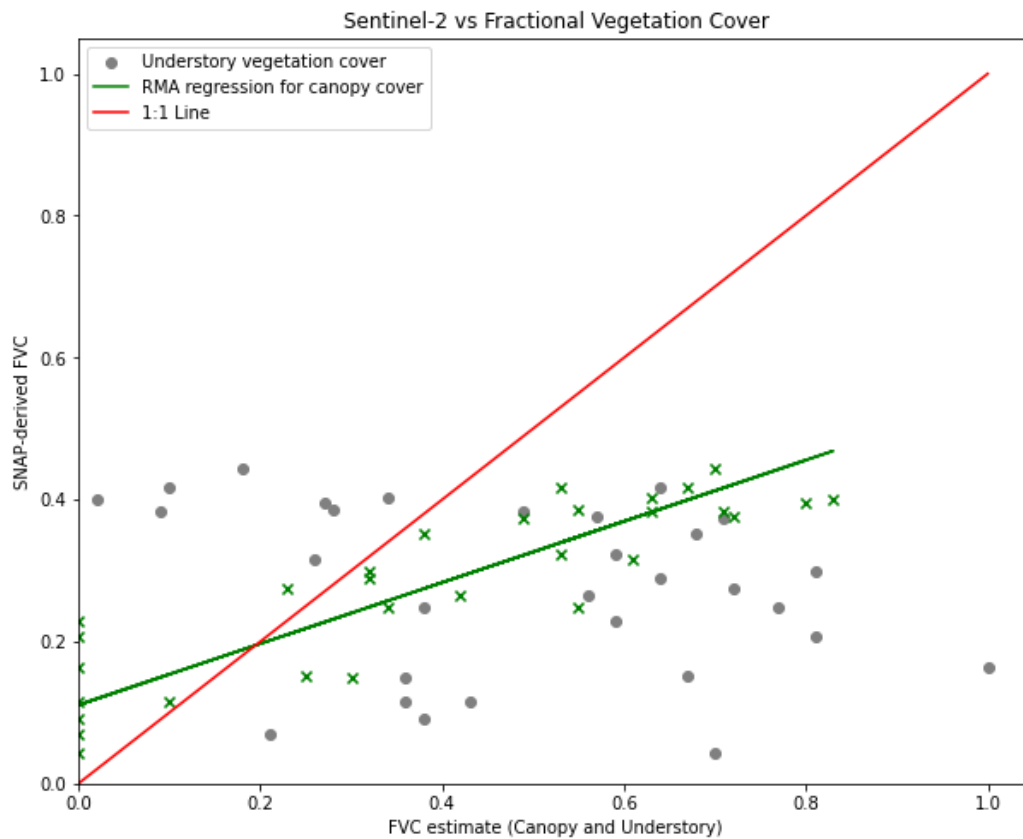
Figure 25. Relationship between SNAP-derived FVC and in-situ FVC. Both canopy (green) and understory (grey) FVC estimations were compared against the SNAP-derived FVC. The RMA regression line for understory consisted of a negative slope and was therefore not included.

Table 6. Statistical results from analysis comparing SNAP-derived FVC and canopy and understory FVC.

		n	MAE	RMSE	CRM	EF	R2	p-value
Karnali floodplain (thesis plots)	Canopy	30	0.17	0.21	-inf	0.41	0.77	0.00
	Canopy (excl. 0%)	23	0.19	0.22	7.05	-0.35	0.66	0.00
	Understory	30	0.32	0.36	-15.13	-1.25	0.08	0.13

SNAP-derived FVC showed stronger similarities to canopy cover estimates as compared to understory estimates, to the point where no RMA regression relationship observed for understory data (figure 25). This was shown with the very low R^2 value of 0.08 (p-value > 0.05; table 6). The opposite was seen with regards to canopy estimates, obtaining a high R^2 value of 0.77 (p-value < 0.05), indicating the RMA regression line significantly represents the variability of the data and demonstrates a strong correlation between SNAP-derived FVC and canopy FVC. However, high MAE and RMSE values (17% and 21%) can be seen. Several grassland plots with 0% canopy cover obtained higher estimates when obtained by the SNAP-derived FVC (green crosses on y-axis in figure 25) and drastically influenced the initial CRM value which came out as −∞. However, when these plots were excluded, the CRM value of 7.05

indicated the SNAP-derived FVC once more tended to underestimate the in-situ data. Excluding these plots however, drastically reduced the EF value (-0.35 from 0.41) indicating that without these low canopy plots, the SNAP-derived FVC does not as accurately quantify the canopy cover. The R^2 value in this instance (0.66) still indicated that whilst SNAP-derived FVC may not accurately quantify canopy cover, there is still considerable correlation between the two.

4.2.3 Surface Soil Moisture

The pixel distributions as well as the required intercepts and slopes of the wet and dry edges of the OPTRAM model that were used to obtain the relationships in this section, can be found in Appendix D. Figure 26 for 23 January in the Karnali shows the general properties of the VI-STR space and the calculated slopes and intercepts required for the OPTRAM SSM calculations.
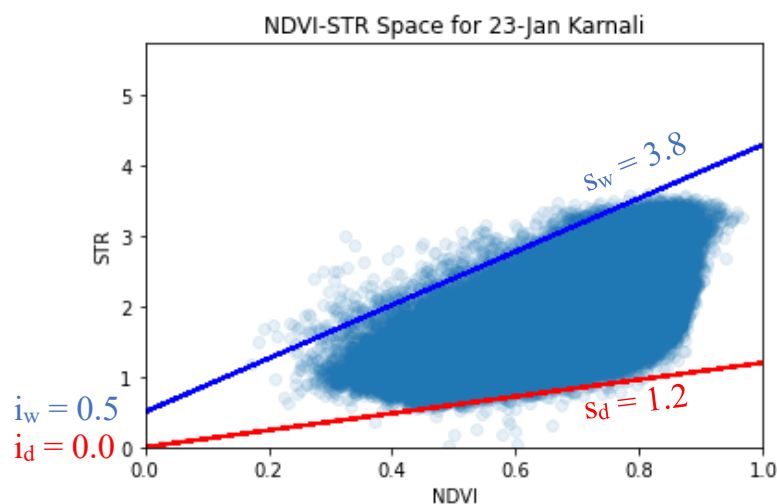
Figure 26. Pixel distribution within the NDVI-STR space for 23 January (calculation for plot SP3). Wet and dry edges represented by blue and red lines respectively. Corresponding intercepts and slopes shown on the figure.
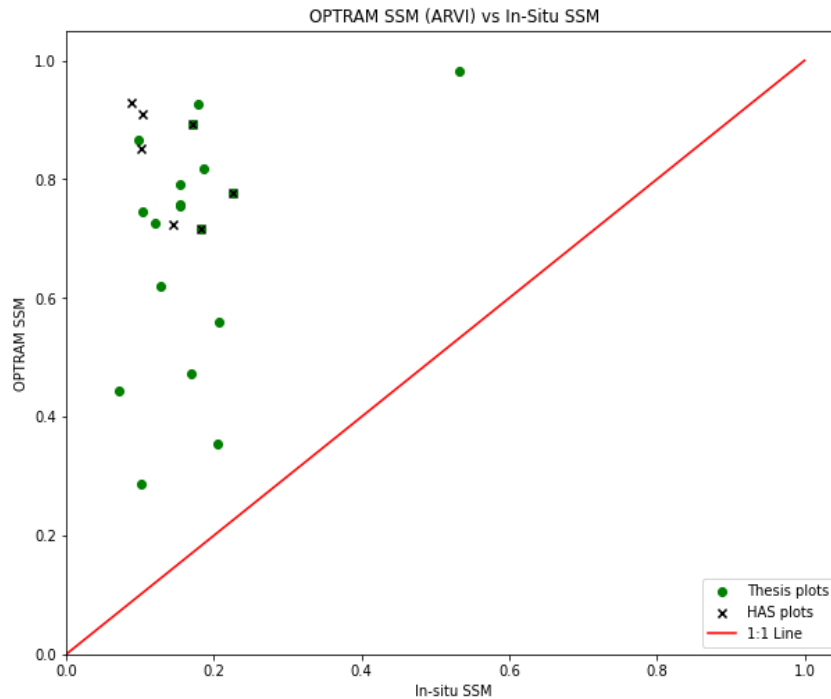
Figure 27. Relationship between OPTRAM SSM retrieval using the best performing vegetation index (ARVI). and in-situ SSM.

Table 7. Statistical results from analysis comparing OPTRAM soil moisture and plot SSM.

		n	MAE	RMSE	CRM	EF	R2	p-value
Karnali floodplain	*NDVI-STR*	20	0.33	0.37	-45.7	-15.18	0.02	0.60
(thesis plots)	*SAVI-STR*	21	0.41	0.45	-58.95	-23.75	0.05	0.34
	ARVI-STR	18	0.52	0.55	-65.19	-31.75	0.16	0.10
Karnali floodplain	*NDVI-STR*	31	0.32	0.35	-69	-18.26	0.02	0.48
(thesis +HAS)	*SAVI-STR*	28	0.45	0.49	-88.55	-34.5	0.05	0.26
	ARVI-STR	22	0.56	0.59	-92.81	-41.37	0.06	0.27

The SSM obtained through the OPTRAM method does not represent the in-situ SSM well, regardless of the vegetation index used. This is evident by the negligible R^2 values (p-values > 0.05) and considerably negative EF values (table 7). It can be seen in figure 27 that the majority of in-situ data is saturated <20% whilst the OPTRAM SSM values show are greater range of values, all >20%. OPTRAM generally performs better when using NDVI (lower RMSE and MAE values), however a stronger relationship is present between OPTRAM SSM and in-situ SSM when using ARVI, although still very weak (R^2 = 0.16; p-value = 0.10) No significant differences are evident between the data collected during the fieldwork of this thesis, and that collected by HAS, with all in-situ data overlapping in range. The scatter plots between OPTRAM SSM and in-situ SSM using NDVI and SAVI can be found in Appendix D.

5. Discussion

The discussion will be organised according to the research questions posed earlier. Following this is a reflection on the protocol combining the insights and the ranges of the values obtained when testing the protocol, as well as the analysis with satellite-derived values. Possible future research avenues are also suggested.

5.1 Research Questions

Research Question 1: *To what extent can an affordable smartphone based indirect LAI method (PocketLAI) be considered a viable alternative to a more established, technical and higher-cost indirect LAI method (AccuPAR-LP80) in heterogenous vegetation in the Terai Arc Landscape?*

The PocketLAI obtained a strong R^2 value of 0.78 when comparing the total plot LAI estimates with the AccuPAR, as well as good EF and R^2 values of 0.64 and 0.67 respectively for canopy LAI, which although lower than the EF and R^2 values obtained in Francone et al. (2014; >0.8 for all comparisons), are still satisfactory. Additionally, the RMSE value obtained in this thesis (0.53) is actually lower than that obtained by Francone et al. (2014; an average of 0.62). The discrepency in EF and R^2 values can potentially be attributed to the different vegetation analysed, as Francone et al. (2014) assessed the PocketLAI for different crops (maize and giant reed) that are extremely homogenous. On the other hand, this thesis investigated the PocketLAI in heterogenous vegetation and therefore, lower EF and R^2 values were anticipated. This is further supported by Orlando et al. (2015) that found that the PocketLAI, when tested on tree species, shows better agreement with other indirect methods when the canopies were more homogenous.

Francone et al. (2014) found very little over- or underestimation in all crops (-0.02 < CRM < 0.00), whereas the plots assessed in this thesis in the Karnali found that the PocketLAI tended to overestimate canopy LAI (CRM = -0.24). This overestimation was more evident in lower LAI ranges and could potentially be a result of these plots not having a continuous canopy - as it was observed in these plots that the PocketLAI would intermittently include vegetation located outside of the plot of interest, potentially resulting in a higher LAI than is representative of the plot. The saturation of PocketLAI values observed for more dense and continuous canopies in this thesis (LAI > 2) was also observed in Casa et al. (2019).

Further research comparing the AccuPAR and PocketLAI, and a direct method as a reference LAI in the context of the TAL could be interesting, as it has been documented by several studies that the AccuPAR tends to underestimate LAI (Confalonieri et al., 2013; Fang et al., 2014; Pokovai & Fodor, 2019), with Finzel et al. (2012) also documenting the AccuPAR's generally poor performance in heterogenous canopies. Therefore given the PocketLAI's tendency to overestimate in comparison to the AccuPAR in this thesis, it could potentially result in more accurate LAI estimations.

Whilst the PocketLAI showed good potential as an alternative to the AccuPAR in the context of the Karnali, this was not observed when extended to the context of the TAL, with EF and R^2 values drastically decreasing. This can potentially be a result of the different vegetation occurring in the different areas, as well as the impact of different light conditions on AccuPAR estimates, with higher PAR values noted by HAS. Pokovai and Fodor (2019) observed a general tendency for AccuPAR LAI estimates to underestimate LAI with lower PAR values. However, the range of AccuPAR LAI values overlap considerably for both measurements in the Karnali and the TAL and therefore the weaker relationship between the PocketLAI and AccuPAR observed in the TAL is more likely a result of issues regarding the PocketLAI than the AccuPAR. This can be argued as canopy LAI values obtained by HAS using the PocketLAI were greatly saturated between 1.4 and 2.0 regardless of the corresponding AccuPAR LAI.

This saturation could be attributed to the specific model of the device the PocketLAI was installed. Confalonieri et al. (2014) investigated the differences when the application was installed on four different devices finding that LAI estimates could vary between high- and low-cost devices by as much as $2.0m^2.m^{-2}$. A saturation effect was also shown for some devices that retained a LAI value of $\sim3.0m^2.m^{-2}$ despite the reference LAI changing from 3.0-5.0 $m^2.m^{-2}$. Therefore, considering the PocketLAI data was obtained by two different devices (Samsung Note 9 for this thesis and a lower cost smartphone, the Hammer Explorer Plus Eco used by HAS), it is more likely that this impacted the results than the vegetation or light condition differences due to the pattern seen in PocketLAI values.

Answering research question 1, the PocketLAI can be considered a viable alternative to the AccuPAR-LP80 in the context of the TAL, especially when considering the low cost and high portability, the latter being extremely useful in such environments. However, further investigation to the effect of the specific model of the smartphone on which the PocketLAI is installed needs to be carried out in the TAL. Additionally, given the large research gap in

literature directly comparing these two LAI measuring techniques especially in natural vegetation, a more rigorous collection of data should be carried out to validate the results obtained in this thesis for the Karnali, particularly to further investigate saturation effects for more dense canopies.

Research Question 2: *To what extent can the SNAP biophysical processor be used to accurately retrieve **LAI** and fvc in the Terai Arc Landscape?*

Both understory and canopy LAI were investigated and given the continuous nature of the canopy for the majority of the forest plots analysed, the understory layer was negligible regarding satellite LAI retrieval. This was shown by the high RMSE (>1.5) and CRM (>16) values for both the PocketLAI and AccuPAR total plot estimates (that included understory vegetation), indicating a very large underestimation of the satellite-derived LAI. Furthermore, the low R^2 values (0.27 and 0.38) indicated a weak overall relationship with total plot estimates inclusive of understory vegetation. However, the statistical results of the total LAI plot estimate obtained in this thesis using equation 2 are comparable with a method proposed by Goeking and Tarboton (2022) that found an R^2 of 0.33 between LandSat LAI and total plot LAI combining understory and canopy.

Goeking and Tarboton (2022) also noted that the satellite is unable to detect understory influences, dependent on the openness (continuousness) of the canopy. This agrees with Meyer et al. (2019) that found an increase in accuracy when omitting shrub vegetation and keeping only the canopy analysis. The same was observed for the results presented in this study with both RMSE values decreasing significantly when only canopy LAI was used.

There is further evidence towards the idea that HAS PocketLAI data is unreliable due to the strong R^2 value (0.74) obtained between PocketLAI values of this thesis and the satellite-derived LAI, a value that considerably decreased when including HAS PocketLAI values. The satellite-derived LAI also tended to perform better against the PocketLAI than the AccuPAR (when omitting HAS data) with most RMSE values <1.0. This also agrees with the previous hypothesis that the PocketLAI may prove more accurate than the AccuPAR in determining LAI in natural vegetation plots, although research into a calibration model is recommended to overcome the saturation effect the PocketLAI experiences at higher LAI values.

The range of RMSE values when SNAP-LAI was compared against in-situ canopy LAI came to be 0.51-1.23 $m^2.m^{-2}$, and is similar range to that of Hu et al. (2020), reporting 0.54-1.16$m^{-2}.m^{-2}$ for a variety of vegetation types. Brown et al. (2019) and Chrysafis et al. (2020) also

reported values of 1.55 and 1.42m^{-2}.m^{-2} respectively for forest vegetation, indicating the results of this thesis actually indicate marginally lower errors. R^2 values for the data obtained in the Karnali ranged from 0.47-0.74 m^{-2}.m^{-2}. These values, agree once more with the literature that presented a range of R^2 of 0.59-0.70 (Hu et al., 2020; Brown et al., 2019; Chrysafis et al., 2020; Meyer et al., 2019), showing that the use of Sentinel-2 and the SNAP biophysical processor in the TAL is comparable to results obtained in other geographical contexts.

The low accuracy of SNAP-derived LAI can be attributed to an aspect of satellite-derived LAI that was consistent in this study and across all the literature cited earlier, the tendency to underestimate in-situ LAI, regardless of the method used to obtain the in-situ data. This is largely due to the different definitions of LAI employed by the PocketLAI, AccuPAR, and SNAP biophysical processor. The biophyscial processor only quantifies the effective LAI (LAI$_{eff}$) that assumes a random distribution of leaves. It also considers only the green contributors (Weiss & Baret, 2016). This effectively outputs a green LAI$_{eff}$. The AccuPAR and PocketLAI however, much like other indirect optical methods grounded in gap fraction analysis, cannot distinguish between leaves and other woody elements, let alone green leaves and other leaves, and therefore outputs a total plant area index (PAI) that includes all elements in a canopy and can significantly overestimate LAI, especially when compared to a green LAI estimate (Bréda, 2003; Francone et al., 2014; Fang et al., 2019).

Answering research question 2 regarding LAI, the SNAP biophysical processor can not be used to accurately retrieve in-situ LAI measurements when using indirect light-based LAI devices. However, there exists the potential of using the SNAP biophysical processor to monitor patterns and relative changes in LAI given the moderate to strong relationships observed and comparability of results with literature. Further validation of satellite-derived LAI should be carried out on large temporal and spatial scales to improve the accuracy of the biophysical processor, especially in forest and natural vegetation environments as these studies are still dominated by crop vegetation analyses. In-situ validation techniques that are able to distinguish between PAI and green LAI whilst still remaining non-destructive should also be investigated to improve accuracy of satellite-sensing products and subsequently ecohydrological modelling.

Research Question 2: *To what extent can the SNAP biophysical processor be used to accurately retrieve LAI and **FVC** in the Terai Arc Landscape?*

The relationships observed between SNAP FVC and in-situ FVC are similar to that described previously for LAI. The SNAP biophysical processor also appeared to not capture understory

vegetation with no significant relationship being observed with in-situ understory FVC estimates, and also shows the tendency to underestimate the canopy data. Once more this is attributed to fact that understory vegetation is often undetectable by satellite-products in these environments, and that only green vegetation is processed (Goeking & Tarboton, 2022; Weiss & Baret, 2016).

Literature comparing SNAP fractional cover and in-situ FVC obtained R^2 values in the range of 0.36-0.94 for a variety of vegetation types (Djamai et al., 2019; Kamenova & Dimitrov, 2021; Hu et al., 2020). This is in agreement with the R^2 value of 0.77 obtained in this thesis for canopy FVC. Hu et al. (2020) obtained an R^2 of 0.55 for forest vegetation that was higher than both crop and grass R^2 values reported (0.34 and 0.32) indicating a stronger relationship between SNAP fractional cover and forest FVC. This was also observed in this thesis as there was no correlation between grass plots and the SNAP fractional cover, as noted in the results section, where in-situ estimates were 0% and corresponding SNAP estimates ranged between 5% and 25%. Whilst obtaining a stronger correlation than Hu et al. (2020), the RMSE value obtained in this thesis for canopy FVC of 0.21 shows an average error 10% greater than the RMSE obtained by Hu et al. (2020) for forests (RMSE = 0.12). This higher RMSE is likely due to the lack of combining canopy and understory vegetation in the protocol, when canopies are intermittently open.

Research question 2 regarding FVC can only be answered regarding the Karnali and not the TAL, as no data was obtained outside the Karnali. The SNAP biophysical processor does not accurately retrieve FVC, largely underestimating fractional cover in the Karnali. However, similar to the comparisons with LAI, there is a strong correlation between SNAP fractional cover and in-situ canopy cover, indicating the potential to use SNAP in exploring the patterns and changes in canopy cover in the Karnali. In-situ data should be collected in other regions of the TAL to determine whether the results obtained in the Karnali are representative of the whole region.

Research Question 3: *To what extent can the OPTRAM method be used to accurately retrieve SSM in the Terai Arc Landscape?*

The OPTRAM method obtained extremely poor R^2 values (<0.2), all with corresponding p-values >>0.05, and very high RMSE values of >0.35cm^3.cm^{-3}, strongly disagreeing with literature which obtained satisfactory to strong R^2 values in the range of 0.53-0.80 (Sadeghi et al., 2017; Hassanpour et al., 2020; Ambrosone et al., 2020). The same studies all reported the

OPTRAM method to have good accuracy with RMSE ranges of 0.039-0.084 $cm^3.cm^{-3}$, substantially lower than the RMSE obtained in this thesis. Chen et al. (2020) obtained an R^2 value <0.13 for two of nine plots, comparable with the result obtained when using ARVI as the vegetation index in this thesis. However, Chen et al. (2020) also obtained low RMSE values (0.05-0.13$cm^3.cm^{-3}$) similar to the other studies mentioned.

It should be noted that these studies were investigating OPTRAM for agricultural fields and grasslands with no forest cover which is likely to affect the performance of the model when compared to dense forest canopy plots. Chen et al. (2020) noted that the applicability of the OPTRAM method is affected in more complex topographic terrains and mixed terrains, an aspect that may have influenced the accuracy and relationships presented in this thesis. The pixel distributions (Appendix D) may support this as about half of the VI-STR spaces show distributions that are not captured well by the trapezoidal geometry, indicating the methods may not apply. Confirming this, Sadeghi et al. (2017) reported a triangular geometry for one distribution noting that this instance does not lead to physically-based theoretical wet and dry edges. The OPTRAM method is also inherently subjective as the slopes and intercepts are determined visually, affecting the uncertainties of the method (Sadeghi et al., 2017; Chen et al., 2020). Further research should be conducted into modifying the OPTRAM method to better, and more objectively, incorporate these different pixel distributions to capture in-situ SSM more accurately in complex environments.

The saturation of in-situ SSM between 10% and 20% over a variety of vegetation classes in combination with the strong disagreement of results to all literature, may however point towards an issue with the in-situ measurements rather than with the applicability of the OPTRAM method in the TAL. This could be a result of the depth of SSM measurement with the SM150T. Inserting the probe directly into the ground results in SSM measurements of only the top 5cm of soil, which given the small radius of influence of the SM150T, may not be sufficient to capture the SSM due to high fluctuations of near surface soil moisture (Wang et al., 2021). Whilst the OPTAM method was employed for SSM at a depth of 5cm (Sadeghi et al., 2017; Hassanpour et al., 2020), this was compared against in-situ methods that are not capacitance-based methods that rely on circuit contact which can be affected greatly in near surface soil moisture (Kojima, et al., 2016). The other studies cited investigated the OPTRAM method with SSM for depths up to 20cm (Chen et al., 2020; Ambrosone, et al., 2020).

To test whether the poor performace of the OPTRAM method in this thesis is a result of the in-situ measurements, SSM measurements should be taken at a depth of 10-15cm. This would entail digging ~5cm of topsoil before inserting the SM150T to record SSM. Furthmore, extensive calibration of the SM150T with soil sampled in the TAL should be carried out according to the manual (Delta-T Devices, 2016). This would enable soil-specific calibration coefficients as opposed to the general coefficients provided by the SM150T. Lastly, the effect of litterfall on OPTRAM SSM retrieval should also be explored, as several plots had ground cover with high litterfall cover with moisture seemingly present, thus potentially impacting the reflectance retrieved by the satellite.

Answering research question 3, the OPTRAM method does not accurately retrieve surface soil moisture in the TAL. This is attributed to errors in the in-situ data collection, although the applicability of OPTRAM in more complex environments should also be investigated.

5.2 Reflection on Protocol

The primary aim of this thesis was to develop a protocol for the sampling of LAI, FVC, and SSM in the TAL. The protocol aimed to provide consistent and reliable data in both a time and cost-efficient manner. The results of this thesis indicate that this aim was generally achieved with the developed protocol showing great potential in its application. The consistency of the data obtained by the protocol was tested with the implementation of the protocol by HAS in other regions of the TAL. The range of values obtained for each investigated parameter were comparable across vegetation classes as those obtained during the fieldwork of this thesis, indicating a level of consistency across the TAL.

The reliability of the data also showed promise with the data capturing expected patterns, such as higher (total plot) LAI values in forest plots than grassland plots and even increased understory with decreased canopy cover (Majasalmi & Rautiainen, 2020). Differences between Sal forest plots and riverine plots were also observed further indicating that the protocol is able to capture differences between vegetation classes. The reliability was also shown, particularly for LAI and FVC, with comparisons to satellite-derived data generally obtaining similar values to that of previous studies that validated satellite-derived data with in-situ data.

Furthermore, the need for the protocol to be time-efficient in its implementation was largely achieved with the time needed at each plot being ~30 minutes using the final plot layout, compared to the initial ~90 minutes.

The results showed the potential in the PocketLAI to quantify in-situ LAI, something which would prove extremely valuable to the Tiger Project due to its increased portability and accessibility, allowing for more researchers to collect LAI data due to its cost and availability compared with the single AccuPAR currently shared within the project. Future implementation of the protocol should be conducted accounting for and investigating the potential effect of the specific smartphone model on saturating values.

There also exists the need to carry out direct LAI measurements to obtain accurate reference in-situ LAI values. Currently the results of this thesis indicate that satellite-based LAI can monitor general patterns, however for detailed modelling the AccuPAR, PocketLAI, and satellite-derived LAI carry too many uncertainties. Therefore, an argument for the investigation

and subsequent inclusion of Specific Leaf Area (SLA) in the protocol is made as SLA can provide reference LAI estimates without being influenced by woody elements, is independent of light influences and can calculate LAI for the entire plot (Kwon et al., 2016). This can help in calibration of the indirect methods as well as contribute to the validation of satellite-based methods. Furthermore, SLA provides valuable information regarding plant chemistry and ecosystem production efficiency (Lymburner et al., 2000), which can prove extremely useful for other lines of research within the Tiger Project. However, the need for accurate LAI modelling must be made certain as SLA collection, whilst not as destructive as other methods if litterfall traps are used, is still a destructive method and a very time-consuming process.

FVC estimation carries a large risk of subjectivity that has not yet been tested regarding the protocol. Furthermore, the relationships observed need to be investigated on a seasonal scale. For both FVC and LAI data, the results showed a strong potential for the monitoring of canopy influences, however, the need for the inclusion of understory presence regardless of the continuity of the canopy should be explored as the interaction between canopy layers and hydrological processes are an important influence on water resources and vegetation type changes (Goeking & Tarboton, 2022). Investigation as to how to record this, in a more methodical and objective manner, should be tested to be included in the protocol.

Exploring the potential of vegetation indices to predict LAI and FVC in the TAL is also recommended as this can potentially increase the consistency between satellite-based and in-situ LAI and provide valuable insights on seasonal relationships between vegetation density and LAI (Lukasová et al., 2014). This could prove highly beneficial in monitoring successional vegetation changes and the subsequent impacts on physiological traits of the ecosystem on a landscape scale. An additional exploratory investigation into this for LAI was conducted during this thesis and can be found in Appendix E.

The largest adjustment to the protocol is needed regarding SSM. The lack of relationships observed in this thesis were attributed to in-situ measurement errors. Increasing the depth of SSM measurements could provide further insight along with extensive on-site calibrations of the SM150T. Furthermore, soil sampling at each plot is suggested to physically measure soil moisture to provide a form of reference values. This would also potentially enable soil type (texture), as well as soil carbon content, to be included in the protocol. Both parameters offer valuable insight into the properties of the soil that can then be related with plant productivity

as well as important hydrologic properties that can contribute to other facets of The Tiger Project.

Future research should investigate whether such high resolution SSM is actually necessary, as perhaps obtaining lower resolution SSM spatial gradients to monitor relationships with river discharge, distance from major rivers, and vegetation changes is sufficient. This would allow for SSM loggers to be installed along transects, allowing for more reliable and consistent data to be collected whilst still providing valuable insights to the SSM of the environment.

Lastly, possible research into the interrelationships and dynamics between LAI, FVC, SSM, as well as established VIs for different phenological phases could be crucial in monitoring vegetation productivity and potentially predicting successional changes.

6. Conclusions

A protocol for the sampling of LAI, FVC, and SSM was developed and tested in the context of the TAL. The protocol was largely able to capture consistent and reliable data for LAI and FVC across vegetation types in the Karnali, whilst showing potential across different regions in the TAL. Furthermore, the viability of a smartphone-based LAI method, the PocketLAI, was investigated and found to be a feasible alternative to the AccuPAR-LP80, although more data across the TAL, and potential calibrations for higher LAI environments is needed. The protocol was also able to capture consistent data for SSM, however the reliability of the data was not sufficient, and adjustments need to be made to improve in-situ SSM measurements.

The data collected whilst testing the protocol was used for validation of satellite products which showed significant relationships with in-situ LAI and FVC. Whilst the satellite products did not accurately retrieve LAI and FVC, largely underestimating values, the results still carry important implications regarding the potential of monitoring patterns of these parameters across the TAL. This was not the case for SSM, once more emphasising the need for improvement regarding the collection of this parameter and subsequent adjustments to the protocol.

The results of the analyses conducted in this thesis, contributes importantly to literature that is largely dominated by agricultural contexts, by exploring these relationships in a natural and heterogenous environment. Furthermore, this thesis provides introductory research into the feasibility and applicability of ecohydrological monitoring within the TAL.

Further iterations of this protocol across different fieldwork campaigns within The Tiger Project will prove vital in establishing a robust protocol, potentially incorporating additional parameters, such as SLA, soil texture, and soil carbon content. The implications of such a protocol will be invaluable in facilitating research on the feedbacks between successional vegetation change, plant physiological properties, and hydrologic processes. This will aid in informing conservation of priority areas regarding tiger habitats, and subsequently aid in guiding conservation management and human development planning in the Terai Arc Landscape.

References

Adab, H., Morbidelli, R., Saltalippi, C., Moradian, M., & Ghalhari, G. (2020). Machine Learning to Estimate Surface Soil Moisture from Remote Sensing Data. *Water, 12*(11), 3223. doi:10.3390/w12113223

Adhakari, B. (2013). Flooding and Inundation in Nepal Terai: Issues and Concerns. *Hydro Nepal: Journal of Water, Energy and Environment,, 12*, 59-65. doi:10.3126/hn.v12i0.9034.

Ambrosone, M., Matese, A., Di Gennaro, S., Gioli, B., Tudoroiu, M., Genesio, L., Toscano, P. (2020). Retrieving soil moisture in rainfed and irrigated fields using Sentinel-2 observations and a modified OPTRAM approach. *International Journal of Applied Earth Observation and Geoinformation, 89*, 102113. doi: 10.1016/j.jag.2020.102113

Andrade, B., Boldrini, I., Cadenazzi, M., Pillar, V., & Overbeck, G. (2019). Grassland vegetation sampling — a practical guide for sampling and data analysis. *Acta Botanica Brasilica, 33*(4), 786-795. doi:10.1590/0102-33062019abb0160

Bajocco, S., Ginaldi, F., Savian, F., Morelli, D., Scaglione, M., Fanchini, D., Bregaglio, S. (2022). On the Use of NDVI to Estimate LAI in Field Crops: Implementing a Conversion Equation Library. *Remote Sensing, 14*(15), 3554. doi:10.3390/rs14153554

Bellard, C., Marino, C., & Courchamp, F. (2022). Ranking threats to biodiversity and why it doesn't matter . *Nature Communications, 13*, 2616. doi:10.1038/s41467-022-30339-y

Berghuis, A. (2019). *MSc Thesis: Groundwater research in Nepal for tiger conservation, A reconnaissance study to groundwater dynamics in an alluvial mega-fan in Bardiya National Park (Terai), focusing on the interaction between groundwater and the Karnali river.* Utrecht University.

Bijlmakers, J. (2020). *MSc Thesis: Environmental drivers of space-time dynamics of vegetation in Bardia National Park, Nepal.* Utrecht University.

Bréda, N. (2003). Ground-based measurements of leaf area index: a review of methods, instruments and current controversies. *Journal of Experimental Botany, 54*(392), 2403-2417. doi:10.1093/jxb/erg263

Brook, B., Sodhi, N., & Bradshaw, C. (2008). Synergies among extinction drivers under global change. *Trends Ecology Evolution, 23*(8), 453–460. doi:10.1016/j.tree.2008.03.011

Brown, A., Ogutu, O., & Dash, J. (2019). Estimating forest leaf area index and canopy chlorophyll content with Sentinel-2: An evaluation of two hybrid retrieval algorithms. *Remote Sensing, 11*, 1752. doi:10.3390/rs11151752

Carter, N., Gurung, B., Viña, A., Campa III, H., Karki, J., & Liu, J. (2013). Assessing spatiotemporal changes in tiger habitat across different land management regimes. *Ecosphere, 4*(10), 1-19. doi:10.1890/ES13-00191.1

Casa, R., Upreti, D., & Pelosi, F. (2019). Measurement and estimation of leaf area index (LAI) using commercial instruments and smartphone-based systems. *Earth and Environmental Science, 275*, 012006. doi:10.1088/1755-1315/275/1/012006

CBS. (2014). *National Population and Housing Census 2011 - Chitwan. Gov. Nepal 06: 1–278.* Retrieved December 10, 2022, from http://cbs.gov.np/image/data/Population/VDCMunicipalityindetail/35Chitwan_VDCLevelReport.pdf

Chai, T., & Draxler, R. (2014). Root mean square error (RMSE) or mean absolute error (MAE)? – Arguments against avoiding RMSE in the literature. *Geoscientific Model Development, 7*, 1247-1250. doi:10.5194/gmd-7-1247-2014

Chen, H., Zhu, G., Zhang, K., Bi, J., Jia, X., Ding, B., Qin, W. (2020). Evaluation of Evapotranspiration Models Using Different LAI and Meteorological Forcing Data from 1982 to 2017. *Remote Sensing, 12*(15), 2473. doi:10.3390/rs12152473

Chen, L., Wang, L., Ma, Y., & Liu, P. (2015). Overview of Ecohydrological Models and Systems at the Watershed Scale. *IEEE Systems Journal, 9*(3), 1091-1099. doi:10.1109/jsyst.2013.2296979

Chen, M., Zhang, Y., Yao, Y., Lu, J., Pu, X., Hu, T., & Wang, P. (2020). Evaluation of the OPTRAM Model to Retrieve Soil Moisture in the Sanjiang Plain of Northeast China. *Earth and Space Science, 7*, e2020EA001108. doi:10.1029/2020EA001108

Chrysafis, I., Korakis, G., Kyriazopoulos, A., & Mallinis, G. (2020). Retrieval of Leaf Area Index Using Sentinel-2 Imageryin a Mixed Mediterranean Forest Area. *International Journal of Geo-Information, 9*, 622. doi:10.3390/ijgi9110622

Confalonieri, R., Foi, M., Casa, R., Aquaro, S., Tona, E., Peterle, M., Cappelli, G. (2013). Development of an app for estimating leaf area index using a smartphone. Trueness and precision determination and comparison with other indirect methods. *Computers and Electronics in Agriculture, 96*, 67-74. doi:10.1016/j.compag.2013.04.019

Confalonieri, R., Francone, C., & Foi, M. (2014). The PocketLAI smartphone app: an alternative method for leaf area index estimation. *International Congress on Environmental Modelling and Software, 41*. Retrieved from https://scholarsarchive.byu.edu/iemssconference/2014/Stream-A/41

Decagon. (2016). *AccuPAR PAR/LAI Ceptometer Model LP-80 Operator's Manual.* Pullman WA: Decagon Devices, Inc.

DEH. (2001). *Developing a Protocol .* Retrieved December 09, 2022, from Department of Environmental Health. University of Washington: https://depts.washington.edu/wildfire/resources/protckl.pdf

Delta-T Devices. (2016). *User manual for the SMT150T soil moisture sensor.* Retrieved June 18, 2023, from https://delta-t.co.uk/wp-content/uploads/2017/01/SM150T-user-manual-version-1.0.pdf

Dhakal, M., & Baral, H. (2015). Tiger Conservation in South Asia: Lessons from Terai Arc Landscapes, Nepal. *2nd International Conference on Tropical Biology "Ecological restoration in Southeast Asia: Challenges, Gains, and Future Directions".* Bogor-INDONESIA, 12-13 October 2015: SEAMEO BIOTROP.

DHM. (2017). *Observed Climate Trend Analysis in the Districts and Physiographic Regions of Nepal (1971-2014).* Kathmandu, Nepal: Department of Hydrology and Meteorology.

Dhungana, R., Savini, T., Karki, J., & Bumrungsri, S. (2016). Mitigating human-tiger conflict: an assessment of compensation payments and tiger removals in Chitwan National Park, Nepal. *Tropical Conservation Science, 9*(2), 776-787. doi:10.1177/194008291600900213

Di Marco, M., Venter, O., Possingham, H., & Watson, J. (2018). Changes in human footprint drive changes in species extinction risk. *Nature Communications, 9*, 4621. doi:10.1038/s41467-018-07049-5

Dinerstein, E. (1979a). An ecological survey of the royal Karnal Bardiya Wildlife Reserve, Nepal. Part II: Habitat/Animal interactions. *Biological Conservation, 16*, 265-300. doi:10.1016/0006-3207(79)90030-2

Djamai, N., Fernandes, R., Weiss, M., McNairn, H., & Goïta, K. (2019). Validation of the Sentinel Simplified Level 2 Product Prototype Processor (SL2P) for mapping cropland biophysical variables using Sentinel-2/MSI and Landsat-8/OLI data. *Remote Sensing of the Environment, 225*, 416-430. doi:10.1016/j.rse.2019.03.020

DNPWC and DFSC (2022). . (2022). *Status of Tigers and Prey in Nepal 2022. Department of National Parks and Wildlife Conservation and Department of Forests and Soil Conservation.* Kathmandu, Nepal: Ministry of Forests and Environment.

Dube, T., Pandit, S., Shoko, C., Ramoelo, A., Mazvimavi, D., & Dalu, T. (2019). Numerical Assessments of Leaf Area Index in Tropical Savanna Rangelands, South Africa Using Landsat 8 OLI Derived Metrics and In-Situ Measurements. *Remote Sensing, 11*(7), 829. doi:10.3390/rs11070829

Eckrich, C., Flaherty, E., & Ben-David, M. (2013). Estimating Leaf Area Index in Southeast Alaska: A Comparison of Two Techniques. *PLoS ONE, 8*(11), e77642. doi:10.1371/journal.pone.0077642

Eigentler, L. (2020). *Intraspecific competition can generate species coexistence in a model for dryland vegetation patterns.* Edinburgh: Heriot-Watt University.

Fan, L., Gao, Y., Bruck, H., & Bernhofer, C. (2009). Investigating the relationship between NDVI and LAI in semiarid grassland in Inner Mongolia using in-situ measurements. *Theoretical and Applied Climatology, 95*, 151-156. doi:10.1007/s00704-007-0369-2

Fang, H., Baret, F., Plummer, S., & Schaepman-Strub, G. (2019). An Overview of Global Leaf Area Index (LAI): Methods, Products, Validation, and Applications. *Reviews of Geophysics, 57*, 739-799. doi:10.1029/2018RG000608

Fang, H., Li, W., Wei, S., & Jiang, C. (2014). Seasonal variation of leaf area index (LAI) over paddy rice fields in NE China: Intercomparison of destructive sampling, LAI-2200, digital hemispherical photography (DHP), and AccuPAR methods. *Agricultural and Forest Meteorology, 198-199*, 126-141. doi:10.1016/j.agrformet.2014.08.005

Finzel, J., Seyfried, M., Weltz, M., Kiniry, J., Johnson, M., & Launchbaugh, K. (2012). Indirect Measurement of Leaf Area Index in Sagebrush-Steppe Rangelands. *Rangeland Ecology & Management, 65*(2), 208-212. doi:10.2111/REM-D-11-00069.1

Francone, C., Pagani, V., Foi, M., Cappelli, G., & Confalonieri, R. (2014). Comparison of leaf area index estimates by ceptometer and PocketLAI smart app in canopies with different structures. *Field Crops Research, 155*, 38-41. doi:10.1016/j.fcr.2013.09.024

GeoTimeDate. (2023). *Sunrise, Sunset for Kathmandu, CR, Nepal.* Retrieved 05 28, 2023, from geotimedate: https://geotimedate.org/sun/nepal/cr/kathmandu

Ginaldi, F., Bajocco, S., Savian, F., Morelli, D., Scaglione, M., Fanchini, D., Bregaglio, M. (2022). Global dataset of empirical functions to convert NDVI into LAI in field crops. *figshare. Dataset.* doi:10.6084/m9.figshare.20359437.v2

Goeking, S., & Tarboton, D. (2022). Spatially Distributed Overstory and Understory Leaf Area Index Estimated from Forest Inventory Data. *Water, 14*, 2414. doi:10.3390/w14152414

Hai-liang, X., Mao, Y., & Ji-mei, L. (2007). Changes in groundwater levels and the response of natural vegetation to transfer of water to the lower reaches of the Tarim River. *Journal of Environmental Sciences, 19*, 1199-1207. doi:10.1016/S1001-0742(07)60196-X

Hasegawa, K., Matsuyama, H., Tsuzuki, H., & Sweda, T. (2010). Improving the estimation of leaf area index by using remotely sensed NDVI with BRDF signatures. *Remote Sensing of the Environment, 114*(3), 514-519. doi:10.1016/j.rse.2009.10.005

Hassanpour, R., Neyshabouri, M., Zarehagi, D., & Feizizadeh, B. (2020). Modification on optical trapezoid model for accurate estimation of soil moisture content in a maize growing field. *Journal of Applied Remote Sensing, 14*(3), 034519. doi:10.1117/1.JRS.14.034519

Hu, Q., Yang, J., Xu, B., Huang, J., Memon, M., Yin, G., Liu, K. (2020). Evaluation of Global Decametric-Resolution LAI, FAPAR and FVC Estimates Derived from Sentinel-2 Imagery. *Remote Sensing, 12*, 912. doi:10.3390/rs12060912

Huete, A. (1988). A soil-adjusted vegetation index (SAVI). *Remote Sensing of the Environment, 25*, 295-309. doi:10.1016/0034-4257(88)90106-X

Hyer, E., & Goetz, S. (2004). Comparison and sensitivity analysis of instruments and radiometric methods for LAI estimation: Assessments from a boreal forest site. *Agricultural and Forest Meteorology, 122*(3), 157-174. doi:10.1016/j.agrformet.2003.09.0133

Jiapaer, G., Chen, X., & Bao, A. (2011). A comparison of methods for estimating fractional vegetation cover in arid regions. *Agricultural and Forest Meteorology, 151*(12), 1698-1710. doi:10.1016/j.agrformet.2011.07.004

Kala, J., Decker, M., Exbrayat, J., Pitman, A., Carouge, C., Evans, J., Mocko, D. (2014). Influence of Leaf Area Index Prescriptions on Simulations of Heat, Moisture, and Carbon Fluxes. *Journal of Hydrometeorology, 15*(1), 489-503. doi:10.1175/JHM-D-13-063.1

Kamenova, I., & Dimitrov, P. (2021). Evaluation of Sentinel-2 vegetation indices for prediction of LAI, fAPAR and fCover of winter wheat in Bulgaria. *European Journal of Remote Sensing, 54*(sup1), 89-108. doi:10.1080/22797254.2020.1839359

Kojima, Y., Shigeta, R., Miyamoto, N., Shirahama, Y., Nishioka, K., Mizoguchi, M., & Kawahara, Y. (2016). Low-Cost Soil Moisture Profile Probe Using Thin-Film Capacitors and a Capacitive Touch Sensor. *Sensors, 16*, 1292. doi:10.3390/s16081292

Kral, M., van Lunenburg, M., & van Alphen, J. (2017). The spatial distribution of ungulates and primates across the vegetation gradient in Bardiya National Park, West Nepal. *Asian Journal of Conservation Biology, 6*(1), 38-44.

Kwon, B., Kim, H., Jeon, J., & Yi, M. (2016). Effects of Temporal and Interspecific Variation of Specific Leaf Area on Leaf Area Index Estimation of Temperate Broadleaved Forests in Korea. *Forests, 7*(10), 215. doi:10.3390/f7100215

Lehmkuhl, J. (1994). A classification of subtropical riverine grassland and forest in Chitwan National Park, Nepal. *Vegetation, 111*, 29-43. doi:10.1007/BF00045575

Lekshmi, S., Singh, D., & Baghini, M. (2014). A critical review of soil moisture measurement. *Measurement, 54*, 92-105. doi:10.1016/j.measurement.2014.04.007

Li, S., Fang, H., Zhang, Y., & Wang, Y. (2022). Comprehensive evaluation of global CI, FVC, and LAI products and their relationships using high-resolution reference data. *Science of Remote Sensing, 6*, 100066. doi:10.1016/j.srs.2022.100066

Loague, K., & Green, R. (1991). Statistical and graphical methods for evaluating solute transport models: Overview and application. *Journal of Contaminant Hydrology, 7*, 51-73. doi:10.1016/0169-7722(91)90038-3

Lukasová, V., Lang, M., & Skvarenina, J. (2014). Seasonal changes in NDVI in relation to Phenological Phases, LAI and PAI of beech forests. *Baltic Forestry, 20*(2), 248-262.

Lymburner, L., Beggs, P., & Jacobson, C. (2000). Estimation of Canopy-Average Surface-Specific Leaf Area Using Landsat TM Data. *Photogrammetric Engineering & Remote Sensing, 66*(2), 183-191.

Ma, T., Duan, Z., Li, R., & Song, X. (2019). Enhancing SWAT with remotely sensed LAI for improved modelling of ecohydrological process in subtropics. *Journal of Hydrology, 570*, 802-815. doi:10.1016/j.jhydrol.2019.01.024

Majasalmi, T., & Rautiainen, M. (2020). The impact of tree canopy structure on understory variation in a boreal forest. *Forest Ecology and Management, 466*, 118100. doi:10.1016/j.foreco.2020.118100

Merritt, D., & Cooper, D. (2000). Riparian vegetation and channel change in response to river regulation: A comparative study of regulated and unregulated streams in the Green River Basin, USA. *Regulated Rivers: Research and Management, 16*(6), 543-564. doi:10.1002/1099-1646(200011/12)16:6<543::aid-rrr590>3.0.co;2-n

Meyer, L., Heurich, M., Beudert, B., Premier, J., & Pflugmacher, D. (2019). Comparison of Landsat-8 and Sentinel-2 Data for Estimation of Leaf Area Index in Temperate Forests. *Remote Sensing, 11*, 1160. doi:10.3390/rs11101160

Nash, J., & Sutcliffe, J. (1970). River flow forecasting through conceptual models part I. A discussion of principles. *Journal of Hydrology, 10*(3), 282-290. doi:10.1016/0022-1694(70)90255-6

Nittu, G., Shameer, T., Nishanthini, N., & Sanil, R. (2022). The tide of tiger poaching in India is rising! An investigation of the intertwined facts with a focus on conservation. *GeoJournal.* doi:10.1007/s10708-022-10633-4

Orlando, F., Movedi, E., Coduto, D., Parisi, S., Brancadoro, L., Pagani, V., Confalonieri, R. (2016). Estimating Leaf Area Index (LAI) in Vineyards Using the PocketLAI Smart-App. *Sensors, 16*, 2004. doi:10.3390/s16122004

Orlando, F., Movedi, E., Paleari, L., Gilardelli, C., Foi, M., Dell'Oro, M., & Confalonieri, R. (2015). Estimating leaf area index in tree species using the PocketLAI smart app. *Applied Vegetation Science, 18*, 716-723. doi: 10.1111/avsc.12181

Panthi, S., Poudel, S., & Mishra, B. (2019). First stop human depredation to double the number of Bengal tigers. *Animal Conservation, 22*, 1-2. doi:10.1111/acv.12451

Parton, W., Haxeltine, A., Thornton, P., Anne, R., & Hartman, M. (1996). Ecosystem sensitivity to land-surface models and leaf area index. *Global Planetary Change, 13*, 89-98. doi:10.1016/0921-8181(95)00040-2

Pask, A., & Pietragalla, J. (2012). Leaf Area, Green Crop Area and Senescence. In A. Pask, J. Pietragalla, D. Mullan, M. Reynolds, & Eds., *Physiological Breeding II: A Field Guide to Wheat Phenotyping* (pp. 58-62). Mexico: CIMMYT. Retrieved June 09, 2023, from https://www.google.com/books?hl=hu&lr=&id=lYVL-db0AtQC&oi=fnd&pg=PA2&dq=+++++Pask+et+al.+2012+leaf&ots=Rmi48ZZSfX&sig=P9VHxybWrtcYtgYfub9a15dyEAM

Pokovai, K., & Fodor, N. (2019). Adjusting Ceptometer Data to Improve Leaf Area Index Measurements. *Agronomy, 9*(12), 866. doi:10.3390/agronomy9120866

Potithep, S., Nagai, S., Nasahara, K., Muraoka, H., & Suzuki, R. (2013). Two separate periods of the LAI–VIs relationships using in situ measurements in a deciduous broadleaf forest. *Agricultural and Forest Meteorology, 169*, 148-155. doi:10.1016/j.agrformet.2012.09.003

Purevdorj, T., Tateishi, R., Ishiyama, T., & Honda, Y. (1998). Relationships between percent vegetation cover and vegetation indices. *International Journal of Remote Sensing, 19*(18), 3519-3535. doi:10.1080/014311698213795

RLB. (2022). *About Bardia National Park*. Retrieved from Rhino Lodge Bardia: https://www.rhinolodgebardia.com/bardianationalpark.php

Rodriguez-Iturbe, I., Porporato, A., Laio, F., & Ridolfi, L. (2000). Plants in water-controlled ecosystems: Active role in hydrologic processes and response to water stress—I. Scope and general outline. *Advances in Water Resources, 24*(7), 695-705.

Rout, C., & Aldous, C. (2016). How to write a research protocol. *Southern African Journal of Anaesthesia and Analgesia, 22*(4), 101-107. doi:10.1080/22201181.2016.1216664

Sadeghi, M., Babaeian, E., Tuller, T. M., & Jones, S. (2017). The optical trapezoid model: A novel approach to remote sensing of soil moisture applied to Sentinel-2 and Landsat-8 observations. *Remote Sensing of Environment, 198*, 52-68. doi:10.1016/j.rse.2017.05.041

Shrestha, S., Tripathi, G., & Laudari, D. (2018). Groundwater Resources of Nepal: An Overview. In *Groundwater of South Asia* (pp. 169-193). Singapore: Springer.

Sinclair, H., Brown, S., Adhikari, B., Attal, M., Borthwick, A., Budimir, M., Dugar, S. (2017). Improving understanding of flooding and resilience in the Terai, Nepal: 1-5. https://infohub.practicalaction.org/oknowledge/handle/11283/620609

Smith, M., Ustin, S., Adams, J., & Gillespie, A. (1990). Vegetation in Deserts: I. A Regional Measure of Abundance from Multispectral Images. *Remote Sensing of the Environment, 31*, 1-26.

Somvanshi, S., & Kumari, M. (2020). Comparative analysis of different vegetation indices with respect to atmospheric particulate pollution using sentinel data. *Applied Computing and Geosciences, 7*, 100032. doi:10.1016/j.acags.2020.100032

Song, W., Mu, X., Ruan, G., Gao, Z., Li, L., & Yan, G. (2017). Estimating fractional vegetation cover and the vegetation index of bare soil and highly dense vegetation with a physically based method. *International Journal of Applied Earth Observation and Geoinformation, 58*, 168-176. doi:10.1016/j.jag.2017.01.015

Stafford, J. (1988). Remote, non-contact and in-situ measurement of soil moisture content: a review. *Journal of Agricultural Engineering Research, 41*(3), 151-172. doi:10.1016/0021-8634(88)90175-8

Tanre, D., & Kaufman, Y. (1992). Atmospherically resistant vegetation index (ARVI) for EOS-MODIS. *IEEE Transactions on Geoscience and Remote Sensing, 30*(2), 261-270. doi:10.1109/36.134076

Thapa, S., de Jong, J., Subedi, N., Hof, A., Corradini, G., Basnet, S., & Prins, H. (2021). Forage quality in grazing lawns and tall grasslands in the subtropical region of Nepal and implications for wild herbivores. *Global Ecology and Conservation, 30*, e01747. doi:10.1016/j.gecco.2021.e01747

Tillack, A., Clasen, A., Kleinschmit, B., & Forster, M. (2014). Estimation of the seasonal leaf area index in an alluvial forest using high-resolution satellite-based vegetation indices. *Remote Sensing of Environment, 141*, 52-63. doi:10.1016/j.rse.2013.10.018

Tucker, C. (1979). Red and photographic infrared linear combinations for monitoring vegetation. *Remote Sensing of the Environment, 8*(2), 127-150. doi:10.1016/0034-4257(79)90013-0

Upadhyaya, S., Musters, C., Lamichhane, B., Snoo, G., & Thapa, P. (2018). An Insight Into the Diet and Prey Preference of Tigers in Bardia National Park, Nepal. . *Tropical Conservation Science, 11*. doi:10.1177/1940082918799476.

Wang, J., Xiong, Q., Lin, Q., & Huang, H. (2018). Feasibility of using mobile phone to estimate forest LeafArea Index: a case study in Yunnan Pine. *Remote Sensing Letters, 9*(2), 180-188. doi:10.1080/2150704X.2017.1399470

Wang, L., & Qu, J. (2009). Satellite remote sensing applications for surface soil moisture monitoring: A review. *Frontiers of Earth Science in China, 3*, 237-247. doi:10.1007/s11707-009-0023-7

Wang, Q., Adiku, S., Tenhunen, J., & Granier, A. (2005). On the relationship of NDVI with leaf area index in a deciduous forest site. *Remote Sensing of Environment, 94*(2), 244-255. doi:10.1016/j.rse.2004.10.006

Wang, Y., Zhang, Y., Yu, X., Jia, G., Liu, Z., Sun, L., Zhu, X. (2021). Grassland soil moisture fluctuation and its relationship with evapotranspiration. *Ecological Indicators, 131*, 108196. doi:10.1016/j.ecolind.2021.108196

Warren-Wilson, J. (1963). Estimation of foliage denseness and foliage angle by inclined point quadrats. *Australian Journal of Botany, 11*, 95-105. doi:10.1071/BT9630095

Wegge, P., & Storaas, T. (2009). Sampling tiger ungulate prey by the distance method: lessons learned in Bardia National Park, Nepal. *Animal Conservation, 12*(1), 78-84. doi:10.1111/j.1469-1795.2008.00230.x.

Weiss, M., & Baret, F. (2016). S2ToolBox Level 2 products: LAI, FAPAR, FCOVER, Version 1.1. *ESA Contract nr 4000110612/14/I-BG;*, 52.

Weiss, M., Baret, F., Smith, G., Jonckheere, I., & Coppin, P. (2004). Review of methods for in situ leaf area index (LAI) determination: Part II. Estimation of LAI, errors and sampling. *Agricultural and Forest Meteorology, 121*(1-2), 37-53. doi:10.1016/j.agrformet.2003.08.001

Wester, P., Mishra, A., Mukherji, A., & Shrestha, A. (eds) (2019). *The Hindu Kush Himalaya Assessment - Mountains, Climate Change, Sustainability and People.* Springer Nature Switzerland AG, Cham: pp. 627.

WWF. (2021). *Terai Arc Landscape | Nepal*. Retrieved May 29, 2023, from World Wildlife Fund for Nature: https://www.wwfnepal.org/our_working_areas/tal2/

WWF. (2022). *WWF's impact on tiger recovery 2010-2022.* . Retrieved December 05, 2022, from Switzerland: World Wildlife Fund for Nature: https://wwfeu.awsassets.panda.org/downloads/wwf_tx2_impact_report.pdf

Yang, R., Liu, L., Liu, Q., Li, X., Yin, L., Hao, X., Song, Q. (2022). Validation of leaf area index measurement system based on wireless sensor network. *Scientific Reports, 12*, 4668. doi:10.1038/s41598-022-08373-z

Younes, N., Joyce, K., Northfield, T., & Maier, S. (2019). The effects of water depth on estimating Fractional Vegetation Cover in mangrove forests. *International Journal of Applied Earth Observation and Geoinformation, 83*, 101924. doi:10.1016/j.jag.2019.101924

Appendices

Appendix A – Final Protocol

Protocol for the sampling of LAI, FVC, and SSM, within the TAL, Nepal

Introduction and Objectives

Grasslands in the Terai Arc Landscape (TAL) are vulnerable to undergoing successional vegetation change that will result in their transformation to forests. A major driving force in this change is the impact of fluvial processes on groundwater levels, where the TAL is expected to experience decreasing groundwater levels throughout important ecological habitats. Therefore, the need to monitor and model ecohydrological relationships and their feedbacks with successional vegetation change is vital for the conservation of biodiversity in the TAL.

This protocol, forming a part of the "Save the Tigers! Save the Grasslands! Save the Water!" (Tiger) project, aims to address the need for consistent and reliable in-situ data collection for ecohydrological parameters that will provide critical insights towards the ecohydrology of the TAL. The data must be collected across a large spatio-temporal scale to ensure a holistic overview of the TAL is provided as well as to ease in the eventual upscaling of the data and improve future validation of remote-sensing techniques. The protocol is intended for use within the Tiger Project where researchers conducting fieldwork, even if unrelated to the specific objectives of the protocol, can contribute to the data described in the protocol. This necessitates a time-efficient sampling process with few technical requirements.

This protocol is introductory and aims to be dynamic in its application, requiring its implementation across many fieldwork campaigns and invites adaptations and additions when deemed necessary for the enhancement of ecohydrological monitoring in the TAL.

Parameters

Leaf Area Index (LAI) is defined as the one-sided leaf area per unit ground area and has often been related to net radiation, net primary production of a canopy, as well as influencing the partitioning of rainfall between evaporation, throughfall, and runoff. It is included in the protocol as it is widely used to model and monitor interactions between radiation, the water and carbon balances, and plant biomass and productivity (Li et al., 2022). LAI sampling is generally categorised as destructive or non-destructive, with the latter being preferred in the case of this protocol due to time and logistical constraints when sampling in protected wildlife inhabited areas. The indirect methods described in the protocol are for the AccuPAR-LP80 ceptometer, and the PocketLAI smartphone application.

FVC is defined as the fraction of ground, or vertical projection area, covered by vegetation and is closely related to LAI in its applications. It is included in the protocol as it can provide a more detailed analysis of understory and canopy influences on ecohydrological relationships than LAI, providing more information regarding the soil-vegetation interface in relation to evapotranspiration (Li et al., 2022).

Soil moisture is another parameter that is widely used for the study of vegetation and water processes as it plays a significant role in regulating runoff, vegetation production, and evapotranspiration (Adab et al., 2020). Surface soil moisure (SSM) in particular refers to the water content of the top ~15cm of the soil layer and is an important parameter in describing fundamental water and energy fluxes at the land surface/atmosphere interface (Wang & Qu, 2009).

Plot Selection

Completely unbiased, randomized plot selections is not feasible in the region of interest, primarily due to accessibility and safety concerns. Given the aim of the protocol to be used by a variety of researchers conducting independent fieldwork that does not necessarily reflect the protocol's specific aims, the plots are likely to be selected based upon sampling selection regarding other research objectives. When sampling specifically to test the protocol to validate the methods or contribute to the protocol, it is essential that a variety of vegetation classes are selected. In short, there is no distinct guide as of yet, for plot selection and in reality this should be determined largely by the local collaborators what is possible in terms of safety.

Field Plot Layout
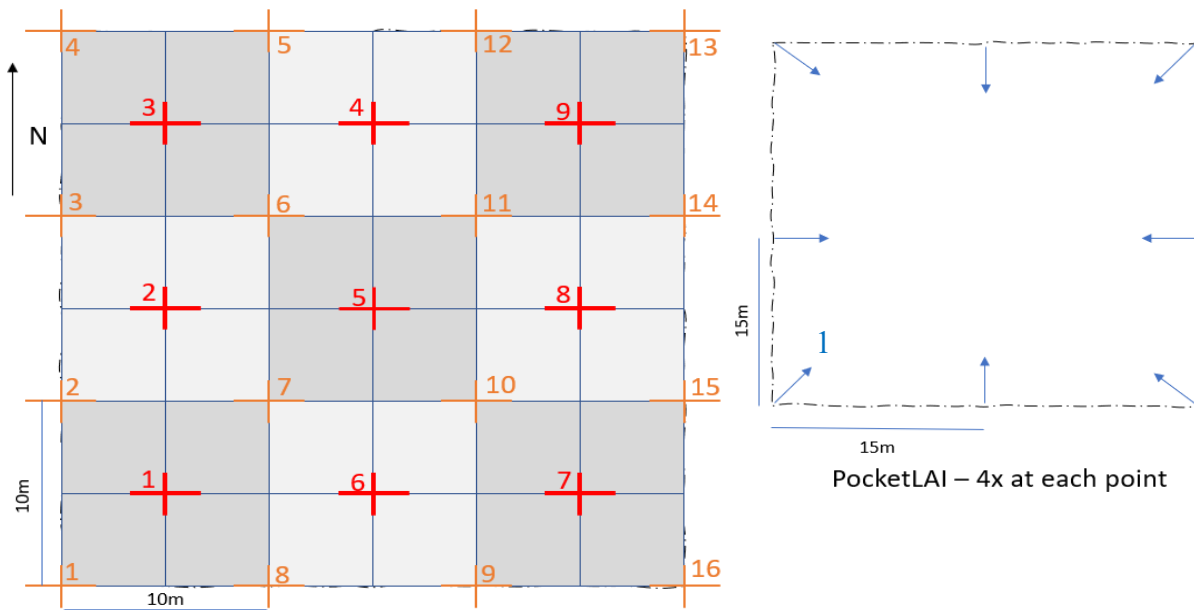
Field plot layout for the sampling of LAI, FVC, and SSM.

The field plot shown in the figure is suggested for the sampling of LAI using the AccuPAR-LP80 and PocketLAI, FVC for understory and canopy through visual estimation, and SSM using the SM-150T. Point measurements should be taken in a snake pattern (as indicated) starting in a south-north direction as this will help comparability between repeat samplings.

The plot borders and, if possible, 5m transects, should be marked using a rope or similar whilst sampling to ensure point measurements are consistent in their locations, this will also considerably speed up data collection. The coordinates of the centre point and the four corners of the plot should be taken.

Sampling Methods

Plots must be sampled within 2 hours of solar noon, approximately 10:00-14:00, however solar noon changes as the year progresses and should therefore be noted for the sampling period. Ideally, sampling as close to solar noon as possible, particularly in winter when beam radiation is generally lower than in summer. The time at which the sampling process for each parameter begins and ends should be noted. Sampling should take place in clear sky conditions, especially when using the AccuPAR, however if this is not possible the sky conditions should be observed and described. The dominant vegetation class (forest, grassland) of the plot should be noted and if possible, further classification (Sal forest, riverine forest, short grasslands, tall grasslands) as well as dominant vegetation species can be noted as this will enable further detailed analysis if desired and can potentially contribute to other investigations within the Tiger Project. This classification of vegetation should be done in collaboration with local knowledge on the species and vegetation in the region. Canopy vegetation is regarded as vegetation with a height >1.5m and understory as <1.5m. If there is no distinct understory-canopy separation or it is clear 1.5m is not the threshold height for a specific plot this should be noted and the relevant adjustments to understory and canopy measurements made where possible.

Other general remarks regarding observations of any other details regarding external (e.g., wind, weather) or plot-specific aspects (e.g., burnt or cut vegetation) are recommended. The relevant safety considerations should be employed upon consultation with local collaborations for samplings within wildlife inhabited areas. This includes but is not limited to working in pairs (up to 4 people in more dense vegetation) and sampling with a guide or person with similar experience and knowledge present. It is estimated that 30 minutes is needed for the sampling of all three parameters according to the field plot layout, where one researcher is responsible for LAI and another for SSM. This may take longer depending on the density of the understory making movement between point measurements, as well as SSM sampling, more difficult. All data should be stored electronically and uploaded or sent to the relevant database or researchers responsible for data treatment.

Leaf Area Index

<u>AccuPAR-LP80</u>

Before sampling it is necessary to calibrate and input the location and local time as per the manual (http://publications.metergroup.com/Manuals/20442_LP-80_Manual_Web.pdf). It is imperative that throughout all measurements, the device is held level.

Canopy LAI measurements (~10 minutes):

1. Take an above-canopy PAR incident measurement (pressing the up arrow) in an open clearing with no vegetation obstructing the sun and the sky directly above the point. If need be, measurements within a 5-minute walk from the plot can be taken if no such clearing is available within the plot.
   - Ensure the number of active segments is 8.
   - Record the PAR, f_b and zenith values.
   - Suggested to take and clear multiple readings noting the PAR values each time ensuring they do not fluctuate before taking the incident measurement to be used.

2. Start taking below-canopy measurements (pressing the down arrow) following the numbering as indicated in the field plot layout.
   - Hold the AccuPAR at ~1.5m, ensuring that it is level.
   - Try to avoid large woody elements that may strongly influence LAI. E.g., avoid positioning a large trunk or thick branches between the AccuPAR and the sun.
   - Note the PAR value at each point and ensure that it does not exceed the incident measurement. If a below-canopy PAR greatly exceeds the above-canopy PAR ($>{\sim}100\mu mol.m^{-2}.s^{-2}$), it indicates that the sky or light conditions have changed since the time of taking the incident measurement. Restart the sampling.
   - Note cloud coverage when sampling in variable light conditions. If a cloud obstructs the sun, pause measurements until the light conditions return to that at the time of the incident measurement. Considering the measurements take approximately 10 minutes, it is recommended to restart the process if a change in light conditions occurs (as with the previous point).
   - Take each measurement when no wind is present.

3. Upon completing measurement at point 16, record the LAI shown on the AccuPAR.

4. Go back to the incident measurement point and repeat the incident measurement, once more noting PAR, f_b and zenith values. In the case where PAR or f_b ($>{\sim}0.1$) has

changed drastically, it is recommended to repeat the measurement process as these values should not vary much within 10 minutes.

All PAR values as well as the incident zenith and f_b values are noted so that LAI can be manually calculated to determine the LAI at each point measurement if needed, using the equation provided in the manual.

Understory LAI measurements (~5 minutes):

1. Note the spatial variation of understory vegetation, including density, size, and fractional cover of the different types of vegetation present. Note the location of shady and sunny areas.
   o This is to guide step 4 for the sampling of the understory present to ensure the measurements are representative of the different vegetation and conditions of the understory.
2. Change the number of active segments to 2, following the instructions in the manual.
   o This allows for smaller vegetation to be sampled more accurately as it changes the effective length of the AccuPAR to 20cm.
   o Using tape, mark 20cm from the tip (60cm from the body of the device), to make it easier to visualise the active portion of the light bar.
3. Repeat step 1. as for the canopy LAI measurements.
4. Take 16 point measurements of the understory, following the same process as in step 2 for canopy LAI measurements.
   o Use step 1 to guide the proportion of measurements for different conditions and vegetation. E.g., if ~75% of understory of similar vegetation type is in the shade, ensure that ~12 measurements of the understory are in shady areas. Use own judgement when a combination of conditions and different vegetation types are observed to ensure the 16 points are representative.
   o Hold the AccuPAR 20cm from the ground beneath the understory vegetation being sampled, ensuring it is level at the instant of sampling.
5. Repeat steps 3 and 4 for the canopy LAI measurements.

<u>PocketLAI</u>

Before sampling, read through help section within the application.

Canopy LAI measurements (~5 minutes):

1. In the application, set the number of averaged shots to 4.
2. Start canopy measurements at point 1, as indicated in the field plot layout. Move clockwise around the plot for each subsequent measurement.

    o Ensure camera of smartphone is wiped clean before sampling, suggested to wipe camera before each point.

    o Hold phone on its side at a height of ~1.8m, ensuring the angle portrayed on the screen is 90 degrees. Push camera icon to start measurements. Once a vibration is felt slowly rotate phone upwards, keeping the height of ~1.8m, until 57 degrees is shown on the screen. The phone will vibrate again at this point indicating that a reading has been taken. Repeat 4 times at each point and note the average LAI as displayed on the screen. This average and all LAI values are stored in the application.

    o In non-continuous canopies, trees and other vegetation that are not located in the plot may be included in the calculations and thus impacting the accuracy of the plot estimate. Confirm that the application is determining the canopy LAI by watching the preview as shown on the screen and if other vegetation is included, note the point and what was observed in the preview camera.

    o Avoid tree trunks and other obstructions directly in front of the camera. Similar to above point, confirm via the preview camera that the canopy is in view. Move to the right or left of the point of measurement, or adjust the height of the phone, if need be, to avoid these obstructions.

3. Average the 8 LAI averages (4 points each), as recorded for each point, to obtain plot canopy LAI.

Understory LAI measurements (~5 minutes):

1. In the application, set the number of averaged shots to 8.
2. Repeat step 1 of the understory LAI measurements described for the AccuPAR.
3. Take 16 point measurements of the understory, following the same guideline regarding representative measurements described in step 4 of the understory LAI measurements described.

- o For vegetation that has a distinct stem and leaves, ensure the phone is held high enough to capture the leaves and not the stem (or the gap between the ground and the leaves). For other vegetation, hold the phone at ground level ~15cm away from the base of the vegetation.
- o The application does not support 16 averaged shots, therefore take two sets of 8 point measurements. Make sure not average LAI after the first 8 readings before moving to the next 8.

4. Average the 2 LAI averages (8 points each) to obtain the plot understory LAI.

<h3 style="text-align:center">Fractional Vegetation Cover</h3>

<u>Visual Estimation</u> (~5 minutes):

It will improve the reliability of the results if at least two researchers independently carry out the plot fractional cover estimations to minimise the subjectivity of the method. If this is not possible, it is recommended at the beginning of a fieldwork campaign to 'calibrate' the visual estimations. This can be done in collaboration with another researcher and independently estimating canopy and understory cover. If values differ significantly, discuss process of estimation pointing out specific gaps observed in vegetation. Repeat until estimations are generally within 5-10% of each other. Recommended to collaborate with a person having strong vegetation background if possible.

1. Stand in the middle of the 10m squares shown in the field plot layout. This corresponds to SSM points, and it is recommended to carry out the visual estimations after SSM measurements have been taken, as the points of these measurements (clearly visible as areas with smoothed soil) will provide a specific point to stand and conduct visual estimations.

2. Estimate understory cover as fraction of leaves (excluding litter) covering bare ground within the 10m square.

3. Estimate canopy cover as fraction of leaves obstructing sky within the 10m square.
   - o For both steps 2 and 3, it is suggested to visually quadrat the 10m square (essentially creating 4x 5m squares) and from the standing position estimate the cover of the 5m squares and averaged for a 10m square estimate. This can make it easier to visually estimate when vegetation changes drastically within the 10m square.
   - o For canopy estimation, it is suggested to walk in a two-step radius from the standing position to confirm that all canopy elements were considered and no

over- or underestimation occurred as a result of parts of the canopies being hidden by lower leaves.

4. Average the 9 fractional understory (canopy) measurements to provide a plot fractional understory (canopy) cover estimate.

Surface Soil Moisture

SM150T (~15 minutes):

Before sampling, read through manual supplied by Delta-T Devices (https://delta-t.co.uk/wp-content/uploads/2017/01/SM150T-user-manual-version-1.0.pdf).

1. Ensure that the reading device (HH150T) attached to the SM150T is set to read 'mineral', following the instructions in the manual.

2. Clear ground vegetation at each of the points indicated in field plot layout, ensuring that bare soil is visible with as little obstruction as possible. Take care not to compact or dig at the points, rather scrape away any vegetation. If thick stems are present, clear ground vegetation as close to original point as possible and take measurement there.

3. Gently push SM150T into soil until the steel rods are fully inserted. Ensure good contact with soil. I.e., when pushing SM150T there must be some resistance as the rods are pushed into the ground, if the rods seem to 'float in', take measurement nearby where there is good soil contact.
   o If strong resistance is felt, do not push harder as the rods may be hitting a rock and may be damaged with further force. Rather take measurement at a new location.
   o Avoid locations with holes in the soil as a result of insects, mice, or other animals.

4. Push the 'on' button (only once the rods are inserted) and press 'read' to display a percentage on the HH150T. Repeat until this percentage stabilizes on one value and note the final percentage.

5. Average the 9-point measurements to provide the plot SSM.

Appendix B – Plots and Raw Data

Thesis Plots – Testing Protocol

All plots with a 'P' (GP, SP, RP), indicate protocol plots. Further results regarding the protocol plots are available upon request

Plot	Date	Time	Latitude	Longitude	Vegetation Class	LAI Accupar	PocketLAI Border	PocketLAI Center	Average PocketLAI	SSM	FVC Canopy	FVC Understory	Understory Accupar	Understory PocketLAI	Plot Estimate Accupar	Plot Estimate PocketLAI
G1	2023/02/17	10:30	28.536909	81.292703	Grassland					20.5	0%	81%	2.72	2.64	2.20	2.14
G2	2023/02/21	10:30	28.514406	81.287194	Grassland					21.2	0%	36%	0.83	0.95	0.30	0.34
G3	2023/02/21	13:00	28.504745	81.288003	Grassland					10.1	0%	59%	3.13	2.49	1.85	1.47
G4	2023/02/23	10:30	28.468553	81.229838	Grassland	0.1	0.16	0.22	0.19	17.1	10%	43%	1.74	1.36	0.81	0.68
G5	2023/02/23	11:30	28.458412	81.226719	Grassland					10.1	0%	21%	1.38	1.1	0.29	0.23
G6	2023/02/23	12:30	28.439890	81.224676	Grassland	0.3	0.36	0.27	0.315	13.1	25%	67%	3.37	3.14	2.36	2.22
G7	2023/02/26	12:00	28.456384	81.238361	Grassland	0.49	0.61	0.5	0.555	27.2	30%	36%	4.31	2.9	1.87	1.43
GP1	2023/02/05	15:00	28.509434	81.252267	Grassland					39.5	0%	100%	3.85	3.72	3.85	3.72
GP2	2023/02/06	10:00	28.493630	81.262683	Grassland					11.4	0%	38%	2.69	2.46	1.02	0.93
GP3	2023/02/05	10:30	28.449808	81.225277	Grassland					23.6	0%	70%	1.87	2.26	1.31	1.58
M1	2023/02/16	12:30	28.580650	81.288536	Mixed	1.71	1.39	1.19	1.29	12.7	32%	81%	3.88	2.79	3.47	2.52
M2	2023/02/21	11:00	28.520443	81.290185	Mixed	1.2	1.45	1.21	1.33	16.9	34%	38%	2.53	2.55	1.71	1.87
R1	2023/02/23	13:30	28.437982	81.227425	Riverine	1.87	1.16	0.86	1.01	7.2	23%	72%	3.66	2.51	3.16	2.13
R2	2023/02/26	10:00	28.466926	81.243085	Riverine	1.88	1.72	1.81	1.765	20.6	42%	56%	3.36	2.74	2.71	2.29
R3	2023/02/26	11:00	28.463917	81.234192	Riverine	1.55	1.48	1.17	1.325	17.9	55%	77%	3.85	2.66	3.32	2.39
R4	2023/02/26	13:30	28.469622	81.229241	Riverine	2.69	1.67	1.49	1.58	15.4	53%	59%	4.94	3.49	4.02	2.74
RP1	2023/02/08	13:00	28.469078	81.248292	Riverine	2.85	2.08	1.83	1.955	9.7	55%	28%	3.83	2.93	3.12	2.32
RP2	2023/02/08	11:30	28.465043	81.245155	Riverine	2.33	2.75	2.34	2.545	18.7	61%	26%	3.56	3.2	2.65	2.87
RP3	2023/02/07	13:00	28.477138	81.236825	Riverine	2.28	1.86	1.31	1.585	17.8	32%	64%	4.68	3.14	3.82	2.68
RP4	2023/02/07	10:30	28.470061	81.245002	Riverine	3.9	2.83	2.52	2.675	53.2	80%	27%	4.69	3.29	4.11	2.95
S1	2023/02/16	10:30	28.604078	81.278895	Sal	2.13	2.06	2.14	2.1	10.4	49%	71%	3.54	3.3	3.13	2.94
S2	2023/02/16	11:30	28.593575	81.284609	Sal	2.37	1.94	2	1.97	15.5	38%	68%	4.05	3.3	3.51	2.86
S3	2023/02/16	14:30	28.536024	81.292297	Sal	3.09	2.16	2.11	2.135	15.4	72%	57%	4.97	3.47	4.16	2.91
S4	2023/02/17	11:30	28.551629	81.275424	Sal	1.44	2.2	1.84	2.02	15.4	63%	34%	2.87	2.8	1.93	2.40
S5	2023/02/17	13:00	28.552282	81.263826	Sal	2.29	2.7	2.5	2.6	12.1	83%	2%			2.24	2.65
S6	2023/02/17	13:30	28.532011	81.263262	Sal	1.92	2.67	2.31	2.49	22.5	71%	49%	2.74	2.96	2.32	2.81
S7	2023/02/21	12:00	28.508595	81.288392	Sal	2.19	2.55	2.54	2.545	18.3	63%	9%	3.56	3.1	2.31	2.60
SP1	2023/02/05	13:00	28.500998	81.258293	Sal	2.31	2.37	2.19	2.28	18.5	70%	18%	3.06	3.22	2.45	2.52
SP2	2023/02/05	13:30	28.493630	81.262683	Sal	2.21	2.1	2.06	2.08	17.5	53%	64%	3.38	3.21	2.96	2.81
SP3	2023/01/31	12:30	28.472557	81.255816	Sal	3.16	2.81	2.39	2.6	17.1	67%	10%			2.84	2.53

HAS Plots – Testing Protocol

Plot properties and in-situ data collected by HAS

	Plots	Date	Time of Sampling	Latitude	Longitude	Vegetation Class	AccuPAR LAI	PocketLAI LAI	SSM
Karnali	B_M_7	20/03/2023	10:40	28.613185900	81.297214700	Forest	1.65	1.13	10.18
	B_S_2	14/03/2023	11:00	28.469679500	81.229289100	Riverine	2.39	2.16	10.28
	B_S_3	14/03/2023	13:05	28.463981200	81.234020500	Riverine	1.22	1.88	14.77
	B_S_7	15/03/2023	10:30	28.551735000	81.275368800	Sal	1.69	1.77	18.78
	B_S_8	15/03/2023	13:04	28.580587800	81.288541600	Mixed	2.98	1.05	14.5
	B_S_9	15/03/2023	14:45	28.604008700	81.279084500	Sal	2.27	1.63	8.91
Babai (BNP)	B_B_B4	23/03/2023	10:30	28.442970792	81.537316819	Sal	0.53	0.51	
	B_B_B6	23/03/2023	12:30	28.452337526	81.537631027	Sal	3.24	1.68	19.53
	B_B_C2	24/03/2023	10:20	28.431838337	81.574267034	Sal	1.9	1.69	20.41
	B_B_C5	24/03/2023	12:50	28.440219539	81.578230237	Forest	2.71	1.86	21.03
	B_B_D3	25/03/2023	13:45	28.405063352	81.608870924	Sal	0.96	1.94	19.32
	B_B_E5	26/03/2023	12:50	28.419353908	81.549035077	Forest	3.04	1.9	27.04
	B_B_E6	26/03/2023	14:20	28.416407138	81.550259457	Mixed	3.18	1.37	16.52
Shuklaphanta (TAL)	S_F_2	06/04/2023	10:00	28.887882899	80.237270471	Riverine	2.9	2.03	
	S_F_3	06/04/2023	11:30	28.865500435	80.218583284	Sal	1.07	1.26	
	S_F_4	06/04/2023	12:40	28.929203020	80.172086203	Sal	1.59	1.2	
	S_F_5	06/04/2023	13:45	28.938105169	80.166300532	Sal	2.36	1.82	
	S_C_2	07/04/2023	10:20	28.884828369	80.239125279	Riverine	4.01	1.93	
	S_C_4	07/04/2023	12:30	28.884394036	80.254091463	Sal	1.7	1.83	
	S_C_5	07/04/2023	14:40	28.910301011	80.259070284	Sal	3.05	2.1	
	S_M_1	10/04/2023	10:00	29.014611847	80.351278919	Riverine	0.75	1.34	
	S_M_2	10/04/2023	11:00	29.006078990	80.346474784	Riverine	1.84	1.22	
	S_M_3	10/04/2023	13:00	28.998172269	80.340658922	Riverine	2.14	1.55	
	S_M_4	10/04/2023	14:00	28.989495585	80.335766984	Sal	2.03	1.72	
	S_O_3	11/04/2023	13:20	28.891502748	80.134256826	Forest	1.04	0.83	
	S_O_4	11/04/2023	14:15	28.902084582	80.126850992	Forest	3.09	1.9	
Chitwan (TAL)	C_A_4	25/4/2023	11:30	27.565690172	84.477205872	Riverine	4.8	1.97	
	C_A_5	25/4/2023	12:40	27.571918141	84.489888743	Riverine	2.48	1.94	
	C_C_2	28/4/2023	10:10	27.509312537	84.277803542	Sal	0.85	1.74	
	C_C_3	28/4/2023	11:15	27.517804794	84.284020450	Sal	0.59	1.74	
	C_C_4	28/4/2023	12:30	27.528008990	84.287667113	Sal	0.53	1.71	
	C_C_5	28/4/2023	13:15	27.537302461	84.291640440	Sal	0.43	1.93	
	C_D_4	30/4/2023	11:10	27.553667066	84.383271265	Sal	0.7	1.89	
	C_D_5	30/4/2023	12:15	27.555165081	84.342044247	Riverine	1.17	1.9	

Satellite Data

The following table shows the satellite data and products used for the plots of this thesis.

Plot	Sense Date	SNAP LAI	SNAP FCover	NDVI	SAVI	ARVI	Level-1C Product
G1	22-Feb	0.44	21%	0.48	0.27	0.42	
G2	22-Feb	0.32	12%	0.29	0.14	0.24	
G3	22-Feb	0.45	23%	0.46	0.26	0.38	
G4	22-Feb	0.33	12%	0.32	0.15	0.27	S2A_MSIL1C_20230222T050821_N0509_R019_T44RNS_20230222T065625
G5	22-Feb	0.31	7%	0.19	0.07	0.13	
G6	22-Feb	0.29	15%	0.38	0.21	0.29	
G7	22-Feb	0.34	15%	0.36	0.17	0.31	
GP1	07-Feb	0.28	16%	0.44	0.26	0.34	
GP2	07-Feb	0.23	9%	0.29	0.16	0.17	S2B_MSIL1C_20230207T050959_N0509_R019_T44RNS_20230207T065750
GP3	07-Feb	0.33	4%	0.17	0.06	0.15	
M1	22-Feb	0.85	30%	0.56	0.28	0.53	
M2	22-Feb	0.62	25%	0.45	0.22	0.42	
R1	22-Feb	0.60	27%	0.51	0.28	0.49	S2A_MSIL1C_20230222T050821_N0509_R019_T44RNS_20230222T065625
R2	22-Feb	0.65	26%	0.53	0.26	0.53	
R3	22-Feb	0.59	25%	0.49	0.24	0.50	
R4	22-Feb	0.87	32%	0.56	0.28	0.57	
RP1	07-Feb	1.20	39%	0.69	0.37	0.71	
RP2	07-Feb	0.88	32%	0.65	0.32	0.67	S2B_MSIL1C_20230207T050959_N0509_R019_T44RNS_20230207T065750
RP3	07-Feb	0.86	29%	0.63	0.29	0.66	
RP4	07-Feb	1.28	40%	0.69	0.36	0.73	
S1	22-Feb	1.20	37%	0.62	0.31	0.58	
S2	22-Feb	1.16	35%	0.63	0.31	0.62	
S3	22-Feb	1.12	38%	0.58	0.31	0.59	
S4	22-Feb	1.27	40%	0.65	0.35	0.65	S2A_MSIL1C_20230222T050821_N0509_R019_T44RNS_20230222T065625
S5	22-Feb	1.25	40%	0.62	0.34	0.62	
S6	22-Feb	1.20	38%	0.60	0.31	0.58	
S7	22-Feb	1.16	38%	0.59	0.32	0.56	
SP1	07-Feb	1.55	44%	0.76	0.39	0.80	S2B_MSIL1C_20230207T050959_N0509_R019_T44RNS_20230207T065750
SP2	07-Feb	1.47	42%	0.74	0.36	0.79	
SP3	23-Jan	1.53	42%	0.79	0.38	0.81	S2A_MSIL1C_20230123T051111_N0509_R019_T44RNS_20230123T065715

The following table presents the satellite data and products for the HAS plots.

Plot	Sense Date	SNAP LAI	NDVI	SAVI	ARVI	Level-1C Product
B_M_7	24-Mar	1.16	0.59	0.32	0.49	S2A_MSIL1C_20230324T050651_N0509_R019_T44RNS_20230324T070313
B_S_2	14-Mar	1.31	0.62	0.36	0.62	
B_S_3	14-Mar	0.62	0.48	0.23	0.46	
B_S_7	14-Mar	1.17	0.56	0.30	0.50	S2A_MSIL1C_20230314T050651_N0509_R019_T44RNS_20230314T070304
B_S_8	14-Mar	0.79	0.52	0.27	0.46	
B_S_9	14-Mar	1.18	0.58	0.32	0.51	
B_B_B4	24-Mar	0.38	0.40	0.25	0.21	
B_B_B6	24-Mar	1.39	0.64	0.38	0.54	
B_B_C2	24-Mar	1.70	0.72	0.40	0.66	
B_B_C5	24-Mar	1.29	0.65	0.36	0.56	S2A_MSIL1C_20230324T050651_N0509_R019_T44RNS_20230324T070313
B_B_D3	24-Mar	1.65	0.76	0.43	0.71	
B_B_E5	24-Mar	1.87	0.79	0.49	0.76	
B_B_E6	24-Mar	1.41	0.69	0.37	0.63	
S_F_2	11-Apr	2.80	0.82	0.53	0.84	
S_F_3	11-Apr	0.83	0.50	0.30	0.39	
S_F_4	11-Apr	1.14	0.65	0.36	0.56	
S_F_5	11-Apr	1.42	0.67	0.39	0.58	
S_C_2	11-Apr	2.44	0.81	0.52	0.83	
S_C_4	11-Apr	1.13	0.63	0.32	0.56	
S_C_5	11-Apr	1.33	0.61	0.37	0.53	S2B_MSIL1C_20230411T051649_N0509_R062_T44RMT_20230411T071407
S_M_1	11-Apr	0.76	0.50	0.28	0.41	
S_M_2	11-Apr	0.80	0.55	0.30	0.47	
S_M_3	11-Apr	0.80	0.55	0.30	0.47	
S_M_4	11-Apr	1.38	0.68	0.39	0.64	
S_O_3	11-Apr	0.72	0.51	0.28	0.43	
S_O_4	11-Apr	1.50	0.72	0.41	0.71	
C_A_4	25-Apr	2.25	0.79	0.50	0.83	
C_A_5	25-Apr	2.30	0.79	0.48	0.83	
C_C_2	25-Apr	0.68	0.47	0.25	0.38	
C_C_3	25-Apr	0.63	0.46	0.24	0.37	S2B_MSIL1C_20230425T045659_N0509_R119_T45RTL_20230425T065542
C_C_4	25-Apr	0.36	0.33	0.17	0.22	
C_C_5	25-Apr	0.61	0.43	0.24	0.33	
C_D_4	25-Apr	0.90	0.51	0.29	0.43	
C_D_5	25-Apr	2.04	0.76	0.47	0.78	

Furthermore, the subsets for each product were created using the following coordinates.

Subset	Babai	SNP	CNP
N	28.46	29.03	27.59
W	81.53	80.1	84.26
S	28.4	28.85	27.49
E	81.62	80.37	84.51

Appendix C – Supplementary Results and Analysis

Protocol Development – Results and discussion

All accompanying statistical results for this section can be found at the end of this report in Appendix F. Raw data can be made available upon request.
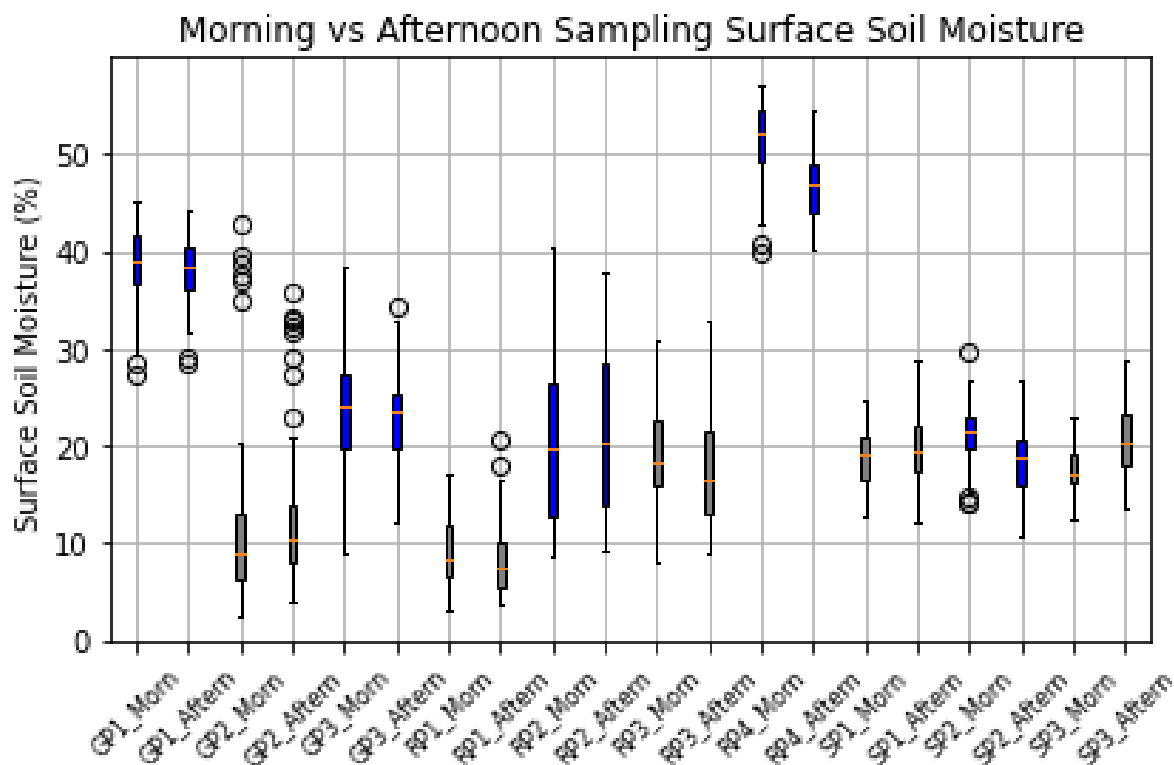

Figure 28. Boxplots of SSM measurements taken at the 10 protocol plots comparing morning sampling with afternoon sampling.

Figure 29 shows the boxplots describing the SSM data obtained at the 10 protocol plots at the different sampling periods. Four plots (RP3, RP4, SP2, and SP3) showed significant differences (p-value<0.05) between SSM measurements taken in the morning and the afternoon. No discernible patterns were observed however, when differences were significant. Some instances saw the morning giving higher estimates (RP3-4 and SP2), whilst the afternoon for SP3 gave a higher estimate. Notable differences in weather were observed for plots RP3 and RP4 for the different sampling periods (overcast conditions and clear sky conditions in the morning and afternoon respectively for RP3 and vice versa for RP4), however the pattern is not consistent with these conditions (RP3 when overcast had a higher SSM whilst the opposite was true for RP4). This points to a variability in SSM that is sensitive to more than one external factor (such

as humidity, wind, temperature) all of which may have experienced small or even significant changes between the times of sampling that could have affected SSM at the plots. These differences were less pronounced when visualized with only RP4 and SP3 indicating ranges that lay outside of each other. Additionally, the means of the soil moisture for these plots differed by at most, 6% (RP4). Therefore, for the purpose of this study, it was concluded that measurements could be taken in the morning or afternoon to obtain a representative estimate of the plot, noting a range of 10%.

The LAI readings obtained by the AccuPAR were first investigated to determine whether two perpendicular readings at each point to decrease the chance of error as a result of light penetration would give different estimates to just one measurement at each point. No statistical differences were observed (lowest p-value = 0.2 for the plot RP3). Therefore, the AccuPAR LAI readings obtained by recording only one measurement at each sampling point was deemed suitable and these values were used for all subsequent analyses involving the AccuPAR.
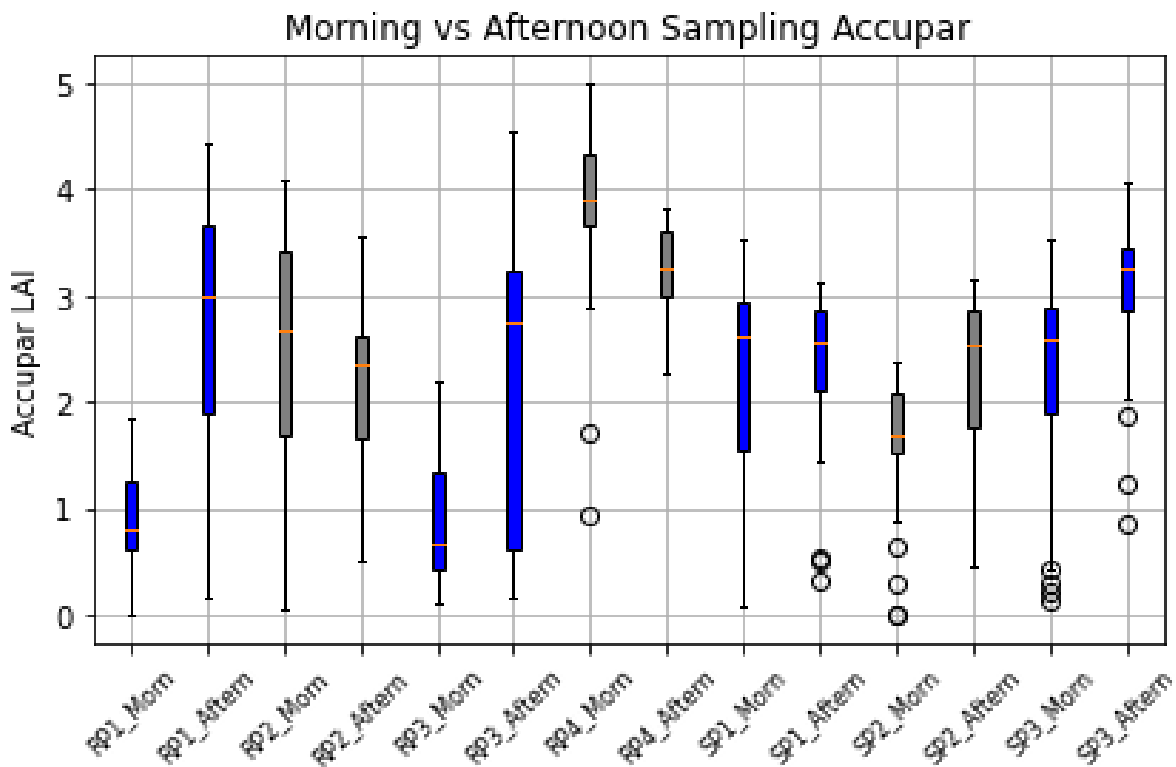

Figure 29. Boxplots of AccuPAR LAI canopy measurements taken at the 10 protocol plots comparing morning sampling with afternoon sampling.

The AccuPAR results for LAI taken in the morning and afternoon with the AccuPAR (figure 30) show larger and more frequently observed differences than the SSM results, indicating that whether measurements are taken in the morning or afternoon will influence the reliability of

results obtained. However, no patterns emerge once more when solely looking at morning measurements against afternoon measurements. The differences are therefore rather a direct effect of the sky conditions at the time of measurement and is reflected when looking at the incident above-canopy PAR readings and f_b values. f_b values <0.1 generally indicate overcast conditions (Pokovai & Fodor, 2019), as was observed in the field for morning measurements at RP1 and RP3 as well as afternoon measurements for RP4. These low f_b values combined with low above-canopy PAR values, results in the AccuPAR underestimating LAI especially in closed canopied as differences in above and below-canopy PAR values become less pronounced, impacting the ratio that calculates LAI This agrees with results from Pokovai & Fodor (2019) who also noted underestimations in overcast conditions. In more ideal conditions (increased PAR and f_b values), no significant differences were observed for RP2 and SP1, however were observed for both SP2 and SP3. This was attributed primarily to the angle of light penetration through the canopy and although is a direct result of measurements taken at different times, is not necessarily a result of morning measurements or afternoon measurements but rather a result of the canopy structure present at each plot.

Despite this, as can be seen in figure 30, there were still large overlaps in the total range of LAI values observed for SP2 with the mean plot canopy LAI differing by 0.6. As canopy structure was not being directly investigated in this research, it was concluded that AccuPAR LAI measurements could be taken in the morning or afternoon as long as non-ideal conditions were avoided to obtain a representative LAI of the plot, noting a possible variance of $0.6m^2m^{-2}$. Measurements should also be taken even closer to solar noon to avoid these differences in the angle of light penetration and reduce the potential variance as a result of canopy structure. Furthermore, it is suggested that the plots should be sampled in a consistent cardinal direction. This would enable potential future analysis, if desired, to compare the effects of the movement of sun on the standard deviations observed within the plot for a specific canopy type. This could provide further insight and improvements when using gap fraction instruments to estimate the LAI. Orienting plots consistently would also help compare specific point measurements for repeated sampling.
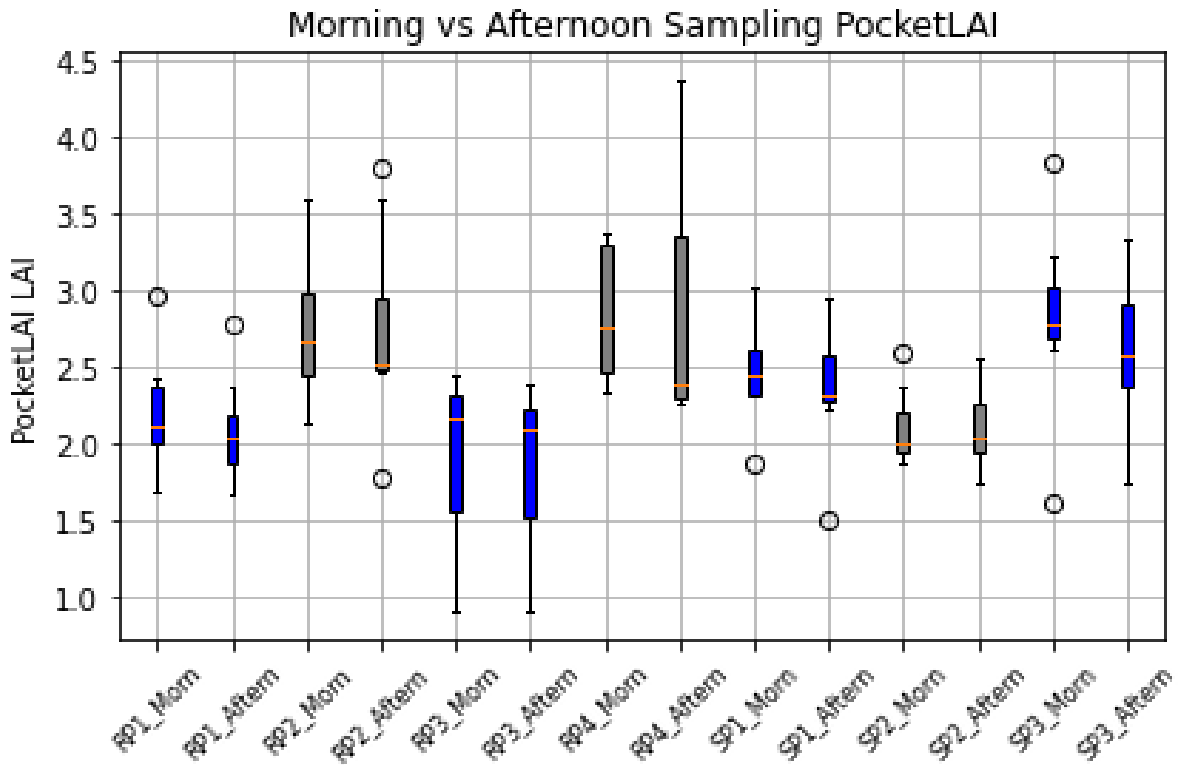
Figure 30. Boxplots of PocketLAI LAI canopy measurements taken at the 10 protocol plots comparing morning sampling with afternoon sampling.

The time of sampling had little effect on the results obtained from the PocketLAI border measurements with only SP1 having a p-value <0.05 (0.04). In any case, the difference in the means obtained for this plot (2.49 for the morning and 2.37 for the afternoon) prove to be small in the context of the protocol aim – representative measurements. Therefore, it was concluded that the time of measurements would not impact the reliability of the LAI estimates provided by the PocketLAI. Furthermore, these results were more consistent and showed less dependency on 'ideal' conditions than the AccuPAR, as significant differences were not observed despite each plot being taken under the same conditions as those for the AccuPAR.
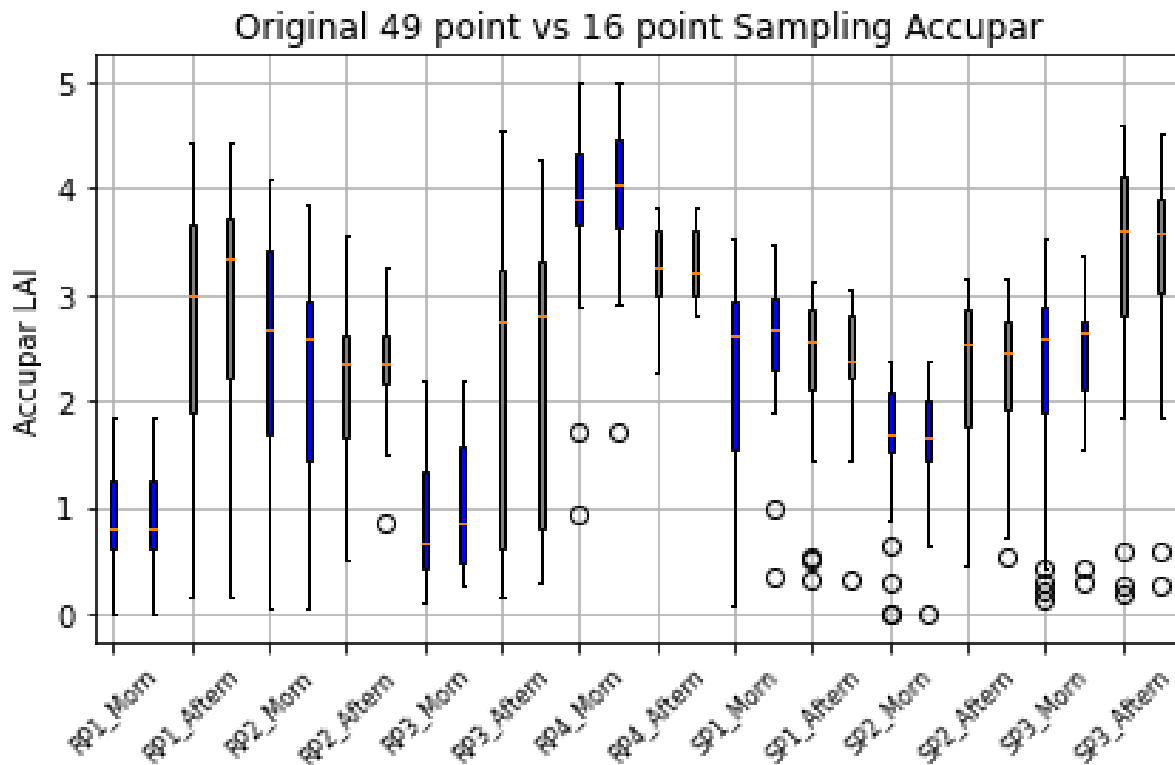
Figure 31. Boxplots comparing full 5m x 5m grid (49 points) measurements and reduced 10m x 10m grid (16 points) taken at the 10 protocol plots. Both sampling periods were included in the analysis to increase the number of data points as differences in time were not being investigated, only the number of points taken when sampling.

Figure 32 shows boxplots comparing canopy LAI estimates for the plots using 49 points of measurement and 16 points of measurement. There were no significant differences observed when reducing the number of sampling points from a 5m x 5m grid (49 points) to a 10m x 10m grid (16 points), indicating that 16 points, as taken in the proposed grid, is a reliable method to obtain an estimation of the plot LAI with a reduced number of measurements. Only the morning measurements at SP1 (p-value = 0.33) showed a reduced range in results when averaging 16 points as opposed to 49, indicating a loss in describing the intra-plot LAI variations. However, the means, and therefore the overall plot estimates which are of greater interest in this study, still gave similar values (2.4 and 2.2 respectively).

For all subsequent analyses, the 16-point plot AccuPAR LAI results are therefore used for the canopy LAI for the protocol plots. Additionally, only one measurement (morning or afternoon) at each plot was used and therefore those taken in the most 'ideal' conditions (high incident above-canopy PAR and closest to solar noon). The corresponding PocketLAI estimates on the same day and time period of sampling were used for the PocketLAI canopy estimates.
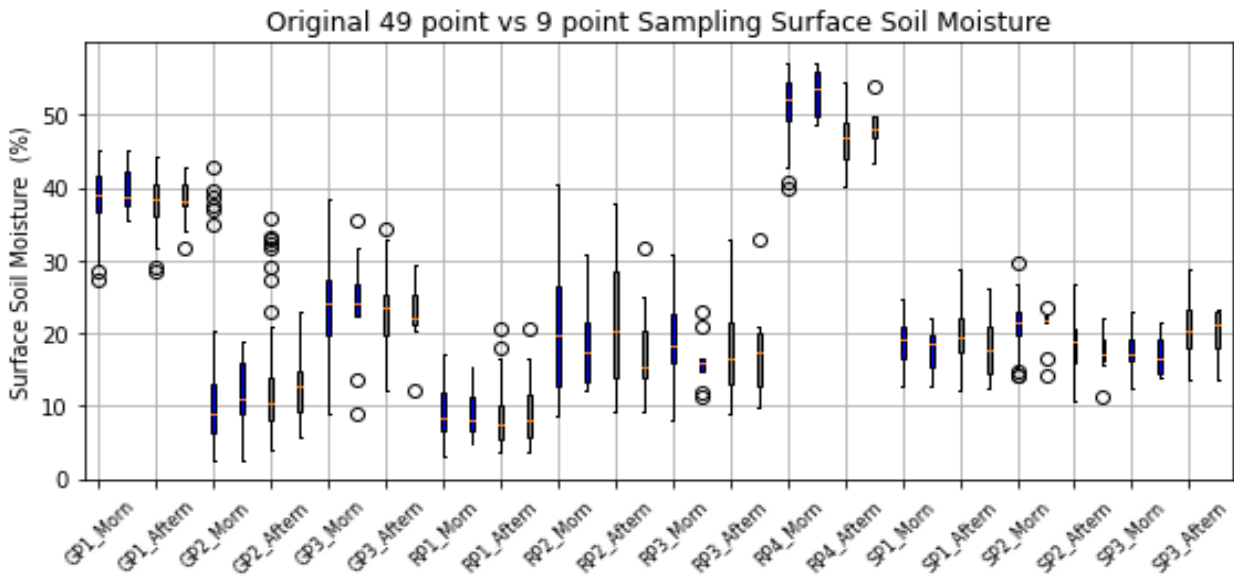
Figure 32. Boxplots comparing full 5m x 5m grid (49 points) measurements and reduced 9-point grid taken at the 10 protocol plots. As with the AccuPAR, both sampling periods were included in the analysis to increase the number of data points as differences in time were not being investigated, only the number of points taken when sampling.

There was only one significantly different result (RP3 morning; p-value = 0.04) between plot SSM measurements when comparing the full grid of 49 points to the proposed 9-point grid. Upon inspecting figure 33 for the morning measurements of RP3, the range is greatly reduced when taking less data points but still lies within the overall range obtained by taking 49 points. Additionally, for the purpose of this protocol, the means also differ by a small enough value (3%) to substantiate the reduced number of sampling points at a plot.
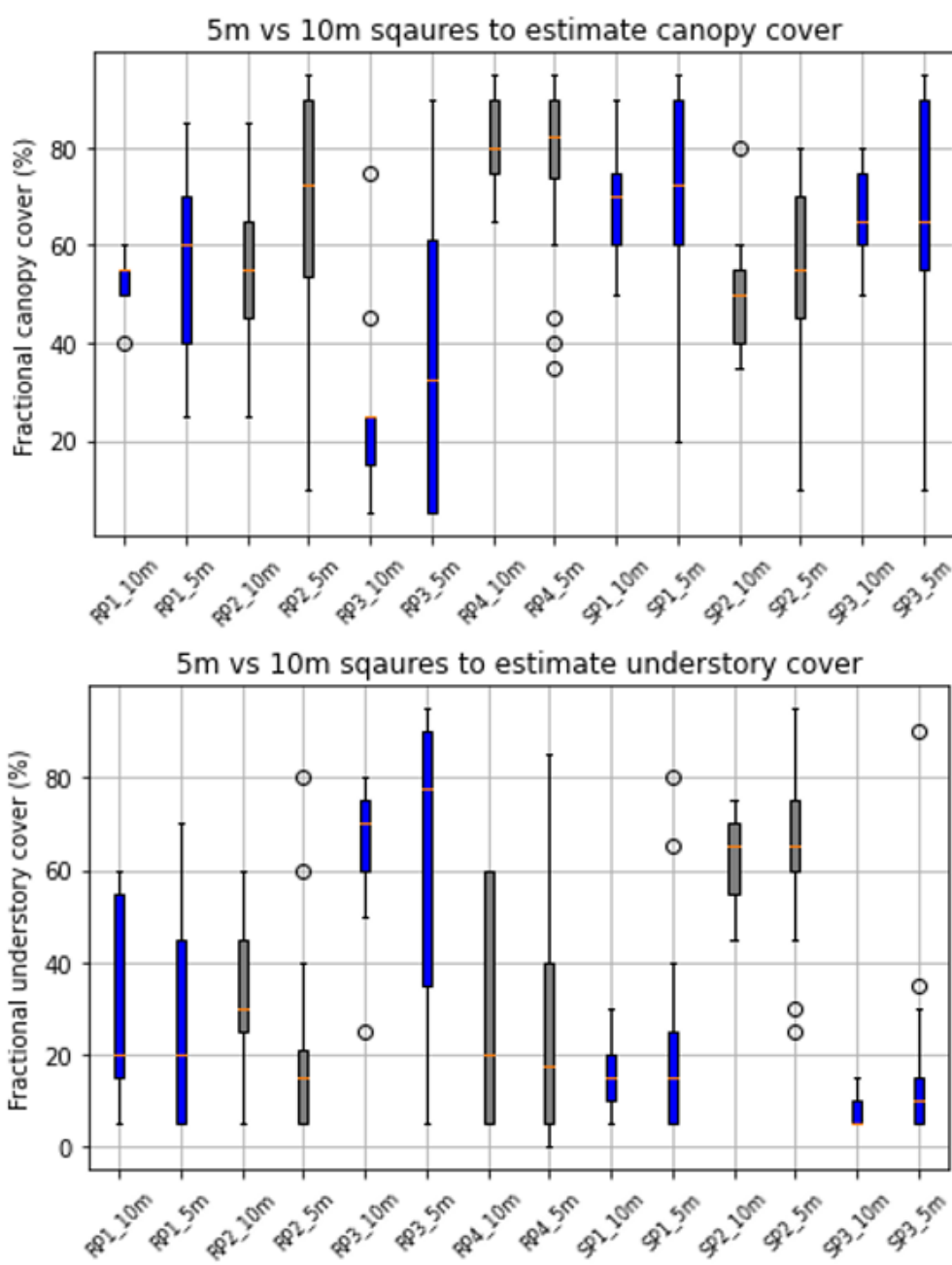
Figure 33. Boxplots of fractional canopy (top) and understory (bottom) estimations using 10m and 5m squares.

Figure 34 shows the vegetation cover estimates when using 5m squares are similar to when using 10m squares. Whilst both RP3 (canopy) and SP3 (understory) had significant differences (p = 0.04 and 0.03 respectively), only the values for RP2 showed a distinct difference in the means obtained for both canopy and understory (11% and 15%). Therefore, increasing the grid size to 10m squares to reduce the overall time spent on plots was deemed suitable for the purpose of this study. Grassland plots GP1-3 were not included as they were completely

covered (100% understory). This method remains very subjective and comparisons and discussion with other researchers, if possible, should be carried out.
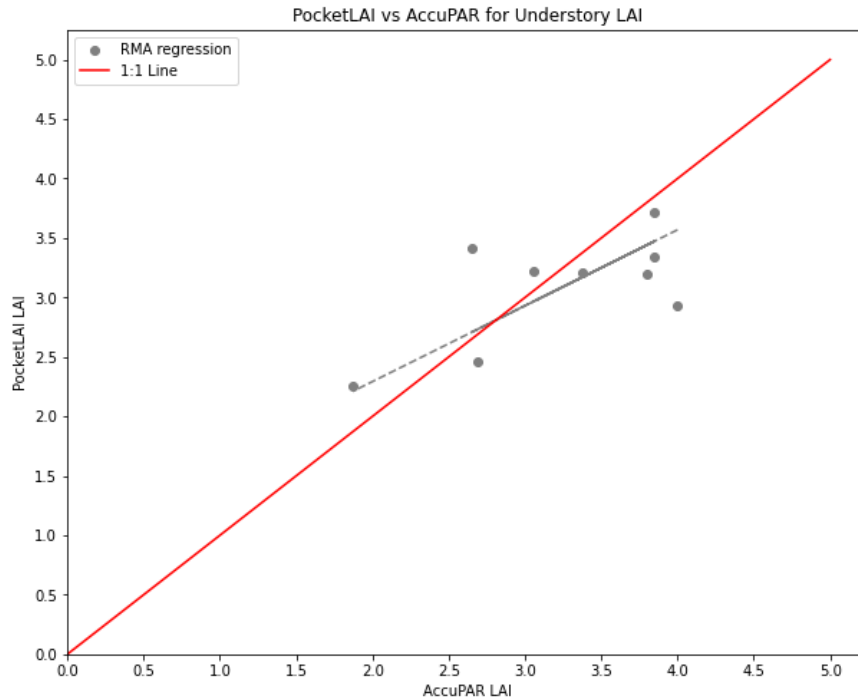

Figure 34. Relationship between understory AccuPAR and PocketLAI measurements. Plots with ideal conditions were used, including data for the grassland plots (GP1).

Table 8. Statistical results from analysis comparing understory LAI taken by the AccuPAR and PocketLAI.

	MAE	RMSE	CRM	EF	R2
AccuPAR vs PocketLAI	0.45	0.54	0.18	0.38	0.43

The results depicted in figure 35 and table 9 indicate that the proposed 16-point representative sampling of the understory is reliable to obtain an estimate of the LAI understory. This is shown with a moderate R^2 value (0.43) and acceptable MAE and RMSE values despite the two instruments sampling at random locations of the understory independent to each other. A saturation effect can be observed at higher LAI values which is also reflected in the increase in error when comparing RMSE and MAE values.
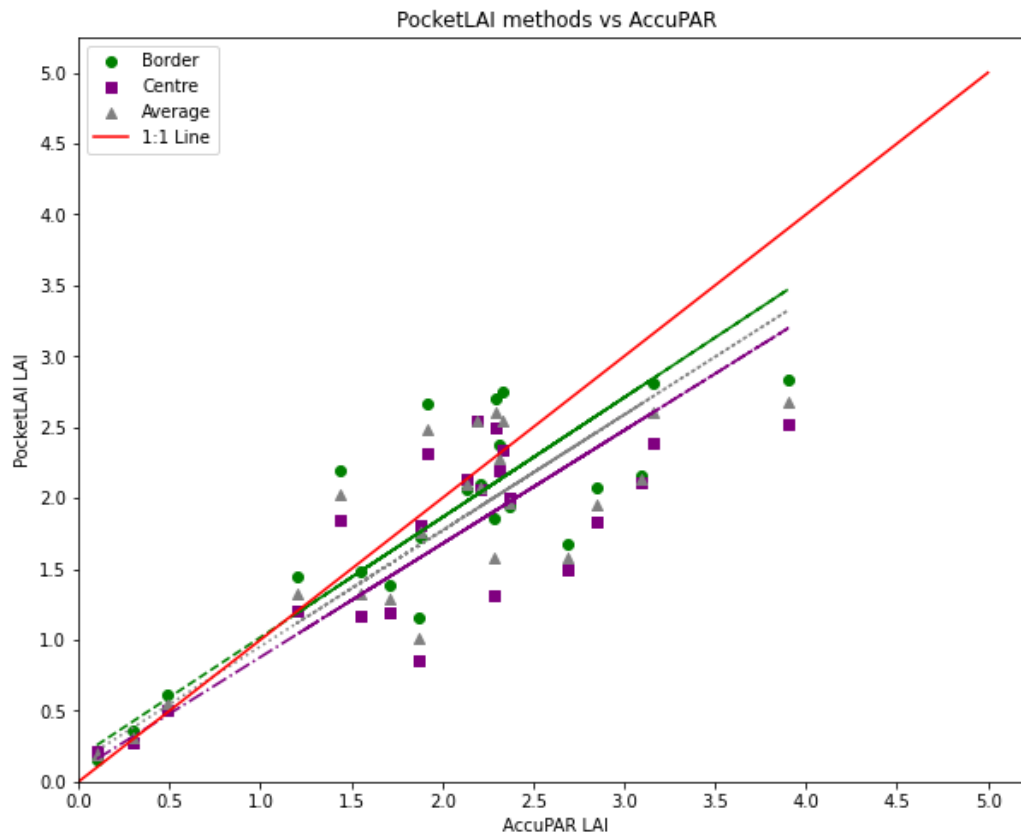
Figure 35. Relationship between PocketLAI canopy LAI and AccuPAR LAI using the three different proposed PocketLAI methods for all 30 plots (most ideal conditions used for protocol plots).

Table 9. Statistical results from analysis comparing different PocketLAI methods to AccuPAR canopy LAI results.

		MAE	RMSE	CRM	EF	R2
PocketLAI Border vs AccuPAR	*Protocol Plots*	0.54	0.65	-2.2	0.33	0.36
	All plots	0.42	0.53	-0.24	0.64	0.67
PocketLAI Centre vs AccuPAR	*Protocol Plots*	0.55	0.71	-0.24	0.20	0.29
	All plots	0.46	0.63	1.68	0.50	0.64
PocketLAI Average vs AccuPAR	*Protocol Plots*	0.54	0.66	-1.22	0.31	0.34
	All plots	0.43	0.57	0.72	0.59	0.66

The three methods for the PocketLAI canopy LAI were investigated initially in the protocol phase with data from the riverine and Sal plots (RP1-4 and SP1-3) using both morning and afternoon measurements (n=14). As can be seen in table 10, the border method performed the best (lowest MAE and RMSE; highest EF and R^2) and was therefore included in the protocol as the preferred method for the PocketLAI. Given the similar MAE and RMSE values, especially between the border and average methods, all three methods continued to be tested on all the plots after the protocol plots (n=23; figure 36). Both MAE and RMSE values decreased for all methods whilst EF and R^2 values considerably increased with more data points. The CRM values initially indicated systemic overestimations for all methods (negative

values) but when all plots were included, both centre and average methods tended to underestimate canopy LAI in comparison to AccuPAR values whilst the border method slightly overestimated LAI, although the low value is also indicative of no significant systemic over- or underestimations. The border measurement of 8 points around the edge of the plot continued to provide the most accurate canopy LAI values in comparison to the AccuPAR, having the lowest MAE and RMSE values of 0.42 and 0.53 respectively and is therefore the proposed method for the protocol. The EF value of 0.64 indicates that this method for the PocketLAI is sufficient in providing consistent LAI estimates with the error margins defined by the MAE and RMSE values. The R^2 value of 0.67 also indicates the RMA regression line sufficiently represents the variability of the results and therefore, the border method being proposed in the protocol was substantiated.

Additional data obtained using protocol

The following figures further showcase the range of data values obtained using the protocol in addition to the figure already presented in the results.
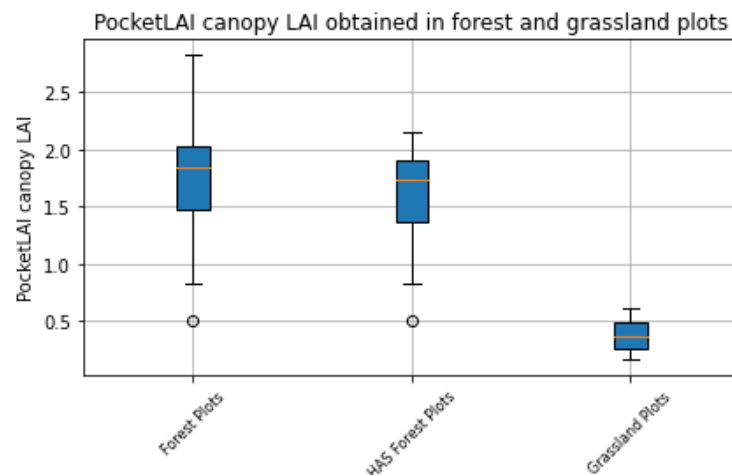

Figure 37. Canopy LAI values recorded with the PocketLAI at forest and grassland plots.
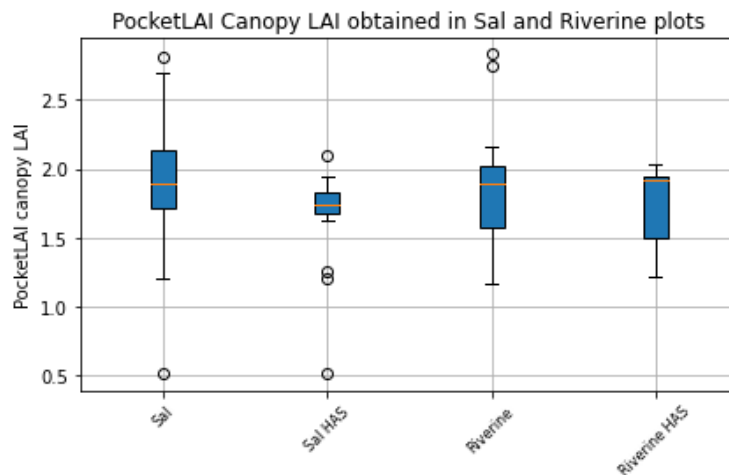

Figure 38. Canopy LAI values recorded with the PocketLAI at Sal forest and riverine forest plots.
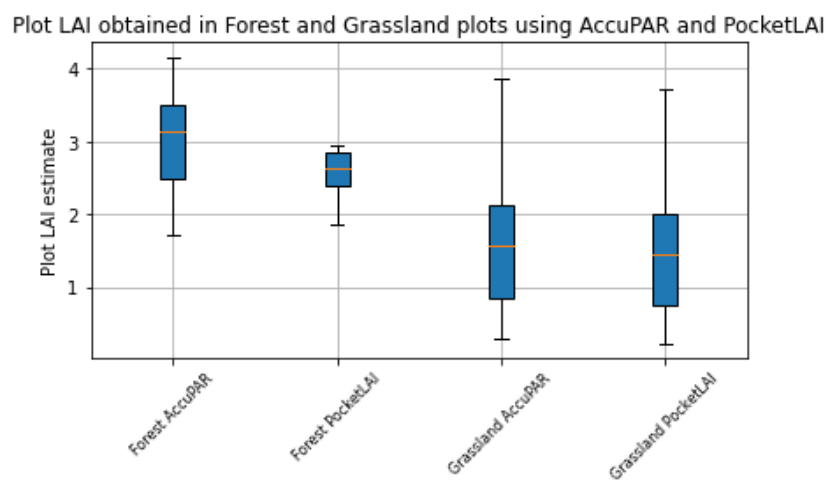
Figure 36. Plot LAI values recorded with the AccuPAR and PocketLAI at forest and grassland plots.
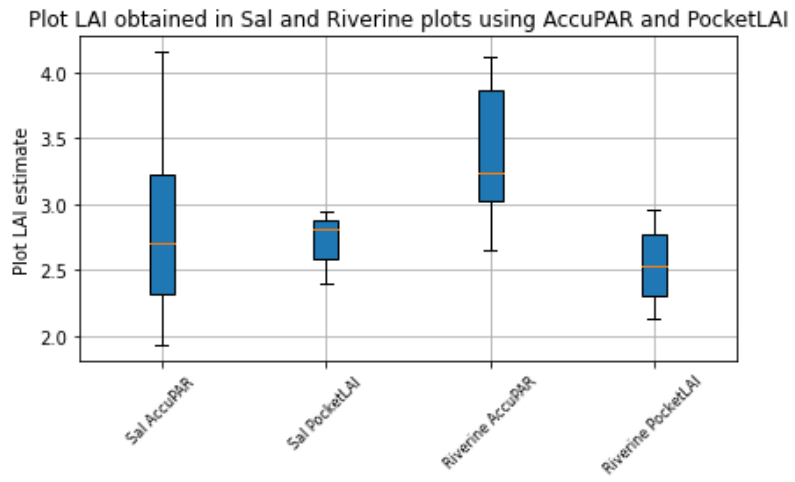
Plot LAI obtained in Sal and Riverine plots using AccuPAR and PocketLAI

Figure 39. Plot LAI values recorded with the AccuPAR and PocketLAI at Sal forest and riverine forest plots.

Appendix D – OPTRAM Method

The different STR-VI (NDVI, SAVI, ARVI) pixel distributions together with the corresponding wet and dry edges, and the pixel STR values that were used to obtain OPTRAM-derived SSM are shown. Following this, the results obtained when using SAVI and ARVI to retrieve SSM through the OPTRAM method are presented.

|	Plot	Date	id	iw	sd	sw	STR	
Thesis Plots (Karnali)	G1	22-Feb	0.5	2.4	0.5	0.8		1.23
	G2	22-Feb	0.5	2.4	0.5	0.8	NaN	
	G3	22-Feb	0.5	2.4	0.5	0.8		1.09
	G4	22-Feb	0.5	2.4	0.5	0.8	NaN	
	G5	22-Feb	0.5	2.4	0.5	0.8	NaN	
	G6	22-Feb	0.5	2.4	0.5	0.8	NaN	
	G7	22-Feb	0.5	2.4	0.5	0.8	NaN	
	GP1	07-Feb	0.1	1.7	1.2	2	NaN	
	GP2	07-Feb	0.1	1.7	1.2	2		2.36
	GP3	07-Feb	0.1	1.7	1.2	2	NaN	
	M1	22-Feb	0.5	2.4	0.5	0.8		1.81
	M2	22-Feb	0.5	2.4	0.5	0.8		1.48
	R1	22-Feb	0.5	2.4	0.5	0.8		1.43
	R2	22-Feb	0.5	2.4	0.5	0.8		1.68
	R3	22-Feb	0.5	2.4	0.5	0.8	NaN	
	R4	22-Feb	0.5	2.4	0.5	0.8	NaN	
	RP1	07-Feb	0.1	1.7	1.2	2		1.82
	RP2	07-Feb	0.1	1.7	1.2	2		1.67
	RP3	07-Feb	0.1	1.7	1.2	2		1.83
	RP4	07-Feb	0.1	1.7	1.2	2		2.06
	S1	22-Feb	0.5	2.4	0.5	0.8		2.09
	S2	22-Feb	0.5	2.4	0.5	0.8		2.13
	S3	22-Feb	0.5	2.4	0.5	0.8		2.19
	S4	22-Feb	0.5	2.4	0.5	0.8		2.13
	S5	22-Feb	0.5	2.4	0.5	0.8		2.06
	S6	22-Feb	0.5	2.4	0.5	0.8		2.16
	S7	22-Feb	0.5	2.4	0.5	0.8		2.02
	SP1	07-Feb	0.1	1.7	1.2	2		2.38
	SP2	07-Feb	0.1	1.7	1.2	2		2.36
	SP3	23-Jan	0.1	0.6	1	3.5		2.48
HAS Plots (Karnali)	B_M_7	24-Mar	0	0.7	1.6	3		1.62
	B_S_2	14-Mar	0.2	1.9	1.2	1.2		1.75
	B_S_3	14-Mar	0.2	1.9	1.2	1.2	NaN	
	B_S_7	14-Mar	0.2	1.9	1.2	1.2		1.93
	B_S_8	14-Mar	0.2	1.9	1.2	1.2		1.44
	B_S_9	14-Mar	0.2	1.9	1.2	1.2		1.75
HAS Plots (Babai)	B_B_B4	24-Mar	0	1	1.8	2		0.91
	B_B_B6	24-Mar	0	1	1.8	2		1.61
	B_B_C2	24-Mar	0	1	1.8	2		1.97
	B_B_C5	24-Mar	0	1	1.8	2		1.61
	B_B_D3	24-Mar	0	1	1.8	2		1.88
	B_B_E5	24-Mar	0	1	1.8	2		2.01
	B_B_E6	24-Mar	0	1	1.8	2		1.79
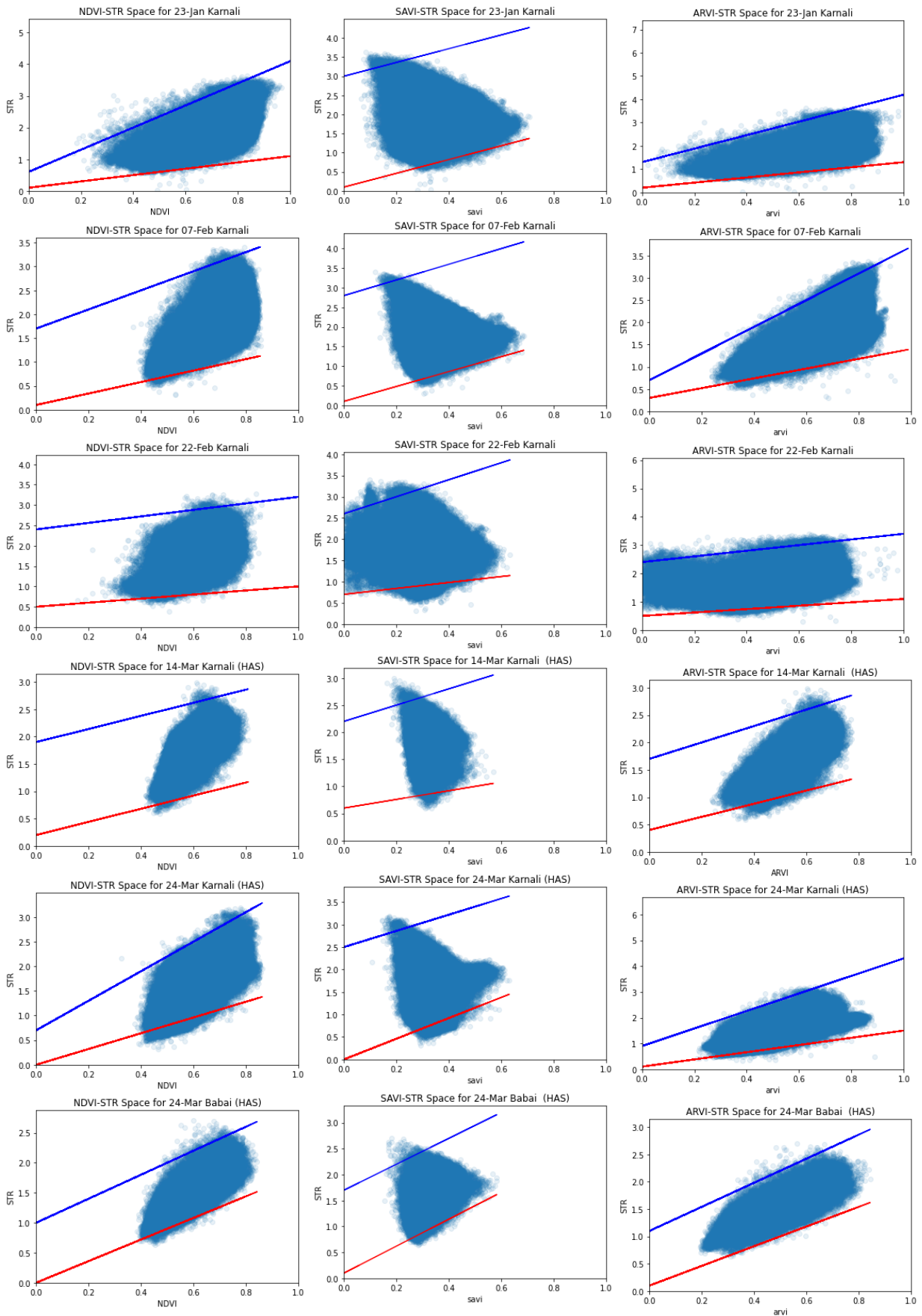
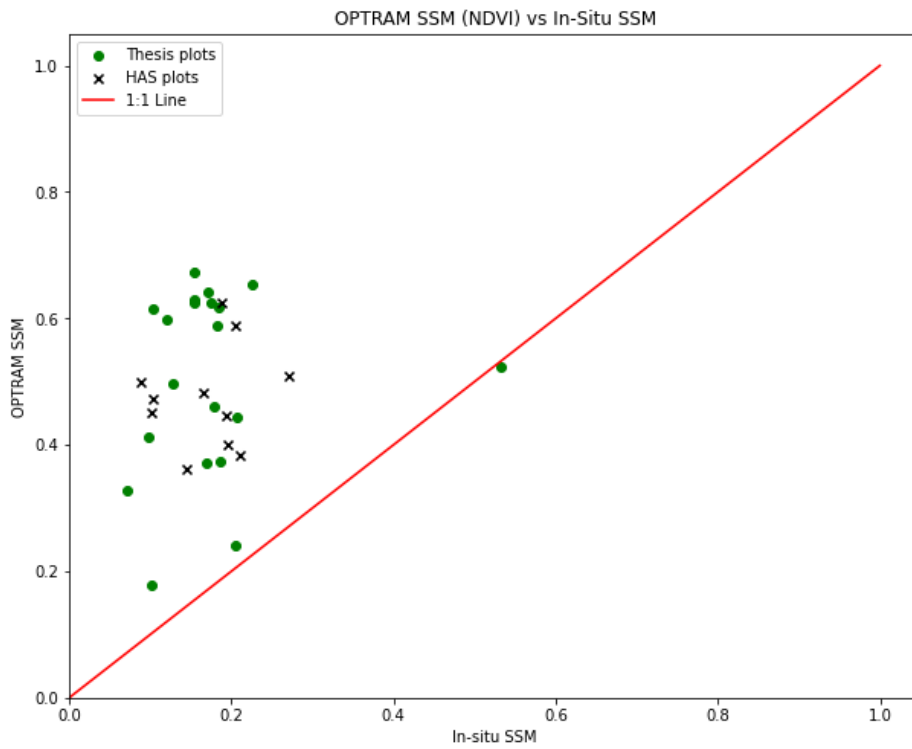*Figure 40. Pixel distributions for STR-VI Spaces*

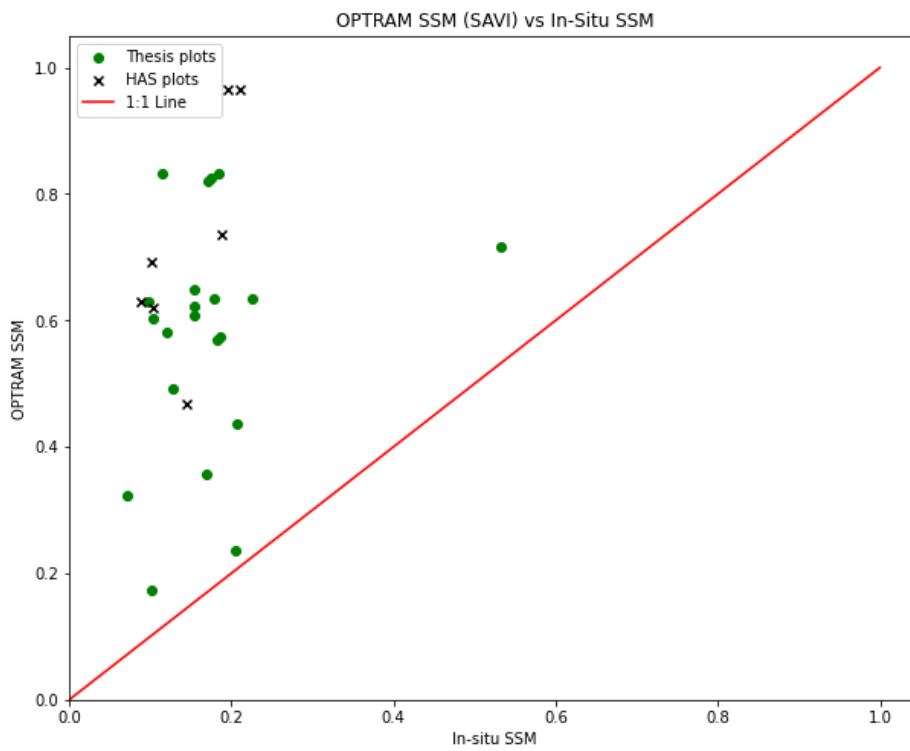*Figure 41. Relationship between OPTRAM SSM and in-situ SSM using NDVI.*

Figure 42. Relationship between OPTRAM SSM and in-situ SSM using SAVI.

Appendix E – Exploration into VI-LAI relationship

The potential of satellite sensing and its applications in the TAL, specifically regarding LAI monitoring was explored as additional research. The Normalized Difference Vegetation Index (NDVI), Soil Adjusted Vegetation Index (SAVI), and Atmospherically Resistant Vegetation (ARVI) were investigated regarding their potential linear relationship with LAI in the TAL.

The relationship between the three vegetation indices (NDIV, SAVI, ARVI) and in-situ canopy and total plot LAI were investigated to determine the potential of using vegetation indices as an alternative to remotely predict LAI in the TAL. The best performing in-situ methods from the analysis with satellite-derived LAI are used. Therefore, canopy and plot LAI PocketLAI data for the thesis plots and canopy AccuPAR LAI data for all plots combined.
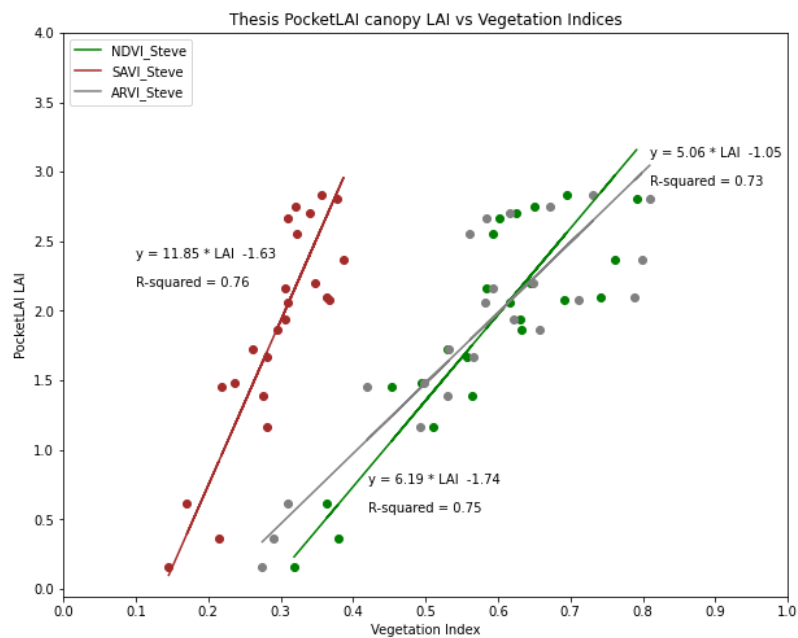

Figure 43. Relationship between in-situ PocketLAI canopy LAI and the three vegetation indices (NDVI, SAVI, ARVI) for thesis plots in the Karnali. R^2 values and regression equations shown on figure, all p-values < 0.01.

Figure 44. Relationship between in-situ PocketLAI total plot LAI (using equation 2) and the three vegetation indices (NDVI, SAVI, ARVI) for thesis plots in the Karnali. R2 values and regression equations shown on figure, all p-values < 0.01.

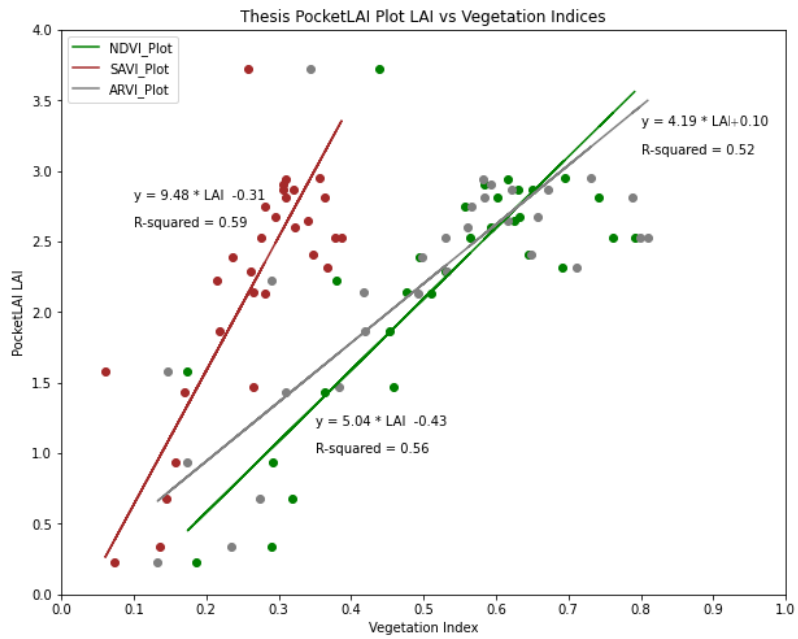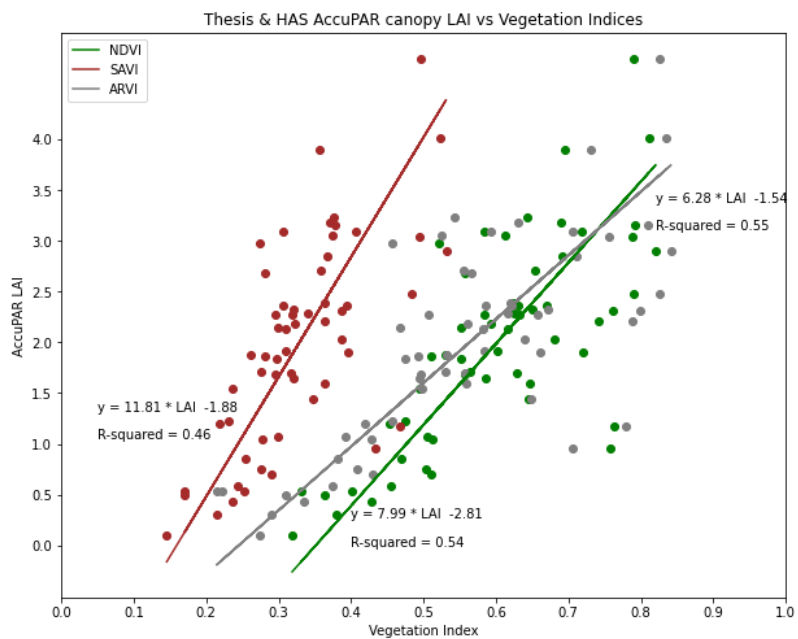
Figure 45. Relationship between in-situ AccuPAR canopy LAI from both thesis and HAS plots, and the three vegetation indices (NDVI, SAVI, ARVI). R2 values and regression equations shown on figure, all p-values < 0.01.

The relationships between each of the different VIs and in-situ LAI showed stronger relationships than the satellite-derived and in-situ LAI. This was especially evident for the total plot LAI estimates, which obtained an R^2 of 0.59 when compared with SAVI, to just 0.38 when compared with the satellite-derived LAI. This implies that VIs derived from Sentinel-2 have a stronger potential in quantifying LAI for the TAL than the direct LAI product.

VIs saturate however, when vegetation canopies close and will no longer show any changes in LAI (Fan et al., 2009). To overcome this, exponential regressions are often used, as is seen in the global dataset of empirical functions to convert NDVI to LAI as presented by Ginaldi et al. (2022). Futhermore, the use of different models based on the phenological phase of vegetation growth is shown to be necessary for accurate VI-LAI models (Potithep et al., 2013; Tillack, Clasen et al., 2014). These functions and relationships should be investigated further in the TAL for different VIs, expanding the range of LAI values collected to accurately quantify LAI using the correct empirical relationship.

Appendix F – Statistical Results

This section presents the relevant statistical results for the results presented in Appendix C for the Protocol Development.

	Morning vs Afternoon								
	Surface Soil Moisture			**Accupar**			**PocketLAI**		
	T-stat	p-value	n	T-stat	p-value	n	T-stat	p-value	n
GP1	1.59	0.12	49						
GP2	-0.78	0.44	49						
GP3	1.08	0.29	49						
RP1	1.00	0.32	49	-13.02	0	49	1.42	0.2	8
RP2	-1.61	0.11	49	1.07	0.29	49	0.13	0.9	8
RP3	2.59	0.01	49	-6.77	0	49	2.08	0.08	8
RP4	7.68	0.00	49	5.73	0	49	-0.14	0.89	8
SP1	-1.15	0.25	49	-0.44	0.66	49	2.51	0.04	8
SP2	7.58	0.00	49	-4.83	0	49	0.05	0.96	8
SP3	-8.30	0.00	49	-5.1	0	49	2.13	0.07	8

	Accupar 2pts vs 1pt		Accupar 49vs16		SSM 49vs9	
	T-stat	p-value	T-stat	p-value	T-stat	p-value
GP1 Morning					0.59	0.57
GP1 Afternoon					0.12	0.91
GP2 Morning					-0.8	0.45
GP2 Afternoon					0.03	0.97
GP3 Morning					-0.03	0.97
GP3 Afternoon					0.43	0.68
RP1 Morning	-0.35	0.73	-0.07	0.74	0.24	0.82
RP1 Afternoon	-0.63	0.53	0.34	0.94	0.73	0.48
RP2 Morning	0.19	0.85	-0.45	0.66	-0.87	0.41
RP2 Afternoon	0.85	0.40	0.46	0.65	-1.61	0.15
RP3 Morning	-1.06	0.30	0.79	0.44	-2.4	0.04
RP3 Afternoon	1.30	0.20	0.24	0.82	0.13	0.9
RP4 Morning	0.67	0.51	0.22	0.83	1.78	0.11
RP4 Afternoon	0.63	0.53	0.58	0.57	1.17	0.28
SP1 Morning	-0.76	0.45	0.99	0.33	-1.23	0.25
SP1 Afternoon	-0.56	0.58	-0.28	0.78	-0.61	0.56
SP2 Morning	1.16	0.25	-0.54	0.6	-0.56	0.59
SP2 Afternoon	0.06	0.95	-0.23	0.82	-0.9	0.4
SP3 Morning	0.27	0.79	0.22	0.83	-0.57	0.58
SP3 Afternoon	0.75	0.45	-0.65	0.52	-0.72	0.49

	FVC Understory 5m vs 10m squares		FVC Canopy 5m vs 10m squares	
	T-stat	p-value	T-stat	p-value
RP1	-1.21	0.23	1.36	0.18
RP2	-5.21	0	2.68	0.01
RP3	-0.43	0.67	2.09	0.04
RP4	-0.41	0.69	-0.52	0.6
SP1	0.99	0.33	0.97	0.34
SP2	1.62	0.11	1.34	0.19
SP3	2.23	0.03	0.27	0.79